

Aus dem Institut für Neurowissenschaften und Medizin des Forschungszentrums Jülich

(INM-3) – Kognitive Neurowissenschaften

**Modulation of behavior and brain activity
by probabilistic inference**

Inaugural-Dissertation

zur Erlangung des Doktorgrades

der Humanwissenschaftlichen Fakultät

der Universität zu Köln

nach der Promotionsordnung vom 18.12.2018

vorgelegt von

Anne-Sophie Käsbauer

aus Bochum

Dezember 2020

Vorwort

Diese Dissertation wurde von der Humanwissenschaftlichen Fakultät der Universität zu Köln im April 2021 angenommen.

Acknowledgements

First and foremost, I want to thank my supervisor Jun-Prof. Dr. Simone Vossel for her continuous support, appreciation, encouragement and excellent mentorship throughout the last four years. Thank you so much Simone for your commitment and enthusiasm in supporting my research, your innovative ideas and thoughts and for all that you have taught me. It was an honor to work with you.

Moreover, I would like to thank Prof. Dr. Gereon R. Fink for providing me the opportunity to accomplish this research at the Institute of Neuroscience and Medicine (INM-3) at the Research Centre Jülich and for sharing his expertise and valuable insights.

Furthermore, I would like to thank Dr. Paola Mengotti who I have been fortunate to collaborate with closely. Thank you for all your advice, work and support to achieve this work. I would like to thank Dr. Claudia Schmidt for her support and our fun times during the lesion mapping. In addition, I like to thank PD Dr. Ralph Weidner for his great scientific advice as well as his mentorship during our kitchen conversations.

Moreover, I would also like to thank Jochen Saliger and Prof. Dr. Hans Karbe for the opportunity to conduct this research at the neurological rehabilitation centre Godeshöhe.

Furthermore, I would like to thank all my current and former colleagues at the INM-3 for the inspiring research environment, great scientific discussions and fun social times. My very special thanks go to Simon Steinkamp, Helen Overhoff, Dr. Sabine Bertleff, Simon Huldreich Kohl, Maren Bell, Dr. Eva Nießen, Alben Reetz, Dr. David Vogel, Mathis Jording and my former office mates Janna Krauß, Max Hommelsen and Dr. Shivakumar Viswanathan for their scientific and most importantly their social support at all times. I would like to thank Prof. Dr. Peter Weiss-Blankenhorn for the great scientific exchange in conducting patient studies and his mentorship in science management.

Most certainly, I am truly grateful to my friends and parents for their unconditional support and infinite trust. Thank you so much for your encouragement, your open ears and for cheering me up, especially in times of trouble. Thank you for always believing in me.

Finally, I would like to express my deepest gratitude to my patients dedicating their time to enable this research.

Abstract

Expectancies and beliefs about upcoming sensory events encoded by the brain play a crucial role in shaping our perception. Therefore, stimulus detection and processing can be facilitated by prior beliefs about the stimulus' location or its features. These beliefs are rapidly generated by former observations/experience of the individual. Bayesian principles can evidently be used to describe this probabilistic inference. The present thesis aimed to characterize the mechanisms underlying probabilistic inference in the healthy and the lesioned human brain.

In healthy participants, probabilistic inference in the context of attentional deployment has already been described with the help of computational models, and the underlying neural mechanisms have been explored with functional neuroimaging (Dombert, Kuhns, et al., 2016; Kuhns et al., 2017; Vossel et al., 2015). However, it is not known how the resting-state network architecture of the brain relates to this process and how the lesioned brain performs probabilistic inference.

To investigate these questions, two experiments have been conducted using modified versions of a Posner-cueing paradigm. In this context, probabilistic inference describes the ability to infer changing probabilities about the validity of a cue and the updating process of the belief about them. By manipulating the percentage of cue validity (%CV) (i.e., the proportion of valid and invalid trials) over the time course of an experiment, the participants had to infer the actual cue validity level (i.e., the probability that the cue will be valid in a given trial), so that probabilistic inference could be assessed.

In Experiment 1, a modified location-cueing paradigm with block-wise changes of the %CV and true and false prior information about the %CV before each block was employed in healthy young participants. A Rescorla-Wagner model was used to characterize probabilistic inference. Moreover, resting-state fMRI was recorded before and after the task and a seed-based correlation analysis was used to define the resting-state functional connectivity (rsFC)

Abstract

of the right temporo-parietal junction (rTPJ). Correlations of each behavioral parameter with the rsFC before the task, as well as with changes in rsFC after the task, were assessed in a ROI-based approach.

It was observed that higher intrahemispheric rsFC between rTPJ and IPS before the task was associated with slower probabilistic inference after false priors. Furthermore, increased interhemispheric rsFC between rTPJ and lTPJ after the task was related to relatively faster probabilistic inference in false blocks. Both findings support previous research and highlight that not only resting-state connectivity per se is relevant for cognitive functions but also that cognitive processing during a task can change connectivity patterns afterwards in a performance-dependent manner.

In Experiment 2, probabilistic inference in stroke patients was investigated to assess a hypothesized relationship with the spatial neglect syndrome (Experiment 2a) as well as commonalities and distinctions between probabilistic inference in different cognitive subsystems (Experiment 2b). Three modified versions of the Posner-cueing task with different cue types were used to investigate spatial attention (location cues), feature-based attention (color cues) and motor-intention (motor-response cues). In contrast to Experiment 1, no prior information about the %CV was provided and probabilistic inference was operationalized by assessing the impact of the %CV manipulation on RTs by means of regression analyses as well as by asking participants to explicitly estimate the %CV. Furthermore, patients were screened for the neglect syndrome using a diverse neuropsychological test battery. Lesion-symptom mapping (VLSM) as well as lesion-network mapping was performed on the relevant behavioral parameters.

The results indicated that patients' probabilistic inference abilities across domains were not per se impaired. However, by trend it was found that some right hemisphere damaged patients exhibited difficulties using their knowledge to adapt their behavior in contralesional space as indicated by a reduced modulation of RTs by %CV in invalid contralesional trials in the spatial attention domain. However, there was no strong evidence for impairments of probabilistic inference being related to the neglect syndrome.

Abstract

Moreover, the correlation of the two probabilistic inference parameters (invalid contralesional %CV regression weight & averaged explicit %CV estimate) within domains revealed no significant relationship between the both, stating them as independent components of probabilistic inference, which was further supported by the VLSM results. However, the correlations across domains revealed some commonalities, which were also in line with the VLSM results. Thus, our data suggests that the neural implementations for probabilistic inference seem to be dedicated to domain-specific subsystems, which share some common nodes.

Consequently, the present thesis provides novel insights into the computational mechanisms of probabilistic inference in the healthy and lesioned brain. The work thereby enables future studies to transfer the gained knowledge from basic research of healthy participants and patients to clinical applications.

Zusammenfassung

Unsere Wahrnehmung wird nicht nur von den physikalischen Eigenschaften unserer sensorischen Umgebung bestimmt, sondern auch entscheidend von internen mentalen Prozessen beeinflusst, wie z. B. den Erwartungen an bevorstehende sensorische Ereignisse, welche von unserem Gehirn kodiert werden. Vorherige Erwartungen über den Erscheinungsort oder die Merkmale eines Stimulus beschleunigen dessen Erkennung und Verarbeitung. Im Alltag werden diese Erwartungen auf der Grundlage vorheriger Beobachtungen schnell entwickelt, und diese probabilistische Inferenz kann plausibel durch Bayes'sche Prinzipien beschrieben werden.

Gegenstand dieser Arbeit ist die Charakterisierung derjenigen Mechanismen, welche der probabilistischen Inferenz im gesunden und im geschädigten menschlichen Gehirn zugrunde liegen. Dazu wurde bereits bei gesunden Probanden die probabilistische Inferenz im Kontext der Aufmerksamkeitssteuerung mit Hilfe von computationalen Modellen beschrieben und die zugrundeliegenden neuronalen Mechanismen mit funktioneller Bildgebung (fMRI) untersucht (Dombert, Kuhns, et al., 2016; Kuhns et al., 2017; Vossel et al., 2015). Bislang ungeklärt ist jedoch, ob es einen Zusammenhang zwischen der Netzwerkarchitektur der funktionalen Konnektivität des Gehirns im Ruhezustand und probabilistischer Inferenz gibt und wie das geschädigte Gehirn, z.B. nach einem Schlaganfall, diese Funktion durchführt.

Um diese Fragen genauer zu untersuchen, wurden zwei Experimente durchgeführt, die beide eine modifizierte Version eines Posner-Cueing-Paradigmas zur Grundlage hatten. Dabei beschreibt der Begriff probabilistische Inferenz die Fähigkeit, wechselnde Wahrscheinlichkeiten in Bezug auf die Vorhersagbarkeit eines Hinweisreizes zu erkennen und die dazugehörige Erwartung zu aktualisieren. Aufgrund der Manipulation der Hinweisreizvalidität ($\% CV = \text{Verhältnis valider und invalider Durchgänge}$) im Verlauf eines Experiments mussten die Probanden auf die tatsächliche $\%CV$ (Wahrscheinlichkeit, dass der Hinweisreiz valide sein wird) schließen und die Fähigkeit zur probabilistischen Inferenz konnte festgestellt werden. In Experiment 1 wurde ein modifiziertes räumliches Hinweisreiz-

Zusammenfassung

Paradigma mit blockweisen Änderungen der % CV und wahren oder falschen Vorabinformationen über die % CV bei gesunden jungen Teilnehmern verwendet. Zusätzlich wurde ein Rescorla-Wagner-Modell benutzt, um probabilistische Inferenz zu charakterisieren. Darüber hinaus wurde die funktionale Konnektivität (rsFC) des Gehirns im Ruhezustand mit der rechten temporo-parietalen Junction (rTPJ) vor und nach der Aufgabe untersucht und Korrelationen jedes Verhaltensparameters mit der rsFC vor der Aufgabe sowie mit Veränderungen der rsFC nach der Aufgabe berechnet.

Ergebnis war ein signifikanter Zusammenhang zwischen einer höheren intrahemisphärischen rsFC zwischen rTPJ und intraparietalem Sulcus vor der Aufgabe und einer langsameren probabilistischen Inferenz nach falschen Informationen. Des Weiteren stand eine erhöhte interhemisphärische rsFC zwischen rTPJ und ITPJ nach der Aufgabe mit einer relativ schnelleren probabilistischen Inferenz in Blöcken mit falscher Information im Bezug. Beide Ergebnisse bestärken frühere Studien und zeigen, dass nicht nur die Konnektivität im Ruhezustand an sich für kognitive Funktionen relevant ist, sondern auch, dass die kognitive Verarbeitung während einer Aufgabe die Konnektivitätsmuster anschließend in verhaltensabhängiger Weise verändern kann.

In Experiment 2 bestand die Stichprobe aus Schlaganfallpatienten und gesunden älteren Probanden. Hierbei wurde eine hypothetische Beziehung zwischen Defiziten in probabilistischer Inferenz und dem räumlichen Neglektsyndrom untersucht (Experiment 2a) sowie Gemeinsamkeiten und Unterschiede zwischen der probabilistischen Inferenz in verschiedenen kognitiven Subsysteme (Experiment 2b) charakterisiert. Drei modifizierte Versionen der Posner-Hinweisreiz-Aufgabe mit unterschiedlichen Hinweisreizen wurden verwendet, um die räumliche Aufmerksamkeit (Orts-Hinweisreiz), die merkmalsbasierte Aufmerksamkeit (Farb-Hinweisreiz) und die motorische Intention (Hinweisreiz zur motorischen Reaktion) zu untersuchen. Im Gegensatz zu Experiment 1 wurden keine Vorabinformationen über die % CV bereitgestellt und die probabilistische Inferenz wurde operationalisiert, indem die Auswirkungen der % CV-Manipulation auf Reaktionszeiten mittels Regressionsanalysen quantifiziert und die Teilnehmer gebeten wurden, die % CV

Zusammenfassung

explizit zu schätzen. Darüber hinaus wurden die Patienten unter Verwendung einer vielfältigen neuropsychologischen Testbatterie auf das Neglektssyndrom untersucht, und es wurden Läsions-Symptom-Mapping (VLSM) sowie Läsions-Netzwerk-Mapping Analysen der relevanten Verhaltensparameter durchgeführt.

Die Ergebnisse zeigten, dass die probabilistische Inferenzfähigkeit der Patienten über Domänen hinweg per se nicht beeinträchtigt war. Trendweise wurde jedoch festgestellt, dass einige rechtshemisphärisch geschädigte Patienten Probleme hatten, ihr Wissen zur Verhaltensänderung im Bereich der räumlichen Aufmerksamkeit zu nutzen. Dies äußerte sich in einer reduzierten Modulation der Reaktionszeiten durch %CV in invaliden kontraläsionalen Durchgängen, jedoch waren ipsiläsionale Durchgänge nicht betroffen. Weiterhin gab es keine eindeutigen Hinweise darauf, dass Beeinträchtigungen der probabilistischen Inferenz mit dem Neglektssyndrom im Zusammenhang standen. Darüber hinaus ergab die Korrelation der beiden probabilistischen Inferenzparameter (die Gewichte der Regressionsanalysen in invaliden kontraläsionalen Durchgängen und die expliziten Schätzungen der % CV) innerhalb einer Domäne keinen signifikanten Zusammenhang zwischen den beiden und daher können sie als unabhängige Komponenten der probabilistischen Inferenz betrachtet werden, was durch die VLSM-Ergebnisse bestärkt wurde. Die domänenübergreifenden Korrelationen zeigten jedoch einige Gemeinsamkeiten, die auch mit den VLSM-Ergebnissen übereinstimmten. Daher legen unsere Daten nahe, dass die neuronalen Strukturen der probabilistischen Inferenz domänenspezifische Subsysteme zugrundeliegen, die aber auch Gemeinsamkeiten aufweisen.

Infolgedessen liefert die vorliegende Arbeit neue Einblicke in die zugrundeliegenden Mechanismen der probabilistischen Inferenz im gesunden und erkrankten Gehirn, sodass zukünftige Studien das gewonnene Wissen aus der Grundlagenforschung gesunder Probanden und Patienten auf die klinische Anwendung übertragen können.

List of Figures

Figure 1.1 Illustration of a classical Posner-cueing paradigm (A) and the validity effect (B)...3

Figure 1.2 Illustration of the Rescorla Wagner model (A), and the hierarchical Bayesian model (B) and the according response model (C).....6

Figure 1.3 Schematic illustrations of neglect symptoms in a cancellation task (A) and a copying task (B) 10

Figure 1.4 Relationship between anatomical distribution of lesions associated with neglect, attentional networks, and damage to fiber tracts (this figure is reproduced with permission of Annual Reviews Inc. and was published in Corbetta et al. 2011). 11

Figure 1.5 Schematic illustration of the central nodes of the dorsal and ventral attention systems (this figure is reproduced with permission of Elsevier and was published in Mengotti, Käsbauer, et al., 2020). 14

Figure 1.6 Schematic illustration of resting-state fMRI (this figure is reproduced with permission of Elsevier and was published in van den Heuvel & Hulshoff Pol 2010).20

Figure 2.1 Experiment 1: A Experimental paradigm with one example trial (valid trial). B Validity effects (RT invalid minus RT valid) for each true and false %CV block 33

Figure 2.2 Positive and negative rsFC of rTPJ across both resting-state runs42

Figure 2.3 Correlation of the parameter of reorienting and the change in rsFC between the rTPJ and the ITPJ after (as compared to before) the task 44

Figure 2.4 Correlations of belief updating and the rsFC between the rTPJ and the rIPS before the task as well as between the rTPJ and ITPJ after (as compared to before) the task45

Figure 2.5 Experiment 2: Experimental paradigm with one example trial (valid trial)67

Figure 2.6 A Block-wise validity effects for each %CV block. B Normalized validity effects for each %CV block..... 76

Figure 2.7 Effect of order on the normalized validity effect..... 78

List of Figures

Figure 2.8 A %CV regression weights for each condition for all three groups. B z-standardized %CV regression weights for the two patient groups	79
Figure 2.9 Effect of order on the estimation of the explicit %CV	80
Figure 2.10 Within-group correlation of the two probabilistic inference parameters (invalid contralesional %CV regression weight & averaged explicit %CV estimate) for RH patients only.....	81
Figure 2.11 Correlations of the neglect and task parameters with all 47 patients	82
Figure 2.12 Within-group correlations of the neglect and task parameters for A RH patients only and B LH patients only	83
Figure 2.13 Lesion distribution of the current sample of stroke patients	83
Figure 2.14 VLSM result for mean LI thresholded at FDR $p < 0.05$ A for all patients (n=46). B RH patients only (n=25)	84
Figure 2.15 VLSM result for PB thresholded at FDR $p < 0.05$ A for all patients (n=47). B RH patients only (n=26).....	84
Figure 2.16 VLSM results thresholded at $p < 0.05$ uncorrected (n=47) for A the absolute values of the z-standardized averaged explicit %CV. B higher RB-scores.....	11
Figure 2.17 VLSM results of RH patients only thresholded at $p < 0.05$ uncorrected (n=26) for A the z-standardized normalized contralesional VE. B the z-standardized invalid contralesional %CV regression weight. C the absolute values of the z-standardized averaged explicit %CV. D higher RB-scores.....	86
Figure 2.18 VLSM results of LH patients only thresholded at $p < 0.05$ uncorrected (n=21) for A the absolute values of the z-standardized averaged explicit %CV. B higher RB-scores....	87
Figure 2.19 Disconnection distribution of the current sample of stroke patients.....	88
Figure 2.20 Behavioral test performances in relation to white matter tract damage for all patients (n=47).....	89
Figure 2.21 Behavioral test performances in relation to white matter tract damage for RH patients (n=26).....	89

List of Figures

Figure 2.22 Behavioral test performances in relation to white matter tract damage for LH patients (n=21).....	90
Figure 2.23 Three different cues were used for investigating spatial attention (Experiment 2a), feature-based attention, and motor-intention.....	104
Figure 2.24 Block-wise validity effects for each %CV block for A the spatial attention task (cf. Experiment 2a). B the feature-based attention task. C the motor-intention task. Normalized validity effects for each %CV block for D the spatial attention task. E the feature-based attention task. F the motor-intention task	105
Figure 2.25 Effect of order on the normalized validity effect of the motor-intention task	111
Figure 2.26 %CV regression weights for each condition for all three groups for A the spatial attention task. B the feature-based attention task. C the motor-intention task. z-standardized %CV regression weights for the two patient groups for D the spatial attention task. E the feature-based attention task. F the motor-intention task.....	114
Figure 2.27 Explicit %CV estimates for each %CV block for all three groups for A the spatial attention task. B the feature-based attention task. C the motor-intention task.....	114
Figure 2.28 Results of the correlations of the two parameters of probabilistic inference across tasks for A the z-standardized contralesional invalid %CV regression weights. B the averaged explicit %CV estimates.....	115
Figure 2.29 VLSM results for the z-standardized invalid contralesional %CV regression weight of all patients (n=46).....	116
Figure 2.30 VLSM results for the z-standardized invalid contralesional %CV regression weight in RH patients only (n=26)	117
Figure 2.31 VLSM results for the z-standardized invalid contralesional %CV regression weight in LH patients only (n=20).....	117
Figure 2.32 VLSM results for the absolute values of the z-standardized averaged explicit %CV of all patients (n=46).....	118

List of Figures

Figure 2.33 VLSM results for the absolute values of the z-standardized averaged explicit %CV in RH patients only (n=26).....	119
Figure 2.34 VLSM results for the absolute values of the z-standardized averaged explicit %CV in LH patients only (n=20)	120
Figure 2.35 Behavioral test performances in relation to white matter tract damage for RH patients (n=26).....	121
Figure 2.36 Behavioral test performances in relation to white matter tract damage for LH patients (n=20).....	121
Figure 2.37 Behavioral test performances in relation to region of interest affection for all patients (n=46).....	122

List of Tables

Table 1 rsFC pattern of the rTPJ across both resting-state runs43

Table 2 Demographic and neuropsychological data of the stroke patients (Experiment 2a).65

Table 3 Overview of patients fulfilling the criteria for extinction and neglect 75

Table 4 Neuropsychological and task parameter data of the two RH neglect patients on their first assessment and six month follow up. 92

Table 5 Demographic and neuropsychological data of the stroke population (Experiment 2b) 101

List of Abbreviations

AAL	Automated anatomical labeling
ACC	Anterior cingulate cortex
ACL-K	Short form of the aphasia checklist
AF	Arcuate fasciculus
ANG	Angular gyrus
ANOVA	Analysis of variance
BCB	Brain Connectivity and Behavior
BOLD	Blood oxygen level dependent
CC	Corpus callosum
cm	Centimeter
CT	Computed tomography
cTBS	Continuous theta burst stimulation
%CV	Percentage of cue validity
DAN	Dorsal attention network
DTI	Diffusion tensor imaging
EEG	Electroencephalography
EPI	Echo-planar imaging
FC	Functional connectivity
FDR	False discovery rate
FEF	Frontal eye fields
fMRI	Functional magnetic resonance imaging
GDS	Geriatric depression scale
HC	Healthy controls
HGF	Hierarchical Gaussian Filter
HPC	Hippocampus

List of Abbreviations

HRF	Hemodynamic response function
Hz	Hertz
IFG	Inferior frontal gyrus
IFOF	Inferior occipitofrontal fasciculus
ILF	Inferior longitudinal fasciculus
IPL	Inferior parietal lobe
IPS	Intraparietal sulcus
JHU	Johns Hopkins University
KAS	Cologne Apraxia Screening
l	Left
LH	Left hemisphere
LI	Laterality index
MFG	Middle frontal gyrus
min	Minutes
mm	Millimeter
MMSE	Mini-Mental State Examination
MNI	Montreal Neurological Institute
MRI	Magnetic resonance imaging
ms	Milliseconds
MWCT	Mesulam Weintraub Cancellation Task
n	Number
NPM	Non-parametric mapping
PB	Perceptual bias
PFC	Prefrontal Cortex
PIST	Parietal inferior-to-superior tract
r	Right
RB	Response bias
RF	Radiofrequency

List of Abbreviations

RH	Right hemisphere
ROI	Region of interest
RS	Response speed
rsFC	Resting-state functional connectivity
RT	Response times
RW	Rescorla-Wagner
sec	Second
SEM	Standard error of the mean
SLF	Superior longitudinal fasciculus
SMG	Supramarginal gyrus
SOA	Stimulus onset asynchrony
SPL	Superior parietal lobe
SPM	Statistical parametric mapping
STG	Superior temporal gyrus
T	Tesla
TMS	Transcranial magnetic stimulation
TPJ	Temporoparietal junction
V	Visual cortex
VAN	Ventral attention network
VE	Validity effect
VFC	Ventral frontal cortex
VLSM	Voxel-based lesion-symptom mapping

Table of Contents

Abstract.....	II
Zusammenfassung	V
List of Figures.....	VIII
List of Tables	XII
List of Abbreviations	XIII
1. General Introduction	1
1.1 Probabilistic Inference, Predictions and Belief Updating	1
1.1.1 Probabilistic Inference in the Domain of Visuospatial Attention.....	2
1.1.2 Computational Models of Probabilistic Inference.....	4
1.1.3 Neuroanatomy of Probabilistic Inference.....	7
1.2 (Visuo-)spatial Neglect.....	9
1.2.1 Clinical Symptoms	9
1.2.2 Neuroanatomy.....	10
1.2.3 Cognitive Models of Spatial Neglect.....	12
1.2.4 Probabilistic Inference, Updating and the Spatial Neglect Syndrome	15
1.3 Functional Neuroimaging Approach.....	18
1.3.1 Physical and Physiological Background	18
1.3.2 Functional Magnetic Resonance Imaging	18
1.3.3 Resting-state fMRI.....	19
1.4 Brain-lesion Approach.....	21

2. Empirical Section.....	24
2.1. Objectives of the Thesis.....	24
2.2 Experiment 1: Computational Modeling and Resting-state fMRI Experiment with Healthy Participants.....	25
2.3 Experiment 2a: Behavioral Experiment and Lesion Mapping - Investigating Probabilistic Inference in the Domain of Spatial Attention and its Relation to Spatial Neglect in Stroke Patients.....	56
2.4 Experiment 2b: Behavioral Experiment and Lesion Mapping - Investigating Probabilistic Inference during Feature-based Attention and Motor-intention in Stroke Patients	98
3. General Discussion.....	128
3.1 Experiment 1	128
3.1.1 The Relationship between Resting-state Functional Connectivity and Attentional Reorienting as well as Probabilistic Inference.....	128
3.1.2 Limitations and Implications.....	132
3.2 Experiment 2	133
3.2.1 The Relationship between Probabilistic Inference in the Domain of Spatial Attention and the Neglect Syndrome.....	133
3.2.2 Limitations and Implications.....	135
3.2.3 Probabilistic Inference in Various Cognitive Domains.....	138
3.2.4 Limitations and Implications.....	140
3.3 Future Perspectives and Concluding Remarks	142
4. References.....	144
5. Curriculum Vitae	169

1. General Introduction

1.1 Probabilistic Inference, Predictions and Belief Updating

Perception and actions are not only determined by the physical characteristics of our sensory environment, but are crucially affected by internal processes, such as beliefs and predictions about upcoming sensory events encoded by the brain. These beliefs and predictions are rapidly produced on the basis of recent observations and statistical regularities of our environment. They can affect the efficiency of perception and actions, resulting in e.g. faster stimulus detection when valid, compared to when not (Pinto et al., 2015). Their relative impact is determined by their relative reliability, i.e. precision (Feldman & Friston, 2010; Mumford, 1992). It has been proposed that the brain acts as a prediction machine steadily matching sensory inputs with beliefs generated based on prior observations. The term probabilistic inference describes the formation of beliefs based on deriving the probability of variables of interest (Clark, 2013; Daunizeau, den Ouden, Pessiglione, Kiebel, Stephan, et al., 2010; Friston, 2005; Friston & Kiebel, 2009). The formation of probabilistic beliefs can be investigated by the application of generative models. There is increasing evidence that this probabilistic inference can plausibly be characterized by Bayesian principles proposing that the formation of beliefs is based on probability distributions (Gershman & Beck, 2017; Pouget et al., 2013). Given data (D), Bayes' rule imposes how to obtain the posterior probability distribution over a variable of interest (V):

$$P(V|D) = \frac{P(V)P(D|V)}{P(D)}$$

Hence, to compute the posterior distribution $P(V|D)$, the prior distribution $P(V)$ is multiplied with the likelihood function $P(D|V)$ and this is then divided by the term $P(D)$ to ensure that the posterior integrates to 1. Probabilistic inference aims to minimize prediction errors about sensory inputs and to increase the posterior probability by updating beliefs when new observations are made (Friston & Kiebel, 2009). It has been shown that models which are

1. General Introduction

based on Bayesian principles outperform normative theories in explaining human behavior (e.g. Behrens, Woolrich, Walton, & Rushworth, 2007; den Ouden, Daunizeau, Roiser, Friston, & Stephan, 2010).

1.1.1 Probabilistic Inference in the Domain of Visuospatial Attention

Previous research has demonstrated that probabilistic inference mechanisms are also involved in the deployment of attention (Feldman & Friston, 2010; Vossel et al., 2015; Vossel, Mathys, et al., 2014). To study the role of beliefs and predictions for attentional deployment, cueing paradigms are suitable tasks (Dombert, Kuhns, et al., 2016; Feldman & Friston, 2010; Käsbauer et al., 2020; Kuhns et al., 2017; Mengotti et al., 2017; Mengotti, Kuhns, et al., 2020; Posner, 1980; Vossel, Mathys, et al., 2014).

These cueing tasks are based on the experimental paradigm which was introduced by Posner in 1980 to investigate orienting and reorienting of attention (Posner, 1980). In this paradigm, participants have to keep central fixation and respond to a target stimulus which can appear in the left or right hemifield. Prior to target presentation, a cue will be displayed informing participants about the most likely location of the target (spatial cue). In most trials the cue will be valid. However, in some trials the cue will be invalid and predict the location of the target incorrectly (see Figure 1.1A). Due to the expectations and shifts of attentional resources of the participants, validly cued targets speed responses, whereas invalidly cued targets induce slower responses since reorienting of attention is required and predictions are violated. The difference in response times (RTs) between invalid and valid trials describes the validity effect (VE), representing the attentional costs of reorienting attention (see Figure 1.1B).

1. General Introduction

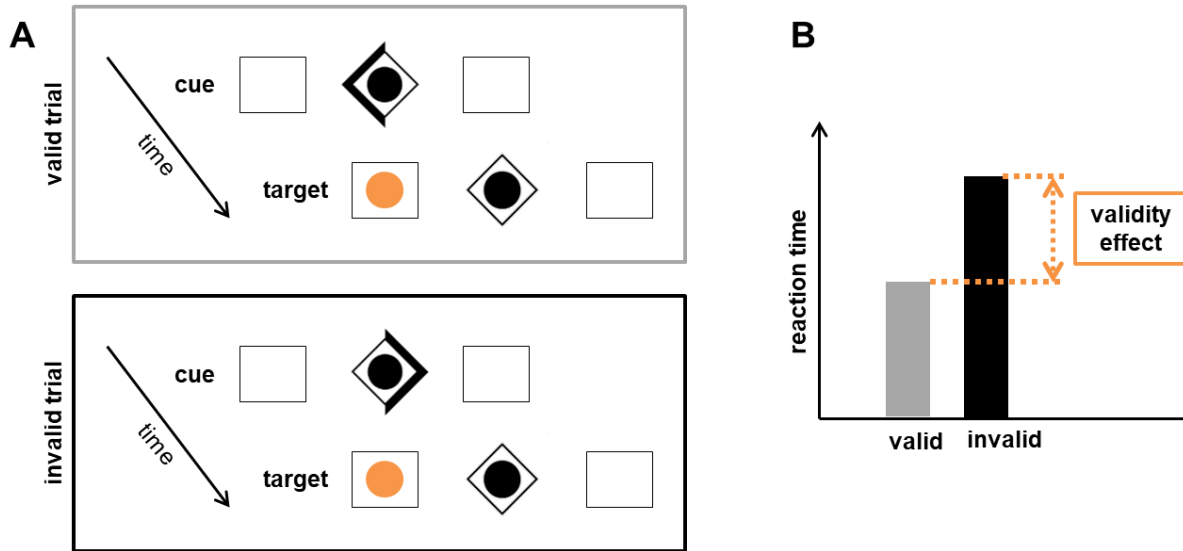


Figure 1.1 Illustration of a classical Posner-cueing paradigm (A) and the validity effect (B)

By using modifications of the classical cueing paradigm, reorienting of attention and probabilistic inference can be investigated within the same task. In classical versions of the Posner task, the percentage of cue validity (%CV) (i.e., the proportion of valid and invalid trials determining the probability that the cue will be valid in a given trial) is kept constant. However, if the percentage of cue validity (%CV) is manipulated throughout the experiment and the participants have to infer the actual %CV level, probabilistic inference can be assessed. Therefore, in cueing paradigms, probabilistic inference equals the learning of cue-target outcomes. While reorienting of attention is reflected in the VE, probabilistic inference can be represented by parameters of computational learning models (e.g., Mengotti et al., 2017; Vossel, Mathys, et al., 2014), weights of regression analyses (how much RTs vary with %CV) or the explicit estimation of the %CV itself.

Previous studies have shown that the VE scales with the proportion of valid to invalid trials, regardless if this is explicitly signaled or not (Dombert, Kuhns, et al., 2016; Kuhns et al., 2017; Mengotti, Kuhns, et al., 2020; Vossel, Mathys, et al., 2014). Attentional gradient models explain this effect by differential resource distributions, since an environment with highly valid cues leads to more costs in case of reorienting (Madden, 1992).

Moreover, it should be noted that the cognitive processes of reorienting and probabilistic inference are not just limited to visuospatial attention, but can also be expanded to feature-

1. General Introduction

based, as well as motor-intentional attention (Dombert, Kuhns, et al., 2016; Kuhns et al., 2017; Mengotti, Kuhns, et al., 2020). Feature-based attention describes in this context the reorienting and probabilistic inference related to a specific feature of a target (e.g. color), whereas motor-intentional attention refers to the required motor response of a target (e.g. button press). Since expectancies about features of a target or about required motor responses speed reaction times similar to expectancies about targets location (Egner et al., 2008; Rushworth et al., 2001), reorienting and probabilistic inference of different cognitive subsystems can be assessed by changing the cue type in the previously described cueing paradigm, i.e. predicting a specific feature of a target or a required motor-response instead of the target's location.

1.1.2 Computational Models of Probabilistic Inference

Previous research has shown that computational learning models can be used to describe the cognitive process of probabilistic inference, in particular the updating of beliefs (e.g. Dombert, Kuhns, et al. 2016; Mengotti et al. ,2017; Vossel et al. 2015). The simplest form is the application of a Rescorla-Wagner (RW) learning model. According to the RW model, the update of a belief equals the product of a learning rate and a prediction error, i.e., the difference between the observed and the predicted response (see exact description Figure 1.2A and paragraph 2.2 methods of Experiment1) (Rescorla & Wagner, 1972). Thus, the learning rate defines the influence of prediction errors changing participants' belief from trial to trial. At the same time, it determines to which extent the past influences participants' beliefs because it specifies the steepness of the exponential decay of the influence of preceding trials (Rushworth & Behrens, 2008). Despite the fact that the RW model is a heuristic model, a significant correlation between the RW learning rate and a subject-specific parameter of updating trial-by-trial estimates about %CV in a hierarchical Bayesian model has been found (Vossel, Mathys, et al., 2014).

The very influential hierarchical Bayesian learning model developed by Mathys et al. (2011) extends the simple RW model since it can quantify the impact of volatile environments on

1. General Introduction

individual learning. In volatile environments, e.g. when the %CV is changing unpredictably over time, beliefs are still formed on the basis of past observations. Thus, the proposed model consists of a hierarchy of states with superordinate levels, which determine the corresponding subordinate levels, e.g. trial-wise beliefs about the probability that a cue will be valid are influenced by higher level beliefs about how volatile the environment is perceived. The model is based on analytical trial-by-trial update equations, which are similar to those of a RW learning model (Behrens et al., 2007; Rescorla & Wagner, 1972), to characterize the formation of predictions based on the updating of beliefs about the environmental state of a trial. Furthermore, it comprises fixed parameters to describe interindividual differences in learning by e.g. the precision-weighting of predictions errors (Daunizeau, den Ouden, Pessiglione, Kiebel, Friston, et al., 2010).

The model has been applied to several empirical data to assess trial-by-trial estimates of prediction errors and their precision for the different levels in the hierarchy (Dombert, Kuhns, et al., 2016; Kuhns et al., 2017; Mengotti, Kuhns, et al., 2020; Vossel et al., 2015; Vossel, Mathys, et al., 2014). In those studies, the %CV in cueing paradigms was changing across the experiment block-wise without the participants knowing when and to which degree the %CV would change. The applied model always consisted of three hierarchical levels (see Figure 1.2B): The first level described the observation if it was a valid or invalid trial. Then, the second level represented the changes in %CV over time. The third and highest level estimated the volatility of the %CV changes. Moreover, two individual parameters accounted for the interindividual differences in updating trial-by-trial estimates about %CV and their volatility.

In both models (RW model and hierarchical Bayesian model), additionally to the previously described perceptual models a response model needs to be defined to derive the observed responses (i.e. reaction times) based on the individual beliefs about the %CV. In the presented models the response model assumes a linear relationship between the response speed and the prediction before the observation of the outcome of the trial to map responses to the individual beliefs about the %CV (see Figure 1.2C).

1. General Introduction

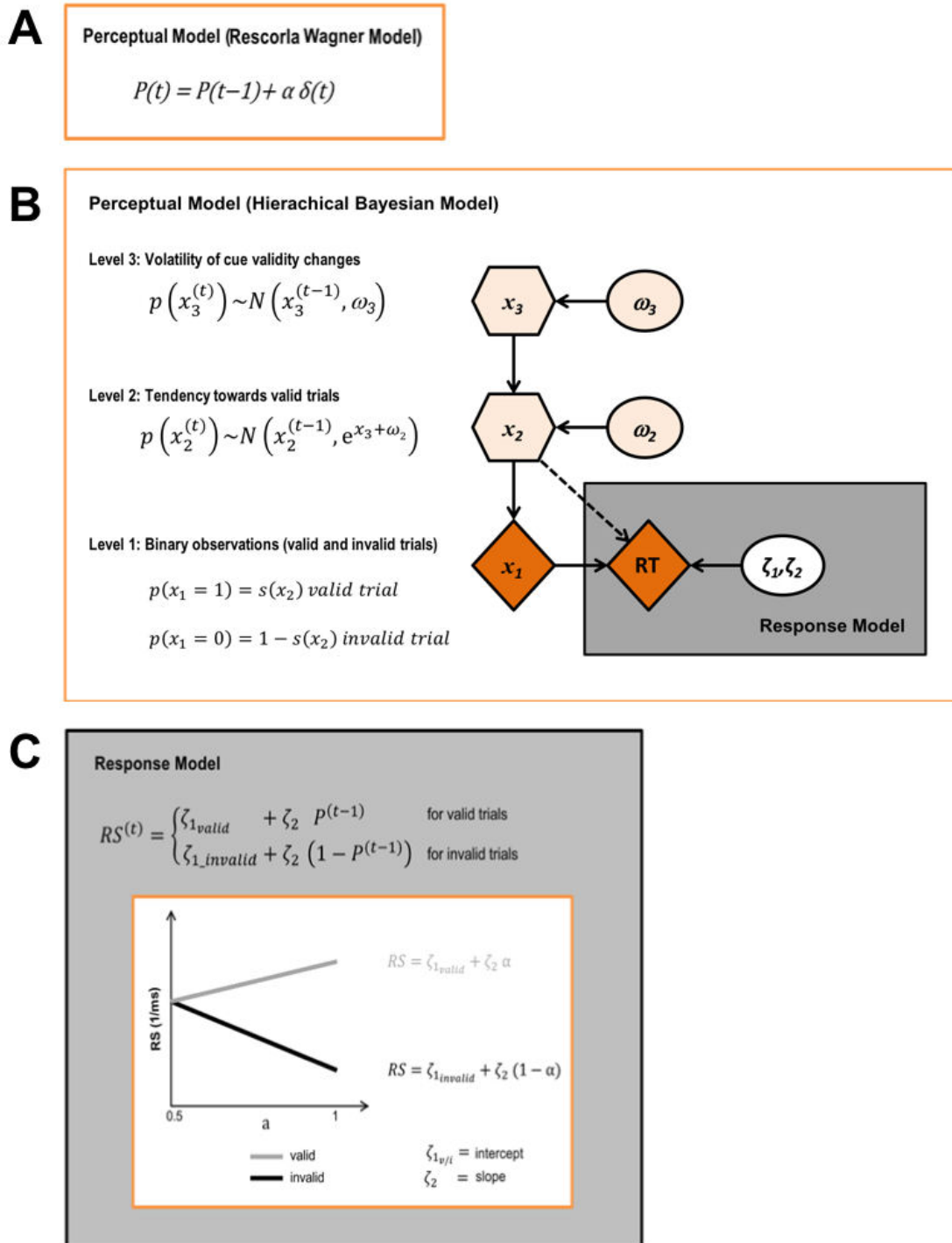


Figure 1.2 Illustration of the Rescorla-Wagner model (A), the hierarchical Bayesian model (B) and the according response model (C)

In summary, the weighting of prediction errors (the discrepancy between observed and predicted responses) by a learning rate defines the updating of beliefs in both models.

1. General Introduction

Whereas the hierarchical Bayesian model is useful in paradigms with a long continuous sequence of trials with volatile changes in the environment, the RW model can still be applied in paradigms with short blocks of trials with a constant environment (and a substantially smaller number of trials entering the modeling) to describe belief updating – a subprocess of probabilistic inference.

1.1.3 Neuroanatomy of Probabilistic Inference

Probabilistic inference is based on multiple sources of information, and correspondingly has different neural correlates depending on where these information are stored in the brain (de Lange et al., 2018). Previous studies in healthy participants have already combined computational modeling with fMRI to characterize the neural correlates of the modulation of discrete attentional systems by probabilistic inference (Dombert, Kuhns, et al., 2016; Kuhns et al., 2017; Vossel et al., 2015). They discovered a relationship between some nodes from the dorsal and ventral attention networks and the cognitive process of probabilistic inference. These two networks are also responsible for the flexible control of attention (Corbetta & Shulman, 2002; see chapter 1.2.3). Whereas the bilaterally organized dorsal attention network (DAN) comprises the frontal eye fields (FEF) and the intraparietal sulcus (IPS) and is crucial for attentional orienting, the more right-lateralized ventral attention network (VAN) consists of the temporoparietal junction (TPJ) and the ventral frontal cortex (VFC) and mediates the reorienting of attention (Corbetta et al., 2008).

Investigating the modulation of spatial attention by probabilistic beliefs using saccadic responses, it was found that the activity of right FEF, TPJ and putamen was particularly modulated during reorienting (Vossel et al., 2015). This result is in line with previous electroencephalography (EEG) research of spatial attention stating that variations of cue probability induce higher effects on attentional reorienting costs than on attentional orienting benefits (Lasaponara et al., 2011).

Due to the fact that preparation of saccades is related to both covert shifts of spatial attention and the preparation of eye movements/motor responses (Deubel, 2008), another

1. General Introduction

study was conducted using manual reaction times (RTs) to differentiate between the effects of probabilistic inference on attention and motor-intention (Kuhns et al., 2017). Here, no common brain structures were found which would relate to the modulation of reorienting by probabilistic inference. However, the involvement of the right TPJ in spatial attention was replicated and it was discovered that activity of the left angular gyrus (ANG) and anterior cingulate cortex (ACC) was modulated by probabilistic inference during motor-intention, respectively. Additionally, connectivity analyses applying psychophysiological interaction analyses revealed that the right hippocampus (HPC) was involved in probabilistic inference-related connectivity alterations (cue-predictability-dependent coupling effects) of all three brain regions. This finding fits to previous research in choice tasks where probabilistic inference-related activity modulation of different brain regions also induced changes of hippocampal activity (Boorman et al., 2016).

Comparing spatial and feature-based attention using manual RTs, probability-dependent attention modulation was associated with activity changes in the (bilateral) precuneus, left posterior IPS, middle occipital gyrus, and right TPJ during spatial attention, and with activity changes in the left anterior IPS during spatial and feature-based attention (Dombert, Kuhns, et al., 2016). No specific modulation of brain regions for feature-based attention was found. Moreover, no significant modulation by probabilistic inference during orienting, as in the previous study on saccadic responses (Vossel et al., 2015), was revealed.

Furthermore, neurostimulation studies have supported these findings by proving a causal involvement of the right TPJ in probabilistic belief updating during spatial attention (Mengotti et al., 2017). Likewise, a causal contribution of the IPS in updating information in a sustained attention task (Leitao et al., 2015) has been demonstrated.

Taken together, these studies have demonstrated that probabilistic inference can discretely affect attentional domains and that common neural substrates exist for some domains, namely the left IPS for spatial and feature-based attention and the right HPC for spatial attention and motor-intention. However, there are no patient studies yet systematically investigating probabilistic inference in different attentional domains and validating these

1. General Introduction

findings. Lesion studies have the advantage that they provide a more causal investigation of the relationship between brain and behavior compared to correlational fMRI in healthy participants. Hence, it still remains to be investigated how the lesioned brain performs the deployment of attention modulated by probabilistic inference and which lesion patterns might be responsible for common and distinct deficits of this cognitive process in different attentional domains.

1.2 (Visuo-)spatial Neglect

1.2.1 Clinical Symptoms

Spatial neglect is a heterogeneous syndrome comprising various symptoms related to impairments of spatial cognition observed after focal brain damage, especially stroke (Li & Malhotra, 2015). The most common disability is the neglect of contralesional stimuli in multiple sensory modalities (Bisiach et al., 1986; Husain & Rorden, 2003; Robertson & Halligan, 1999). Since neglect cannot be attributed to a failure of the sensory systems (e.g., hemianopia), it is often regarded as an attentional disorder. Depending on the spatial bias, diverse subtypes of neglect can be classified, e.g. sensory-attentional, motor-intentional and representational neglect, ego- and allocentric neglect, personal, peri- and extrapersonal neglect (Rode et al., 2017). Neglect can be diagnosed by using simple paper-pencil tests, e.g. cancellation tasks (Azouvi et al., 2002) (see Figure 1.3), functional tasks (Azouvi, 2017), more advanced computer tasks (Rengachary et al., 2009) or virtual reality tasks (Pedroli et al., 2015). Regarding the occurrence, it has been shown that neglect is more frequently observed and severe after right hemispheric lesions (Karnath & Rorden, 2012), although it can also result after left hemispheric ones (Beume et al., 2017). Despite the spontaneous recovery in the acute phase, approximately 40% of patients suffer from persisting symptoms (Nijboer et al., 2013). Therefore, due to the resulting impairments in the activities of daily living, neglect adversely affects recovery after stroke (Barker-Collo et al., 2010; Rengachary et al., 2011).

1. General Introduction

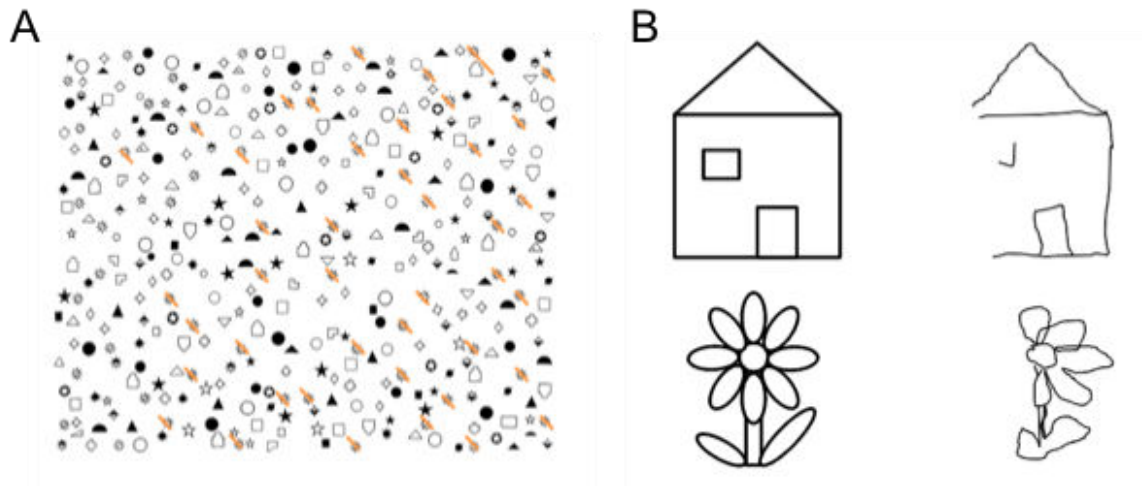


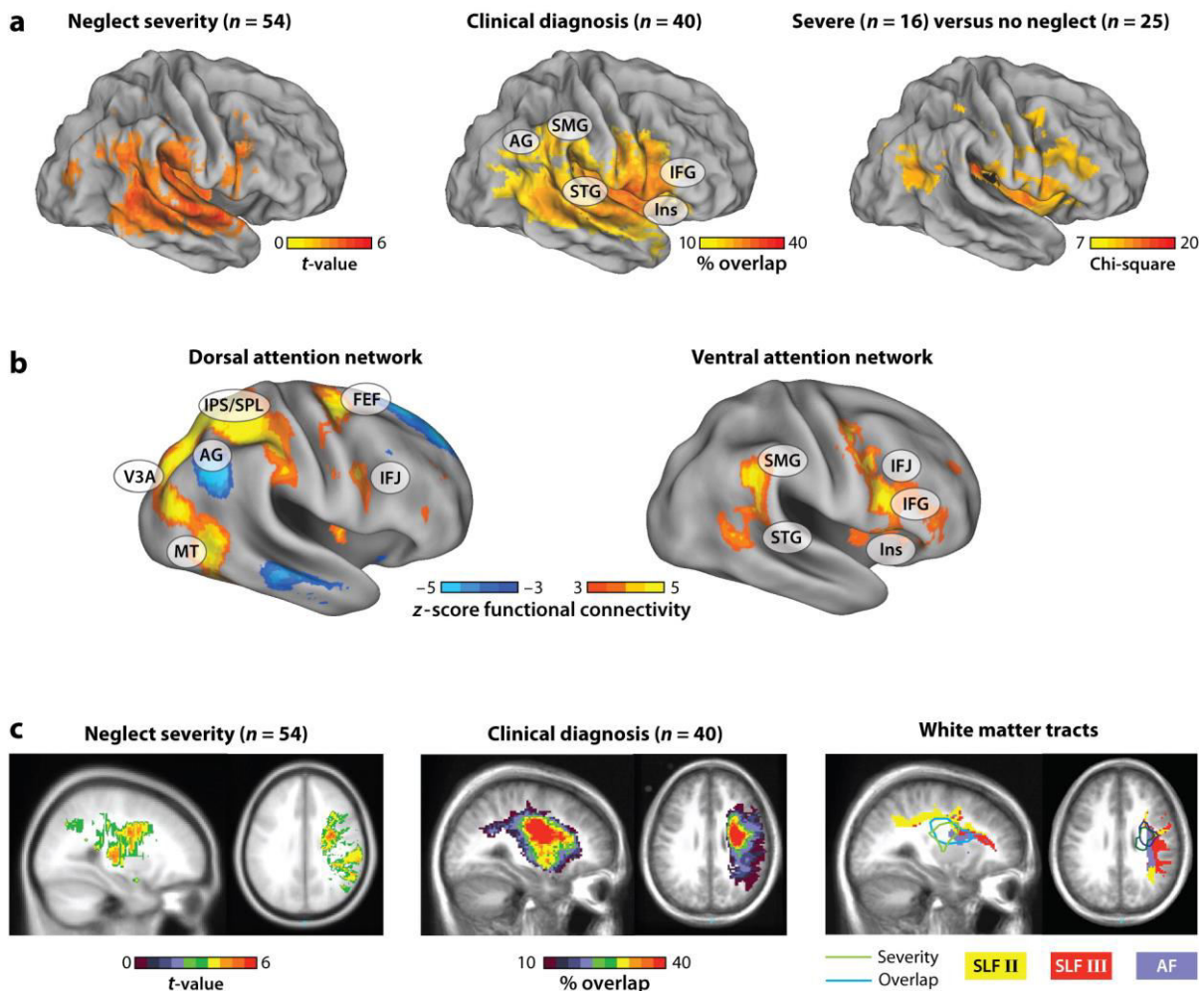
Figure 1.3 Schematic illustrations of neglect symptoms in a cancellation task (A) and a copying task (B)

1.2.2 Neuroanatomy

Historically, lesions to the posterior parietal cortex have been related to spatial neglect (Heilman & Watson, 1977; Vallar & Perani, 1986). However, various studies have shown that there is not one critical lesion location that is responsible for the development of the spatial neglect syndrome (Chechlacz et al., 2012; Rode et al., 2017; Vuilleumier, 2013). In line with the variety of behavioral symptoms, heterogeneous lesion patterns are associated with differing behavioral impairments (see Figure 1.4): Cortical lesions of the TPJ, including inferior parietal lobule (IPL), supramarginal gyrus (SMG) and ANG, the superior temporal gyrus (STG), the middle and inferior frontal cortex as well as subcortical lesions affecting the basal ganglia and parts of the thalamus are related to neglect (Karnath & Rorden, 2012; Thiebaut De Schotten et al., 2014; Vuilleumier, 2013). Further, it has been shown that disconnections of white matter pathways, especially of the second and third branch of the superior longitudinal fasciculus (SLF II and III), the arcuate fasciculus (AF), the inferior longitudinal fasciculus (ILF) and the inferior occipitofrontal fasciculus (IFOF), play an essential role for the spatial neglect syndrome (Carter et al., 2017; Herbet et al., 2017; Lunven et al., 2015; Thiebaut De Schotten et al., 2014; Toba et al., 2020; Vaessen et al., 2016). Moreover, recent evidence also states the importance of interhemispheric

1. General Introduction

connections, in particular as a predictor for the chronicity of the symptom (Lunven & Bartolomeo, 2017; Nyffeler et al., 2019).



Corbetta M, Shulman GL. 2011. *Annu. Rev. Neurosci.* 34:569–99

Figure 1.4 Relationship between anatomical distribution of lesions associated with neglect, attentional networks, and damage to fiber tracts. a) Anatomical regions associated with neglect, as shown by lesion-symptom mapping (left panel), overlap of lesions in patients diagnosed with neglect (middle panel), and comparisons of groups of patients with severe neglect vs. no neglect (right panel). b) The dorsal (left panel) and ventral (right panel) attention networks as determined by resting-state functional connectivity in 25 healthy controls. c) Slice representations from the anatomical distributions of A) (left and middle panel) and white matter tracts corresponding to the arcuate fasciculus (AF) and superior longitudinal fasciculus (SLF) II and III, as determined by diffusion tensor imaging (DTI) in 30 healthy controls (right panel). (this figure is reproduced with permission of Annual Reviews Inc. and was published in Corbetta et al. 2011).

1. General Introduction

1.2.3 Cognitive Models of Spatial Neglect

There are several cognitive models of spatial attention which try to explain the neglect syndrome. One of the most influential theories was proposed by Posner et al. (1984) postulating that covert shifts of attention rely on three mental actions: (1) the disengagement of attention from a stimulus, (2) the shift of attention to a target and (3) the engagement of attention to the target. In case of the neglect syndrome, this theory postulates that lesions of the parietal lobe mainly lead to a disengagement deficit resulting in increased reaction times or a failure to respond to invalidly cued contralesional targets.

Another account to explain spatial neglect is the “hemispatial” theory proposing that the right hemisphere (RH) is responsible for allocating spatial attention to both hemispaces, whereas the left hemisphere (LH) allocates attention only to the contralateral hemispace (Heilman & Van Den Abell, 1980; Mesulam, 1981). Therefore, damage to the RH would lead to spatial neglect of the left hemispace since the LH would not be able to compensate.

The “interhemispheric competition” theory postulates that both hemispheres allocate attention to the contralateral hemispace and that the balance is maintained through interhemispheric inhibition (Kinsbourne, 1977). The LH is supposed to create a stronger contralateral bias compared to the RH, leading to an increase imbalance if damage occurs. This matches a modern view focusing on evolutionary factors, stating a predominant role of the RH in attentional processing. Here the LH is thought to process familiar events and the RH unexpected and possibly threatening, therefore behaviorally more relevant stimuli (Bartolomeo & Seidel Malkinson, 2019). Furthermore, this assumption is in line with the fact that neglect occurs more frequently after damage to the RH (Karnath & Rorden, 2012). Furthermore, supporting this competition theory, Vuilleumier et al. (1996) observed a single case where a patient exhibited the neglect syndrome after a stroke affecting the RH (in particular the angular gyrus), which was ameliorated by a second stroke of the LH (in particular the frontal eye fields).

1. General Introduction

However, this theory has also been challenged by a functional magnetic resonance imaging (fMRI) study of RH damaged patients with and without neglect investigating the specificity of the hemispheric imbalance for neglect (Umarova et al., 2011).

A more recent approach emphasizes that spatial attention is regulated by two distinct neural networks and neglect is related to a dysfunction of these networks (Bartolomeo et al., 2012; Corbetta & Shulman, 2011). The DAN, consisting of the FEF and the IPS, mediates attentional orienting and is considered to be bilaterally organized (Corbetta & Shulman, 2002). The VAN, comprising the TPJ and VFC, promotes the detection of unexpected stimuli and reorienting of attention and is regarded more right-lateralized (Corbetta et al., 2008). As stated, both systems are specialized for distinct attentional subprocesses (see Figure 1.5). Hence, their dynamic interplay is essential for the flexible control of attention (Vossel, Geng, et al., 2014). Furthermore, these networks control spatial attention across various sensory modalities (Macaluso, 2010), although most research has been done in the domain of visuospatial attention.

Initially, the DAN and VAN model was based on results from task-based fMRI studies in healthy participants, however the two networks have also been revealed in resting-state fMRI studies (Fox et al., 2006; He et al., 2007). The white matter pathways SLF (Thiebaut de Schotten et al., 2011), and parietal inferior-to-superior tract (PIST; Catani et al., 2017) connect both networks structurally.

It was found that neglect is mainly associated with structural damage to the VAN, although behavioral deficits relate more to the DAN (Corbetta & Shulman, 2011). This controversial finding can be explained by the strong interconnections of both networks. Thus, structural damage of the VAN indirectly induces dysfunction of the DAN (Corbetta et al., 2005; He et al., 2007). In line with this, damage to SLF, connecting VAN and DAN, has been shown to be a good predictor for spatial neglect (Lunven et al., 2015; Ramsey et al., 2017; Thiebaut De Schotten et al., 2014). Moreover, to support this assumption, it was found that non-invasive brain stimulation of these structurally intact but functionally impaired regions can

1. General Introduction

ameliorate the spatial bias in patients suffering neglect (Nyffeler et al., 2019; Sparing et al., 2009).

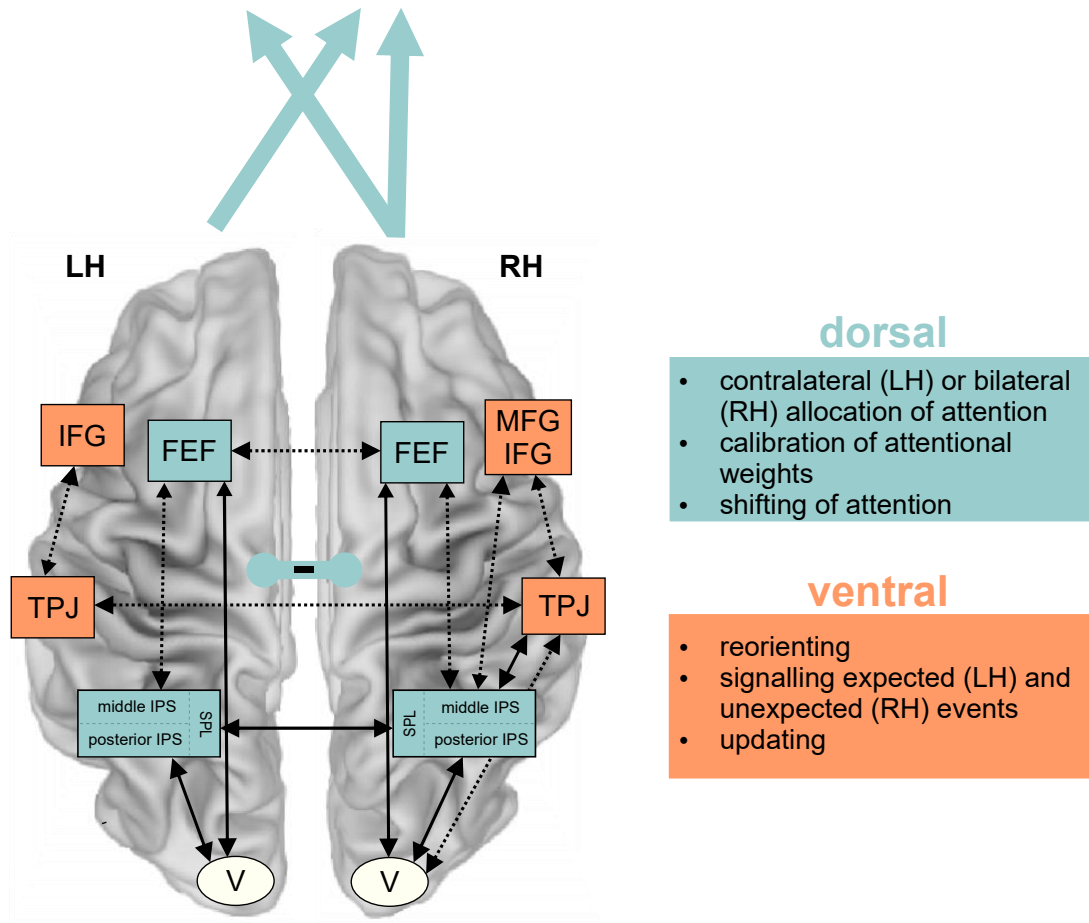


Figure 1.5 Schematic illustration of the central nodes of the dorsal (light blue) and ventral (orange) attention systems. Bidirectional arrows exemplarily depict connections between the nodes. Solid lines depict connections for which there is evidence both from correlational (e.g., fMRI) and causal techniques (e.g., TMS). Dotted lines depict connections with evidence from correlational techniques only. Visual areas are depicted in white. Blue arrows illustrate the organization of the allocation of attention by the dorsal system according to the hemispatial theory, whereas the blue interhemispheric connection indicates interhemispheric inhibition. LH: left hemisphere; RH: right hemisphere; IFG: inferior frontal gyrus; MFG: middle frontal gyrus; FEF: frontal eye fields; TPJ: temporoparietal junction; IPS: intraparietal sulcus; SPL: superior parietal lobe; V: visual cortex. (this figure is reproduced with permission of Elsevier and was published in Mengotti, Käsbauer, et al., 2020).

1. General Introduction

Nevertheless, neglect symptoms can also result from focal lesions to the IPS (Gillebert et al., 2011) or damage to regions of the DAN (Pedrazzini et al., 2017; Ptak & Schnider, 2010) highlighting the importance of both networks for proper functioning. Furthermore, this is supported by studies investigating the functional connectivity (FC) of both networks in stroke patients revealing a relationship between neglect symptoms and a reduced interhemispheric FC, in particular of the DAN (Baldassarre et al., 2014; Carter et al., 2010; He et al., 2007; Ramsey et al., 2016; Siegel et al., 2016). Additionally, recovery of attentional functions was related to a restoration of previously depressed interhemispheric FC (He et al., 2007; Ramsey et al., 2016; Umarova et al., 2016).

1.2.4 Probabilistic Inference, Updating and the Spatial Neglect Syndrome

Although many neuroimaging findings support the proposed neuroanatomical model of attention by Corbetta and colleagues (Corbetta et al., 2005; Corbetta & Shulman, 2011; He et al., 2007), there is also evidence that this model might not account for the whole complexity of the neglect syndrome. In particular, the fact that neglect patients exhibit many non-spatial deficits challenges the traditional view of a spatial attention disorder.

Corbetta and colleagues (2008) already raised some concerns themselves whether the TPJ, a major node of the VAN, is exclusively responsible for the function of attentional reorienting or might play a more general role. Further, this idea has been supported by more recent research (Danckert et al., 2012; Geng & Vossel, 2013) proposing an advanced model of neglect as a more general disorder of representational updating (Filipowicz et al., 2016; Shaqiri et al., 2013; Stöttinger et al., 2014, 2018).

According to this new approach, representational updating describes the ability to generate mental models of the environment and to update these in relation to occurring change. Furthermore, this ability depends on subprocesses of priming, working memory and statistical learning (Shaqiri et al., 2013).

Historically, Bisiach and Luzzatti (1978) were one of the first to show that neglect patients suffer from representational deficits since they displayed neglect of features for mental

1. General Introduction

imaginings of locations. Additionally, it has been shown that neglect patients exhibit many non-spatial symptoms: They are also impaired in non-spatial sustained attention (Bartolomeo et al., 2012; Husain & Rorden, 2003; Robertson et al., 1998), working memory (Danckert & Ferber, 2006; Striemer et al., 2013), temporal estimation (Danckert et al., 2007; Merrifield et al., 2010) and show a prolonged attentional blink (Husain et al., 1997).

Moreover, although color priming in neglect patients is preserved, they demonstrate deficits in location priming (Kristjánsson et al., 2005; Shaqiri & Anderson, 2012, 2013). This can be linked to results in healthy participants indicating that especially the RH and frontal and inferior parietal areas of the brain are related to priming (Kristjánsson et al., 2007) and neglect patients often exhibit lesions of these areas (Corbetta & Shulman, 2002).

Furthermore, statistical learning, the implicit learning of regularities of the environment (Aslin & Newport, 2012), seems to be impaired to some extent in neglect patients. First, preserved abilities (Geng & Behrmann, 2002, 2006) were found in a simple search task. However, this result was questioned and could not be reproduced (Walthew & Gilchrist, 2006). More recent studies detected deficits for statistical learning in RH neglect patients, although deficits were to some extent also present in RH patients without neglect symptoms (Shaqiri & Anderson, 2012, 2013). In addition, the importance of the RH for statistical learning is further supported by results from split-brain patients (Roser et al., 2011). Statistical learning is crucial for the cognitive process of probabilistic inference since updating processes can only be performed sufficiently if the detection of the environmental regularities is intact.

In conclusion, all these non-spatial deficits in neglect patients can be related to the more general failure to update the mental models and beliefs of the changing environment, hence also the cognitive process of probabilistic inference.

So far, only a small amount of studies has investigated probabilistic inference, in particular the updating of mental models, in neglect patients. However, the results are not yet conclusive and have not purely focused on probabilistic inference in the visuospatial attention domain. Danckert and colleagues (2012) found that RH patients performed worse than LH patients in the children's game "rock, paper, scissors" against a computer opponent

1. General Introduction

which covertly altered its strategy. Severe impairment was not present in neglect patients per se and it was rather related to lesions of the insula and putamen. Applying the same task to a different sample of RH and LH patients, it was found that RH and LH patients were similarly impaired, although the authors propose different reasons for the deficits. Deficits in LH patients were supposed to be caused by working memory damage, while in RH patients by the general impaired updating of the belief about the opponent's strategy (Stöttinger et al., 2014). In the same study, an additional task was conducted where updating performance was assessed with a picture morphing task. There, RH patients performed again worse than LH patients and low performance was again related to insula damage (Stöttinger et al., 2014, 2018). Furthermore, investigating the neural correlates of this task in healthy participants showed that activity of a network comprising insula, medial and inferior frontal regions and the inferior parietal cortex was associated with updating behavior (Stöttinger et al., 2015). A recent review further suggests that these regions are involved in a potential RH dominant network mediating the updating of mental models, hence also the cognitive process of probabilistic inference. Accordingly, a current model of a person is maintained in the anterior insula. The IPL supposedly compares new information with the predictions generated by the model, and the medial PFC, including the ACC, explores alternative models (Filipowicz et al., 2016).

Since IPL and TPJ overlap and are not easy to distinguish (Igelström & Graziano, 2017), the proposed view fits to existing results of the involvement of right TPJ in updating (Mengotti et al., 2017) and its function of matching expected and unexpected events (Doricchi et al., 2010).

Importantly, although the cognitive function of updating is impaired in some patients, it is not completely abolished. Single case studies have proven that neglect patients can perform the desired response, they just need more resources (e.g. more time or information) (Shaqiri & Anderson, 2012). Hence, training neglect patients in the subprocesses (i.e. statistical learning) or the main process of updating or probabilistic inference can be seen as a new rehabilitation approach (Shaqiri et al., 2013).

1. General Introduction

Nonetheless, more systematic patients studies are needed to gain a deeper understanding of the relationship of neglect, the contribution of the two hemisphere, updating and probabilistic inference.

1.3 Functional Neuroimaging Approach

1.3.1 Physical and Physiological Background

Magnetic resonance imaging (MRI) is a non-invasive technique to image the structure and function of the human brain in vivo. Historically, it was first discovered in 1970s (Lauterbur, 1973). It is based on the principle that every human cell contains hydrogen nuclei with protons with a spin property and a magnetic moment. By manipulating the orientation of the hydrogen nuclei, an image can be created as followed. In an external magnetic field, these hydrogen nuclei become aligned towards the direction of the field and precess with a frequency which is proportional to the strength of the field. By applying a radiofrequency (RF) pulse, the hydrogen nuclei become excited and their orientation of the magnetic moment is changed (if the frequency of the RF pulse equals the frequency of the nuclei). By terminating the RF pulse, the hydrogen nuclei return to their original state (a process termed relaxation) and emit the energy of the RF pulse. The emission can be measured with coils and translated into images. Due to the fact that different brain tissues (i.e. grey matter, white matter and cerebrospinal fluid) have differing relaxation properties, images with tissue-specific contrasts can be generated (Horowitz, 1995; Jezzard & Clare, 2001).

Besides the possibility of imaging the structural formation of the brain, MRI also contributes to the investigation of the functional organization of the brain (Raichle, 2003).

1.3.2 Functional Magnetic Resonance Imaging

Functional magnetic resonance imaging (fMRI) employs the MRI technique to examine brain functions based on the assumption that active neurons cause an increase in metabolic activity which leads to a regional change of blood flow and oxygenation in the brain. This

1. General Introduction

change can be measured using the blood oxygen level-dependent (BOLD) effect to indirectly assess brain activity. The BOLD effect is based on the principle that hemoglobin has different magnetic properties according to its level of oxygenation. Oxygenated hemoglobin is diamagnetic and therefore increases the MR signal, while deoxygenated hemoglobin is paramagnetic leading to inhomogeneity of the MR signal (Kim & Ogawa, 2012; Kwong et al., 1992; Ogawa et al., 1990). The time course of the BOLD signal is termed haemodynamic response function (HRF) (Aguirre et al., 1998). Combined imaging and intracortical recordings in monkeys have confirmed a high correlation between the HRF and local field potentials (Logothetis, 2002; Logothetis & Pfeuffer, 2004). Therefore, fMRI indirectly enables inferences which brain regions are involved in a particular task (Fellows et al., 2005).

1.3.3 Resting-state fMRI

There are different types of fMRI studies to investigate the brain-function relationship: task-based and task-independent (so called resting-state) fMRI studies. In task-based fMRI studies, the difference between an experimental task of interest relative to a control condition is investigated (Gusnard & Raichle, 2001).

However, in resting-state fMRI studies, participants are at rest and not engaged in any task. In most studies, they are just instructed to keep their eyes open so that they do not fall asleep. Here, the functional organization of the brain can be studied by investigating the functional connectivity (FC) of brain regions (Yeo et al., 2011). FC can be defined as the temporal dependency between spatially remote neurophysiological events (Friston, 2011). Hence, functional brain networks can be revealed by analyzing spontaneously correlated low-frequency (0.01–0.08 Hz) activity fluctuations across the brain (Biswal, 2012; Biswal et al., 1995). There are several methods to investigate FC. Most commonly used are seed-based (see Figure 1.6), model-free (e.g. like independent component analysis) or network analysis (e.g. graph theory) approaches (Smitha et al., 2017). The connectivity patterns of regions forming a network at rest are similar to those during task-related activity (Fox et al.,

1. General Introduction

2006; Hampson et al., 2006). Moreover, these findings also relate to the structural connectivity of the respective brain regions (Greicius et al., 2009; Honey et al., 2009).

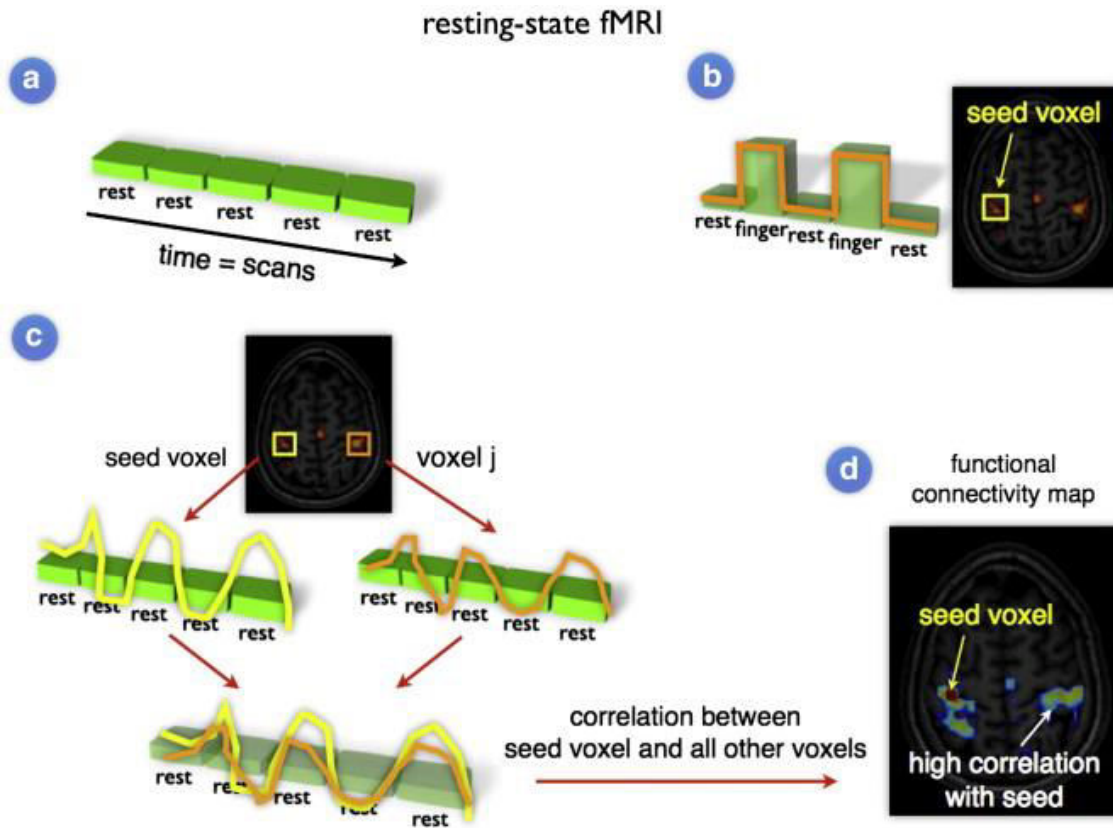


Figure 1.6 Resting-state fMRI studies are focused on measuring the correlation between spontaneous activation patterns of brain regions. Within a resting-state experiment, subjects are placed into the scanner and to think of nothing in particular, without falling asleep. Similar to conventional task-related fMRI, the BOLD fMRI signal is measured throughout the experiment (panel a). Conventional task-based fMRI can be used to select a seed region of interest (panel b). To examine the level of functional connectivity between the selected seed voxel i and a second brain region j (for example a region in the contralateral motor cortex), the resting-state time-series of the seed voxel is correlated with the resting-state time-series of region j (panel c). A high correlation between the time-series of voxel i and voxel j reflects a high level of functional connectivity between these regions. Furthermore, to map out all functional connections of the selected seed region, the time-series of the seed voxel i can be correlated with the time-series of all other voxels in the brain, resulting in a functional connectivity map that reflects the regions that show a high level of functional connectivity with the selected seed region (panel d). (this figure is reproduced with permission of Elsevier and was published in van den Heuvel & Hulshoff Pol 2010).

1. General Introduction

Furthermore, patient studies have demonstrated that resting-state FC networks become altered in the presence of diseases (e.g. Siegel et al., 2016) as well as during healthy aging (Wu et al., 2007). Hence, resting-state fMRI is a powerful tool to gain a better understanding of the functional connections of the brain and how these connections change in disease as well after therapy (Varsou et al., 2014).

To examine the link of brain and behavior with this approach, correlations can be used to relate behavioral differences to different patterns of functional connectivity between brain regions across participants (Baldassarre et al., 2012; Hampson et al., 2006; Lewis et al., 2009; Rosenberg et al., 2016).

1.4 Brain-lesion Approach

Before functional imaging was established, lesion analyses were the only approach available to assess brain-function relationships. In contrast to fMRI in healthy participants, i.e. the non-invasive correlational neuroimaging approach, lesion studies allow a more causal investigation of the link between brain and behavior. However, both kinds of studies share the issues of interindividual differences in the neuroanatomical organization of the brain and that a single cognitive process cannot be assigned to a single brain region (Fellows et al., 2005).

Historically, (single) case studies of patients with acquired brain damage have provided first evidence for the function of brain regions (e.g. Broca, 1861). Subsequently, group studies of brain-lesioned patients investigating particular cognitive functions with experimental tasks have then expanded the general knowledge about which neural correlates underlie those functions. Group studies are particular useful, since lesions of patients are rarely restricted to a single region of interest (ROI), and as mentioned before the distribution of brain regions underlying cognitive processes differs between individuals (Robertson et al., 1993).

Nonetheless, all lesion studies rely on the assumption that distinct brain structures are fundamental to perform a specific cognitive function and that damage to these structures

1. General Introduction

leads to an impairment of behavior and this cognitive function, respectively. Therefore, they enable to infer which brain regions are relevant and necessary to accomplish a particular cognitive process (Fellows et al., 2005; Rorden & Karnath, 2004). It should be noted, however, that cognitive impairments are often not only due to the local effect of a lesion, but rather to the dysfunction of anatomically intact structures connected to the lesioned area (Bartolomeo, 2011).

Most lesion studies are performed in stroke patients due to the sudden onset of a stroke and its relatively well-demarcated affected brain structures, particular considering the modern imaging and lesion delineation techniques (de Haan & Karnath, 2018). Traumatic head injuries and tumors are less suitable for structure-function inferences, since trauma generally results in diffuse brain damage (Büki & Povlishock, 2006) and tumors affect surrounding brain tissue which complicate precise delineation (Scherer, 1940) and evolve slowly over time leaving sufficient time for the brain to reorganize (Fisicaro et al., 2016).

Lesion-symptom mapping has revolutionized our understanding of the functioning of the human brain. There are different analysis approaches to relate lesion location to performance (de Haan & Karnath, 2018): The simplest approach is a lesion subtraction analysis where two lesion overlap maps for patients showing a cognitive deficit or not are subtracted (Rorden & Karnath, 2004). Another well-established approach is an univariate lesion analysis like voxel-based lesion-symptom mapping (VLSM; Bates et al., 2003). In VLSM, statistical tests on the behavioral scores are performed at each voxel, with groups defined by the presence or absence of damage in each voxel. Thereby, voxels in which damage is associated with a behavioral deficit can be identified. To ensure meaningful statistical inferences, data should be thresholded for a sufficient minimum lesion overlap (e.g. only include voxels affected by a minimum of 10% of patients; see Kimberg et al., 2007) as well as corrected for multiple comparisons (Mirman et al., 2018) and lesion volume (Sperber & Karnath, 2017).

However, since it was discovered that lesions may not be randomly distributed across the brain but follow the underlying vasculature (Mah et al., 2014), new multivariate approaches

1. General Introduction

have been developed to account for the non-independence between voxels (Karnath et al., 2018; Sperber et al., 2019). Multivariate lesion-symptom methods are considered to be superior to univariate methods as they take into account the functional relation between brain areas. However, they cannot overcome all limitations of univariate lesion mapping (Sperber, 2020).

Lesion-symptom methods are powerful tools to study brain functions and their underlying cortical anatomy. However, results are primarily driven by overlapping areas where statistical power is high, (Kimberg et al., 2007). To investigate the impact of lesions beyond the immediate tissue damage, new techniques such as lesion-network mapping have been developed using connectome data (Boes et al., 2015; Foulon et al., 2018; Fox, 2018). Here, a patient's lesion is referenced to an atlas of the structural or functional connections generated from healthy subjects and the tracts and regions affected by the lesion are derived to indirectly estimate the impact of the lesion on the whole brain connectome. By comparing disconnection patterns of patients with and without a symptom of interest, the specificity of disconnection can be assessed. These techniques have the advantage that no direct functional or structural connectivity measurements obtained with fMRI or DTI from the patients are needed since network dysfunction is estimated indirectly. However, Salvaggio et al. (2020) compared these new techniques in stroke patients and found that the indirect estimation of structural connectivity damage successfully predicted behavioral deficits, whereas the indirect estimation of functional disconnection did not. Furthermore, it was revealed that the indirect estimation of functional disconnection was not equivalent to the direct functional connectivity measurements for predicting behavioral deficits. Hence, these novel techniques should be further investigated and applied with care, although they especially highlight the impairments beyond the lesion that have been underrepresented in the endeavor to map the structure and function of the brain.

2. Empirical Section

2.1. Objectives of the Thesis

The present thesis aimed at investigating the mechanisms underlying probabilistic inference in the healthy and the lesioned human brain. The empirical section will describe two experiments which have been conducted to address the following research questions:

1. Does the resting-state fMRI pattern of regions from the dorsal and ventral attention networks relate not only to reorienting of attention but also probabilistic inference (Experiment 1)?
2. Which impairments of probabilistic inference in the domain of visuospatial attention are exhibited by stroke patients, especially those showing the neglect syndrome (Experiment 2a)?
3. Do stroke patients exhibit impairments of probabilistic inference in other cognitive domains such as feature-based attention and motor-intention, and are such impairments related to differing lesion patterns (Experiment 2b)?

Declaration of Authorship

Both experiments were conducted in collaboration with co-authors. The author of the present thesis essentially contributed to the operationalization of the experiments, to the collection and analysis of the data, as well as to the writing of the paper.

Note

In Experiment 1 the term belief updating will be used corresponding to probabilistic inference.

2.2 Experiment 1: Computational Modeling and Resting-state fMRI Experiment with Healthy Participants

Käsbauer AS., Mengotti P., Fink G.R., Vessel S.(2020). Resting-state Functional Connectivity of the Right Temporoparietal Junction Relates to Belief Updating and Reorienting during Spatial Attention. *J Cogn Neurosci*, 32(6),1130-1141.

(Reprinted from Journal of Cognitive Neuroscience, 32(6), Resting-state Functional Connectivity of the Right Temporoparietal Junction Relates to Belief Updating and Reorienting during Spatial Attention, 1130-1141, Copyright 2020, with permission of MIT Press.)

Resting-state Functional Connectivity of the Right Temporoparietal Junction Relates to Belief Updating and Reorienting during Spatial Attention

Anne-Sophie Käsbauer^{1,*}, Paola Mengotti¹, Gereon R. Fink^{1,2}, Simone Vessel^{1,3}

¹Cognitive Neuroscience, Institute of Neuroscience & Medicine (INM-3), Research Centre Juelich, 52425 Juelich, Germany

²Department of Neurology, Faculty of Medicine and University Hospital Cologne, University of Cologne, 50937 Cologne, Germany

³Department of Psychology, Faculty of Human Sciences, University of Cologne, 50923 Cologne, Germany

***Corresponding author:**

Anne-Sophie Käsbauer

Cognitive Neuroscience, Institute of Neuroscience and Medicine (INM-3)

Research Centre Juelich,

Leo-Brandt-Str. 5, 52425 Juelich, Germany

Email: a.kaesbauer@fz-juelich.de

Conflict of Interest

The authors declare no competing financial interests.

Acknowledgments

This work was supported by funding from the Federal Ministry of Education and Research to SV (BMBF, 01GQ1401). We are grateful to our colleagues from the INM-3 and INM-4 for valuable support and discussions.

2. Empirical Section

Abstract

Although multiple studies characterized the resting-state functional connectivity (rsFC) of the right temporoparietal junction (rTPJ), little is known about the link between rTPJ rsFC and cognitive functions. Given a putative involvement of rTPJ in both reorienting of attention and the updating of probabilistic beliefs, this study characterized the relationship between rsFC of rTPJ with dorsal and ventral attention systems and these two cognitive processes.

Twenty-three healthy young participants performed a modified location-cueing paradigm with true and false prior information about the percentage of cue validity to assess belief updating and attentional reorienting. Resting-state fMRI was recorded before and after the task. Seed-based correlation analysis was employed, and correlations of each behavioral parameter with rsFC before the task, as well as with changes in rsFC after the task, were assessed in an ROI-based approach.

Weaker rsFC between rTPJ and right intraparietal sulcus before the task was associated with relatively faster updating of the belief that the cue will be valid after false prior information. Moreover, relatively faster belief updating, as well as faster reorienting, were related to an increase in the interhemispheric rsFC between rTPJ and left TPJ after the task. These findings are in line with task-based connectivity studies on related attentional functions and extend results from stroke patients demonstrating the importance of interhemispheric parietal interactions for behavioral performance. The present results not only highlight the essential role of parietal rsFC for attentional functions but also suggest that cognitive processing during a task changes connectivity patterns in a performance-dependent manner.

Keywords: resting-state networks; fMRI; attention; cue validity; learning rate.

2. Empirical Section

Introduction

The analysis of functional connectivity in resting-state fMRI time series has proven to be a useful approach to investigate the functional organization of the brain (Yeo et al., 2011). In resting-state functional connectivity (rsFC) studies, participants are not engaged in any particular task during data acquisition, and functional brain networks are revealed, for example, by analyzing spontaneously correlated low-frequency activity fluctuations across the brain (Biswal et al., 1995). Regions forming a network at rest also show similar connectivity patterns during task-related activity (Fox et al., 2006; Hoffstaedter et al., 2014)—and these findings also relate to the structural connectivity of the respective brain regions (Greicius et al., 2009; Honey et al., 2009).

In the attention domain, regions that are coactivated in task-related fMRI studies show strong rsFC (Fox et al., 2006). More specifically, the dorsal and ventral attentional networks (Corbetta & Shulman, 2002) can be differentiated based on their resting-state connectivity patterns. Here, the temporoparietal junction (TPJ) is positively connected with the ventral attention network as well as the anterior insula, the dorsolateral PFC, and the midcingulate cortex (Bzdok et al., 2013; Kucyi et al., 2012; Mars et al., 2012). Moreover, these connections are stronger for the right TPJ (rTPJ) than the left TPJ (lTPJ; Kucyi et al., 2012). Additionally, recent evidence suggests that anatomically and functionally distinct rTPJ subregions may exist (Bzdok et al., 2013; Mars et al., 2012). Strong rsFC was found between the lateral anterior PFC and a dorsal rTPJ cluster in the inferior parietal lobule. Conversely, an anterior ventral rTPJ subregion was more strongly connected to the ventral PFC and the anterior insula, and a posterior subregion showed stronger rsFC with the anterior medial PFC and a parietal network (Bzdok et al., 2013; Mars et al., 2012). Similar observations supporting the idea of functionally independent subregions in TPJ were also found for the lTPJ using a multivariate analysis of the BOLD signal (Silvetti et al., 2016).

The TPJ has been associated with a wide range of cognitive functions (see Igelström & Graziano, 2017, for a review), and it is still unclear whether this region mediates a general cognitive process or whether it is involved in multiple domain-specific functions. Distinct

2. Empirical Section

subregions have been postulated to be associated with different functions, with the anterior region being linked to attention processes and the posterior region to social cognition (Bzdok et al., 2013; Krall et al., 2016). As a major node within the ventral attention network, the proposed primary attentional function of the rTPJ is reorienting attention toward unexpected stimuli, that is, acting as a “circuit breaker” for the dorsal top-down attention system consisting of the intraparietal sulci (IPS) and FEFs (Corbetta et al., 2008; Corbetta & Shulman, 2002). However, rTPJ has more recently also been associated with the more general function of “contextual updating” (Doricchi et al., 2010; Geng & Vossel, 2013; Mengotti et al., 2017; Vossel et al., 2015), that is, the ability to update internal models of the current behavioral context for creating appropriate expectations and responses.

It remains to be investigated whether rTPJ subserves both reorienting and updating, respectively, and whether different rTPJ connectivity patterns underlie the two processes. Using modifications of the classical locationcueing paradigm (Posner, 1980), reorienting of visuospatial attention, and belief updating can be investigated within the same task. To this end, the percentage of cue validity (i.e., the proportion of valid and invalid trials) is manipulated throughout the experiment, and the participants have to infer the actual cue validity level (i.e., the probability that the cue will be valid in a given trial). Whereas reorienting is reflected in the RT difference between unexpected and expected target locations, belief updating is assessed by parameters of computational learning models based on single-trial RTs reflecting the adaptation of behavior to the inferred validity of the spatial cue (e.g., Mengotti et al., 2017; Vossel, Mathys, et al., 2014).

Although little is known about the link between TPJ rsFC and cognitive functions, first evidence for a significant relationship between rsFC networks and deficits in reorienting of attention has been provided by studies in stroke patients (Baldassarre et al., 2014; Carter et al., 2010; Corbetta et al., 2015; He et al., 2007; Siegel et al., 2016). For instance, impaired reorienting towards contralesional targets has been related to decreased interhemispheric rsFC of the IPS (Baldassarre et al., 2014; Carter et al., 2010; He et al., 2007) as well as decreased interhemispheric rsFC of the supramarginal gyri (He et al., 2007).

2. Empirical Section

Given that the role of rsFC of rTPJ for the trial-wise updating of probabilistic beliefs has not yet been addressed and that rTPJ is putatively involved in both reorienting of attention and belief updating, this study aimed at characterizing the relationship between rsFC of rTPJ and these two cognitive processes. Task-based fMRI studies employing effective connectivity analyses have shown that connectivity changes between regions of the dorsal and ventral attention network are related to behavioral performance in spatial attention paradigms (Vossel et al., 2012, 2015; Weissman & Prado, 2012; Wen et al., 2012). Effective connectivity between ITPJ and rTPJ has been related to enhanced filtering of distractors (Vossel et al., 2016). Connectivity from rTPJ to the right IPS (rIPS) and from rTPJ to the right inferior frontal gyrus (rIFG) has been associated with reorienting of attention, especially when invalid targets are less expected (Vossel et al., 2012). Moreover, connectivity from rTPJ to FEF has been related to trial-wise belief updating about cue validity in a saccadic version of the location-cueing paradigm (Vossel et al., 2015).

In this study, we asked if reorienting and belief updating are related to rTPJ connectivity patterns at rest before the task—as well as to rsFC changes after the task. We chose an rTPJ seed linked to belief updating based on previous fMRI and TMS work (Mengotti et al., 2017; Vossel et al., 2015). In a first step, we characterized the rsFC pattern of this particular rTPJ region. In a second step, we correlated measures of belief updating and reorienting in a modified location-cueing task with rsFC of this area with dorsal and ventral network nodes before the task and with the rsFC changes from before to after the task. We predicted that the resting-state network architecture of rTPJ with the ventral and dorsal system would be related to behavioral performance, and we explored the specificity of the resulting associations for reorienting and belief updating, respectively.

2. Empirical Section

Methods

Participants

The study was approved by the ethics committee of the German Psychological Society, and written informed consent was obtained from all participants. All procedures in this study followed the Code of Ethics of the World Medical Association (Declaration of Helsinki).

For the resting-state measurements, we recruited 29 healthy volunteers with no history of neurological or psychiatric disorders. They had a normal or corrected-to-normal vision and were naïve to the purpose of the experiment. All participants were right-handed, as assessed with the Edinburgh Handedness Inventory (Oldfield, 1971).

After data acquisition, six participants had to be excluded from further analysis: one because of poor task performance (more than 2 SDs below the mean accuracy of all participants), one for a technical problem with the recording of the manual responses, and four because of excessive head movements ($>1^\circ$ in rotation parameters) during resting-state fMRI. Therefore, the final sample comprised 23 participants (14 women; age range = 20–36 years, mean age = 27 years).

Procedure

The data for this study were derived from a more comprehensive neurostimulation experiment, which consisted of three sessions distributed over 3 days. According to a within-participant crossover design, each participant underwent two experimental sessions preceded by a preparation session. The data collected on the first day consisted of a high-resolution anatomical scan, preparatory measures for the neurostimulation, and practice of the experimental paradigm. In the second and third experimental sessions, active, continuous theta burst stimulation (cTBS) or “sham stimulation” was delivered (note that because of the use of a placebo [sham] coil, the sham stimulation did not involve any magnetic stimulation). In the sham session, the placebo coil was placed over the vertex. Each day started with a resting-state scan (~7 min duration), during which participants had no task apart from maintaining fixation on a central cross. Subsequently, the active motor

2. Empirical Section

threshold was determined to define the intensity of the stimulation, and the stimulation was delivered outside the scanner. After the stimulation (sham or active cTBS), the participant was transported to the scanner, and task-based fMRI (~23 min duration) as well as a second resting-state scan were performed. The task-based fMRI measurements started on average 5.37 min (SD = 43 sec) after the neurostimulation.

For our present research question on the role of rTPJ functional connectivity for belief updating and reorienting, we here exclusively focus on the resting-state scans and behavioral data from the task-based fMRI of the sham session of the study. Given that the sham session could be performed before or after the active cTBS session according to a crossover design, we tested for any session order effects in this data set (see below).

Paradigm during Task-based fMRI

We used a modified version of a location-cueing paradigm with central cueing (Posner, 1980) to assess attentional reorienting and belief updating about cue validity (%CV), as described in the study of Mengotti et al. (2017). Stimuli were presented on a 30-in. LCD screen behind the scanner at a distance of 245 cm. Participants saw the monitor via a movable mirror installed on top of the head coil. As a fixation point during the total duration of the task, a central diamond on a gray background was presented (see Figure 2.1A). In each trial, a spatial cue, consisting of an arrowhead pointing to either the left or right side, appeared for 400 ms to indicate in which hemifield the target would appear. After an 800 ms SOA, two diamonds appeared for 350 ms on the left and right side of the fixation point (5.8° eccentric in each visual field). The target was a diamond with a missing upper or lower corner. Participants had to press a button with the index or middle finger of their right hand to indicate which part of the target diamond (upper or lower corner) was missing. The response mapping was counterbalanced across participants. The intertrial interval was 2000 ms. During each experimental session, participants performed one run of eight blocks. Each block comprised 48 trials, resulting in 384 trials. The percentage of %CV, that is, the ratio of valid and invalid trials, was manipulated between blocks but was kept constant within each

2. Empirical Section

block. %CV within each block amounted to ~90% (87.5%), ~70% (71%), ~30% (29%), or ~10% (12.5%), respectively. In the 30% and 10% CV blocks, the cue was counterpredictive, as the majority of trials were invalid. At the beginning of each block, precise information about the %CV was given. However, in half of the blocks, the given information was false—resulting in misleading prior expectations. In these false blocks, the expected %CV was inverted concerning the true %CV. Participants were not instructed how many blocks were false and how distant the false %CV would be from the true one. They only knew that, in some blocks, false information could be given. Hence, the participants were instructed to use the spatial cues depending on how much they “trust” them and to estimate the true %CV. At the end of each block, participants had to explicitly state their estimated %CV using a 9-point scale ranging from 10% to 90%, as well as the confidence in their rating. For the main trials, RTs and accuracy of the target discrimination were measured. Each participant completed a short practice before each experimental session consisting of two runs: One consisting of one block with a constant true 80%CV and the other comprising three blocks, with two blocks with true and one with false prior information about %CV.

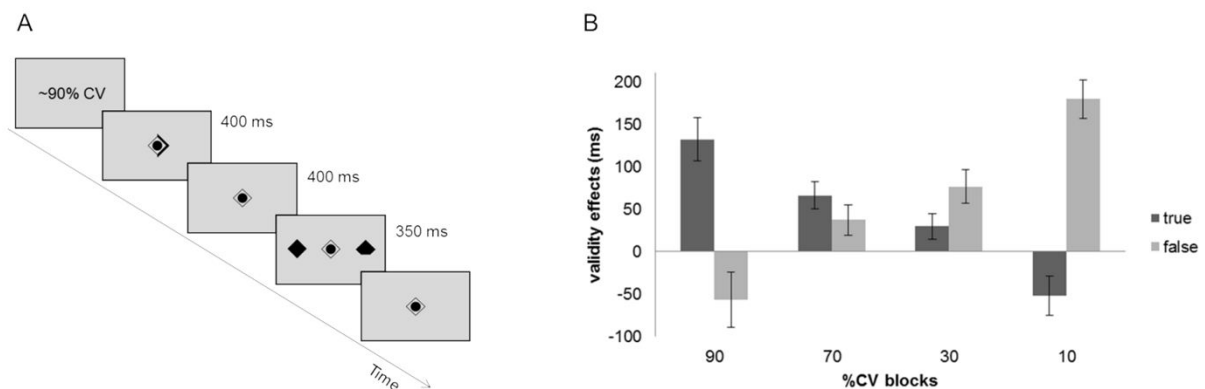


Figure 2.1 A Experimental paradigm with one example trial (valid trial). At the beginning of each block, the %CV (either true or false) was shown. This value was used as prior before the observation of the first trial in the modeling approach. On each trial, participants indicated whether the upper or lower corner of the target was missing. The participants were asked to maintain central fixation throughout the experiment. **B** Validity effects (RT invalid minus RT valid) (mean \pm SEM) for each true and false %CV block. The validity effects vary linearly with actual %CV.

2. Empirical Section

Each participant was presented with the same sequence of trials within each block with two different block sequences for participants. Using constant trial sequences is a standard procedure in computational studies of learning processes that require inference on conditional probabilities in time series (e.g., Daunizeau, den Ouden, Pessiglione, Kiebel, Stephan, et al., 2010; Iglesias et al., 2013). The duration of the paradigm was around 23 min.

Behavioral Data Analysis

Reorienting of Attention - Validity Effects

RTs were measured for each trial to allow an analysis of the behavioral data. Anticipations (RT < 100 ms), misses, and incorrect responses were excluded from the analyses, and mean RT was computed separately for valid and invalid trials.

The above-described paradigm requires the orientation of attention to the most likely target location. In valid trials with %CV > 50%, participants direct their attention covertly to the position indicated by the cue. The validity effect (VE) is the difference in RTs between invalid and valid trials and reflects the time necessary to reorient attention from an expected to an unexpected location (Posner, 1980). However, in the present paradigm, %CV was <50% in some blocks. In these counterpredictive blocks, the target was more likely to appear at the uncued location. To test whether the participants' behavior was affected by the different %CV levels (i.e., if they indeed inferred the actual %CV in the different blocks), the VE was calculated separately for each %CV block (see Figure 2.1B).

For the group-level analyses, averaged blockwise accuracy scores expressed in percentage of correct responses were used in a 2 × 2 within-participant ANOVA with the factors Prior (true, false) and Validity (valid, invalid). Because the manipulation of %CV was expected to mainly influence the speed of responding, mean RTs in each %CV block were subjected to a 2 × 4 × 2 within-participant ANOVA with the factors Prior (true, false), Block (90%CV, 70%CV, 30%CV, 10%CV), and Validity (valid, invalid). Because the blockwise VE was

2. Empirical Section

expected to vary linearly with the actual %CV, a subsequent 2×4 ANOVA on the VE (RT difference between invalid and valid trials) with the factors Prior (true, false) and Block (90%CV, 70%CV, 30%CV, 10%CV) was used. Here, we expected to find a significant linear trend for the Prior \times Block interaction effect, because this would reflect the adaptation of behavior to %CV, that is, inference of the actual %CV levels by the participants. All group-level analyses were performed with SPSS (SPSS Statistics for Windows, Version 25.0, IBM). Results from these analyses are reported at a significance level of $p < .05$ after Greenhouse–Geisser correction where applicable.

To obtain an overall measure of reorienting speed for the correlation analyses with rTPJ rsFC (see below), the sign of the VE was inverted for counterpredictive blocks (where invalid trials were more frequent than valid trials), and the blockwise VEs were averaged. This measure should reflect the general magnitude of the reorienting costs at unexpected locations (i.e., target locations with an actual probability $<50\%$, irrespective of the direction of the cue). To check for any session order effects, we conducted a two-sample t test on the mean VE between those participants who completed the sham before and after the cTBS session.

Belief Updating - Computational Modeling

A measure of belief updating about the actual validity of the spatial cue in this paradigm was derived from a computational learning model. For the modeling, single-trial RT was converted to response speed ($RS = 1/RT$) because RSs tend to be more normally distributed (Brodersen et al., 2008; Carpenter & Williams, 1995). To quantify belief updating about the %CV in true and false blocks, we applied a Rescorla-Wagner (RW) model to trial-wise RSs in the different blocks. Due to the smaller number of trials entering the model and the block structure of the task with constant %CV in each block, a RW model, rather than a previously used hierarchical volatility-based Bayesian model (Vossel et al., 2014, 2015), was chosen, as in Mengotti et al. (2017). It has been shown that the RW learning rate is significantly

2. Empirical Section

correlated with the Bayesian parameter describing the updating of %CV (Vossel et al., 2014). In both types of models, updating is influenced by the weighting of prediction errors (the discrepancy between observed and predicted outcomes) by a learning rate. Each block was modeled separately, and a higher learning rate was expected for false than true blocks. In the RW model, updating of the belief that a cue will be valid in a single given trial equals the product of a learning rate α and the prediction error $\delta^{(t)}$, i.e., the difference between the observed and the predicted outcome in the respective trial t . The updated prediction after experiencing the trial t , $P^{(t)}$, is then given by the sum of the prediction from the previous trial and the product of learning rate and prediction error:

$$P^{(t)} = P^{(t-1)} + \alpha \delta^{(t)}$$

Hence, the learning rate α determines the extent to which prediction errors influence the subject's belief from trial to trial. Considering that the learning rate α affects the steepness of the exponential decay of the influence of preceding trials (Rushworth & Behrens, 2008), it also reveals to which extent past events change the subjects' predictions. To estimate the RW learning rate α in each block, single-trial RSs were used. A linear relationship between $RS^{(t)}$ and the prediction before the observation of the outcome of the trial $P^{(t-1)}$ was assumed by the response model which was employed to map from the subject's belief about %CV to observed responses (RSs) (see Mengotti et al., 2017 and Vossel et al., 2014 for a similar procedure):

$$RS^{(t)} = \begin{cases} \zeta_{1_valid} + \zeta_2 P^{(t-1)} & \text{for valid trials} \\ \zeta_{1_invalid} + \zeta_2 (1 - P^{(t-1)}) & \text{for invalid trials} \end{cases}$$

ζ_{1_valid} , $\zeta_{1_invalid}$, and ζ_2 are additional subject-specific parameters that are estimated from the data. ζ_{1_valid} and $\zeta_{1_invalid}$ define the constants of the linear equation (i.e., the overall levels of RSs), and ζ_2 governs the slope of the affine function (i.e., the strength of the increase in RS with increased estimated %CV $P^{(t-1)}$). The learning rate α and the three parameters from the observation model were estimated from trial-wise RSs using variational

2. Empirical Section

Bayes as implemented in the HGF toolbox (www.translationalneuromodeling.org/tapas/) running on MATLAB (R2014a, The MathWorks, Inc.). Variational Bayes optimizes the (negative) free-energy F as a lower bound on the log-evidence, such that maximizing F minimizes the Kullback-Leibler divergence between exact and approximate posterior distributions or, equivalently, the surprise about the inputs encountered (for details, see Friston, Mattout, Trujillo-Barreto, Ashburner, & Penny, 2007).

The learning rate α was averaged separately for the blocks with true and false prior information concerning %CV. As in our previous study (Mengotti et al., 2017), we expected a higher learning rate α in blocks with false prior information, since here contextual updating is required to estimate the true %CV. To test this assumption, a paired-sample t-test on the learning rate α was calculated to compare blocks with true and false priors.

To obtain a measure of belief updating for the correlation analyses with rTPJ rsFC (see below), the difference in learning rates between false and true blocks was used. This difference score reflects the differential updating after false prior information has been provided. Additionally, to check for a session order effect, we conducted a two-sample t-test on this difference score.

Resting-state fMRI Data Acquisition and Preprocessing

During the two resting-state measurements before and after task-based fMRI, participants had no task apart from maintaining fixation on a central cross. Using a 3T MRI System (Trio; Siemens), 180 T2*-weighted volumes were acquired applying an echo-planar imaging sequence with BOLD contrast with a repetition time of 2.2 sec and an echo time of 30 ms. Each volume consisted of 36 axial slices with interleaved slice acquisition. The field of view was 200 mm, using a 64 × 64 image matrix, which resulted in a voxel size of 3.1 × 3.1 × 3.3 mm³. The first five volumes were discarded from the analysis to allow for T1 equilibration effects. The remaining 175 volumes were analyzed using the Statistical Parametric Mapping software SPM12 (Wellcome Department of Imaging Neuroscience; Friston et al., 1995; www.fil.ion.ucl.ac.uk/spm) and FC toolbox CONN, version 18.a (McGovern Institute for Brain

2. Empirical Section

Research, Massachusetts Institute of Technology; Whitfield-Gabrieli & Nieto-Castanon, 2012; www.nitrc.org/projects/conn). For the preprocessing, images were bias-corrected. Slice acquisition time differences were corrected using sinc interpolation to the middle slice. During spatial realignment, a mean EPI image was computed for each subject and spatially normalized to the MNI template using the segmentation function. Subsequently, the obtained transformation was applied to the individual EPI volumes to translate the images into standard MNI space and resample them into $2 \times 2 \times 2$ mm³ voxels. Finally, the normalized images were spatially smoothed using an 8 mm full-width half-maximum Gaussian kernel. The pre- and post-task resting-state data were passed through several additional preprocessing steps using the CONN toolbox (Whitfield-Gabrieli & Nieto-Castanon, 2012) for MATLAB R2017b (MathWorks, Inc). Data were detrended and high-pass filtered (0.01 Hz). Head movement artifacts were removed with the artifact detection tools scrubbing procedure. White-matter, cerebrospinal fluid, and movement parameters were extracted as nuisance covariates following the CompCor strategy (Behzadi et al., 2007) and taken out by linear regression. Temporal derivatives of these confounds were also included in the linear model, accounting for time-shifted versions of spurious variance.

Seed-Based Functional Connectivity of rTPJ

rsFC was analyzed with seed-based correlation analysis. This method computes the temporal correlation between the BOLD activity from a given seed voxel to all other voxels in the brain using a general linear model approach (Biswal et al., 1995; Fox et al., 2005). First, to identify areas showing positive or negative functional connectivity with the specific rTPJ region, a voxel-wise map was computed for the seed Region of Interest (ROI), which was an 8 mm radius sphere centered at $x = 56$, $y = -44$, $z = 12$. This MNI-coordinate was derived from a previous fMRI and TMS study investigating belief updating and reorienting (Vossel et al., 2015; Mengotti et al., 2017). The BOLD time series were averaged over all voxels in the seed ROI and the voxel-wise Pearson correlation coefficients between that ROI, and all other voxels were computed. After that, the Fisher z transformation was applied.

2. Empirical Section

Participant-specific contrast images reflecting standardized correlation coefficients were used for the second-level random-effects analysis in SPM. We computed one-sample t-tests to determine the main positive and negative rsFC maps of the rTPJ seed across pre- and post-task runs, respectively. To investigate differences in rsFC from pre- to post-task, we computed paired t-tests. All results were thresholded at a voxel-wise $p < 0.05$ FWE corrected with an extent threshold of ≥ 20 voxels. The locations of activation were derived from the Anatomy Toolbox for those regions that have been mapped cytoarchitectonically (Eickhoff et al., 2005). Additionally, to check for any session order effects, we conducted a within-participant ANOVA with the factors session order (active cTBS first, sham first) and run (pre-task, post-task) on the rsFC.

Brain-Behavior Relationship

To examine the relationship between pre-task rsFC and the parameters of reorienting of attention and belief updating in the location-cueing task, we computed the Pearson correlation coefficient between each behavioral parameter (mean VE and the difference in learning rates α for false and true blocks) and the strength of rTPJ rsFC and six target ROIs. These six ROIs were chosen to comprise the critical regions of the dorsal and ventral attentional networks in both hemispheres (lIPS, rIPS, lFEF, rFEF, lTPJ, and rIFG). The coordinates of these ROIs were extracted from the local maxima in the respective anatomical areas in the main positive and negative rsFC maps of the rTPJ seed across pre- and post-task runs. The same analyses were performed using the differences in rTPJ connectivity from post- to pre-task to investigate the relationship of the behavioral parameters with changes in rsFC after the task.

To check if outliers drove the correlations, we calculated Cook's distance (Cook, 1977). If Cook's distance values were > 1 (Stevens, 1996) for a given participant, the correlations were recalculated without this participant to check if the significant relationship persisted.

As control analyses, we also performed the above-mentioned analyses with more general task measurements, i.e., overall RS and accuracy.

2. Empirical Section

To investigate the specificity of our results for reorienting or belief updating, respectively, we used step-wise linear regression analysis with rsFC as dependent and the two behavioral parameters as independent predictor variables. This analysis determines the smallest set of predictor variables with the best model fit. The (minimum) Corrected Akaike Information Criterion (AICC) was used to evaluate the effect of adding or removing the reorienting or belief updating parameter to/from the regression model. Here, it should be noted that both measures should be independent in the present paradigm, since we used a global measure for reorienting (averaged over all blocks with reversed signs for blocks with counter-predictive cues).

Eye Movement Recording

To verify that participants followed the instructions to maintain fixation, eye movements were monitored with an Eye-Link® 1000 (SR Research) eye-tracking system with a sampling rate of 500 Hz on scans during the practice session outside the scanner. At the start of the experiment, calibration and validation of the eye-tracker were performed (validation error $<1^\circ$ of visual angle). Analysis of the data was performed using MATLAB (R2014a, The MathWorks, Inc.). The timing and stimulus configurations of the practice session were identical to the fMRI task. However, the targets were presented with an eccentricity of 8.9° . The critical period analyzed for gaze deviations from the center was the time window between the presentation of the cue and the target display (cue-target period). Saccades were identified as gaze deviations from fixation $>1.5^\circ$ visual angle in the cue-target period, and they were determined and expressed as a percentage score over the total number of trials. Three participants had to be excluded from this analysis because of the bad quality of the signal. Therefore, eye-movement data from 20 of the 23 participants were analyzed.

2. Empirical Section

Results

Behavioral Results

Participants maintained fixation on average in 96% ($\pm 1.2\%$, SEM) of the trials. Overall, the average accuracy amounted to 95% (± 1.56 SEM). The within-participant ANOVA on accuracy scores with the factors *prior* (true, false), and *validity* (valid, invalid) revealed a main effect of *validity* ($F(1,22) = 5.1$, $p=0.034$, $\eta_p^2=0.189$) with higher accuracy in valid trials. The factor *prior* and the interaction did not reach significance.

The within-participant ANOVA on mean RT in each condition with the factors *prior* (true, false), *block* (90%CV, 70%CV, 30%CV, 10%CV), and *validity* (valid, invalid) revealed a main effect of *prior* ($F(1,22) = 7.8$, $p=0.011$, $\eta_p^2=0.261$) with higher RTs in false blocks, a main effect of *validity* ($F(1,22) = 20.9$, $p=1.5 \times 10^{-4}$, $\eta_p^2=0.487$) with higher RTs in invalid trials, as well as a significant *prior* \times *block* \times *validity* interaction ($F(1.46,32.04) = 22.7$, $p=3 \times 10^{-10}$, $\eta_p^2=0.508$). To further interpret the interaction, we subjected the difference in RTs between invalid and valid trials, i.e., the VE, to a 2×2 within-participant ANOVA with the factors *prior* (true, false) and *block* (90%CV, 70%CV, 30%CV, 10%CV). The linear trend for the *prior* \times *block* interaction was significant ($F(1,22) = 33.3$, $p=8 \times 10^{-6}$, $\eta_p^2=0.602$). As expected, VEs varied linearly with CV%, and this effect had a reversed direction in false blocks reflecting learning of the actual %CV (see Figure 2.1B). This confirms that the participants inferred the actual %CV levels in the present paradigm.

Regarding belief updating, we compared the learning rate α of the RW learning model between blocks with true and false priors using a paired-samples t-test. As hypothesized, this revealed a significant difference ($t(22) = -2.7$, $p=0.012$), with a higher learning rate in blocks with false priors, i.e., when more belief updating was required.

Because the study was performed on multiple days, we additionally tested with dedicated two-sample t-tests whether there were any session effects for the mean VE or the belief updating parameter (i.e., the difference between true and false blocks of the learning rate α).

2. Empirical Section

These analyses did not reveal any significant session order effects (VE: $t(21)=0.38$, $p=0.708$; learning rate difference: $t(21)=-0.993$, $p=0.332$).

We also checked if the mean VE and the difference score of the learning rate α were correlated. The correlation between both measures was not significant ($r=-0.235$, $p=0.28$).

Resting-State Functional Connectivity of rTPJ

Seed-based analysis of rsFC of the specific rTPJ coordinate across pre- and post-task runs revealed significant positive rsFC with bilateral TPJ, right inferior frontal gyrus (IFG), and right frontal eye fields (FEF). Significant negative rsFC of the rTPJ was found with the left superior frontal gyrus, left superior orbital gyrus, and the cerebellum (Figure 2.2; see Table 1 for full list).

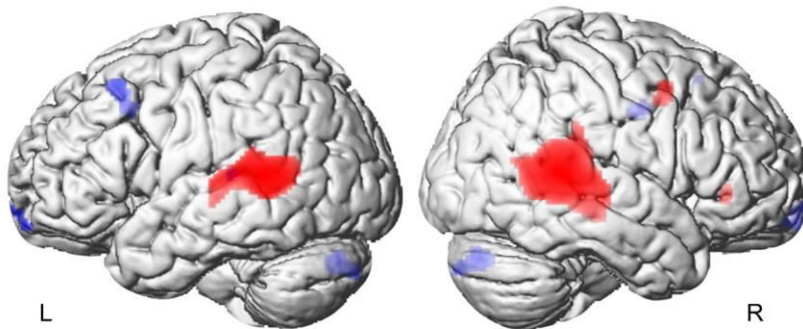


Figure 2.2 Positive (red) and negative (blue) rsFC of rTPJ across both resting-state runs.

The comparison between pre-task and post-task runs did not reveal any significant results.

As for behavioral data, there were also no significant session order effects.

2. Empirical Section

Table 1 rsFC pattern of the rTPJ across both resting-state runs

Region	Cluster size	Side	T	Peak voxel (MNI coordinates)		
				x	y	z
<u>Positive functional connectivity</u>						
superior/middle temporal gyrus (TPJ)	2457	R	39.07	60	-44	12
superior/middle temporal gyrus (TPJ)	1080	L	14.24	-62	-52	14
IFG	20	R	8.43	40	30	4
precentral gyrus (FEF)	45	R	8.08	42	2	46
<u>Negative functional connectivity</u>						
superior frontal gyrus	82	L	9.59	-22	16	52
middle cingulate gyrus/white matter	20	R	8.62	18	-8	40
posterior cingulate gyrus/white matter	29	L	8.53	-4	-34	12
superior/middle orbital gyrus	40	L	8.12	-26	60	-12
cerebellum	92	R	7.82	4	-82	-26

Linking rTPJ Functional Connectivity and Behavior

Reorienting of Attention

ROI-based correlation analyses between behavior and rsFC of rTPJ were performed with six pre-defined ROIs, with coordinates derived from the local maxima in the respective anatomical region from the rsFC maps of rTPJ across both resting-state runs (ITPJ: $x=-62$, $y=-52$, $z=14$; rIFG: $x=42$, $y=12$, $z=12$; lFEF: $x=-56$, $y=-2$, $z=48$; rFEF: $x=42$, $y=2$, $z=46$; lIPS: $x=-26$, $y=-72$, $z=42$; rIPS: $x=26$, $y=-72$, $z=56$). Pre-task rsFC of rTPJ was not significantly related to the general speed of reorienting, i.e., to the overall magnitude of the VE. However, the VE was negatively correlated with the change in rsFC between rTPJ and ITPJ from pre- to post-task ($r=-0.59$, $p=0.003$, Figure 2.3). Stronger interhemispheric rsFC between left and right TPJ after (as compared to before) the task was associated with a smaller overall VE.

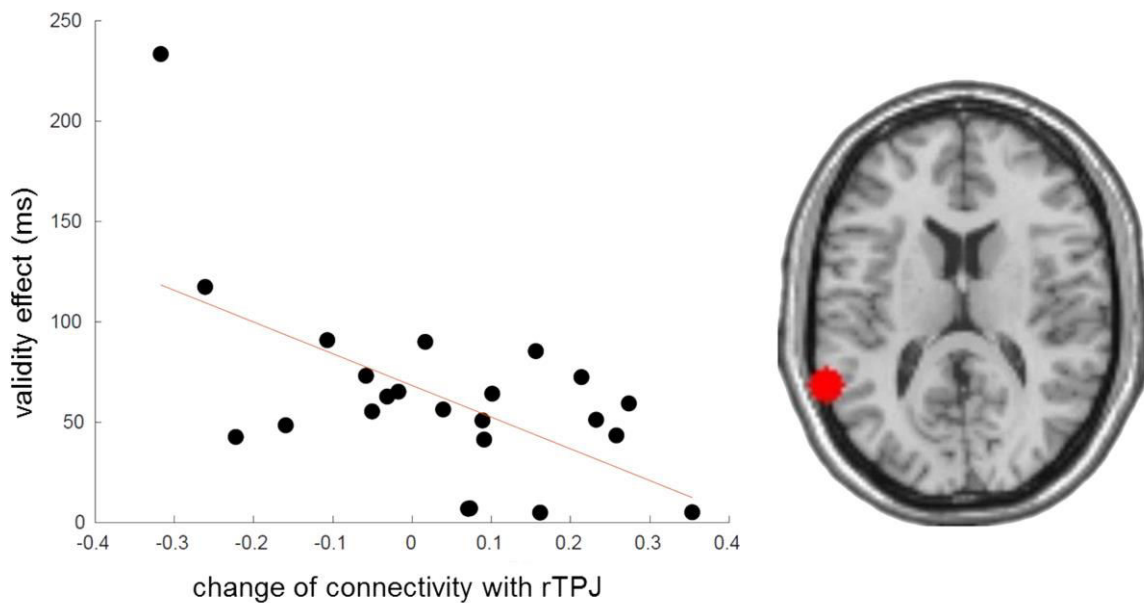


Figure 2.3 Correlation of the parameter of reorienting (mean VE) and the change in rsFC between the rTPJ and the ITPJ after (as compared to before) the task.

The analysis of Cook's distance revealed one outlier (>1). However, the correlation remained significant when excluding this outlier ($r=-0.44$, $p=0.042$). A step-wise linear regression revealed that besides the VE, the belief updating parameter also contributed to the explanation of the rsFC changes between rTPJ and ITPJ (AICC=-86.52 for both predictor variables versus AICC=-85.26 for VE as the only predictor variable).

2. Empirical Section

Belief Updating

For the association between behavior and pre-task rsFC, we found a significant negative correlation between belief updating (as reflected in the difference in learning rates for false and true blocks) and the strength of rsFC between the rTPJ and right intraparietal sulcus (rIPS) ($r=-0.44$, $p=0.037$, Figure 2.4 A). Here, stronger rsFC between rTPJ and rIPS before the task was related to reduced updating (i.e., a smaller difference in learning rates). According to a step-wise linear regression, the belief updating parameter was the only relevant predictor variable (i.e., the VE was eliminated from the regression model) for rTPJ-rIPS connectivity. All of Cook's distance values were below 1.

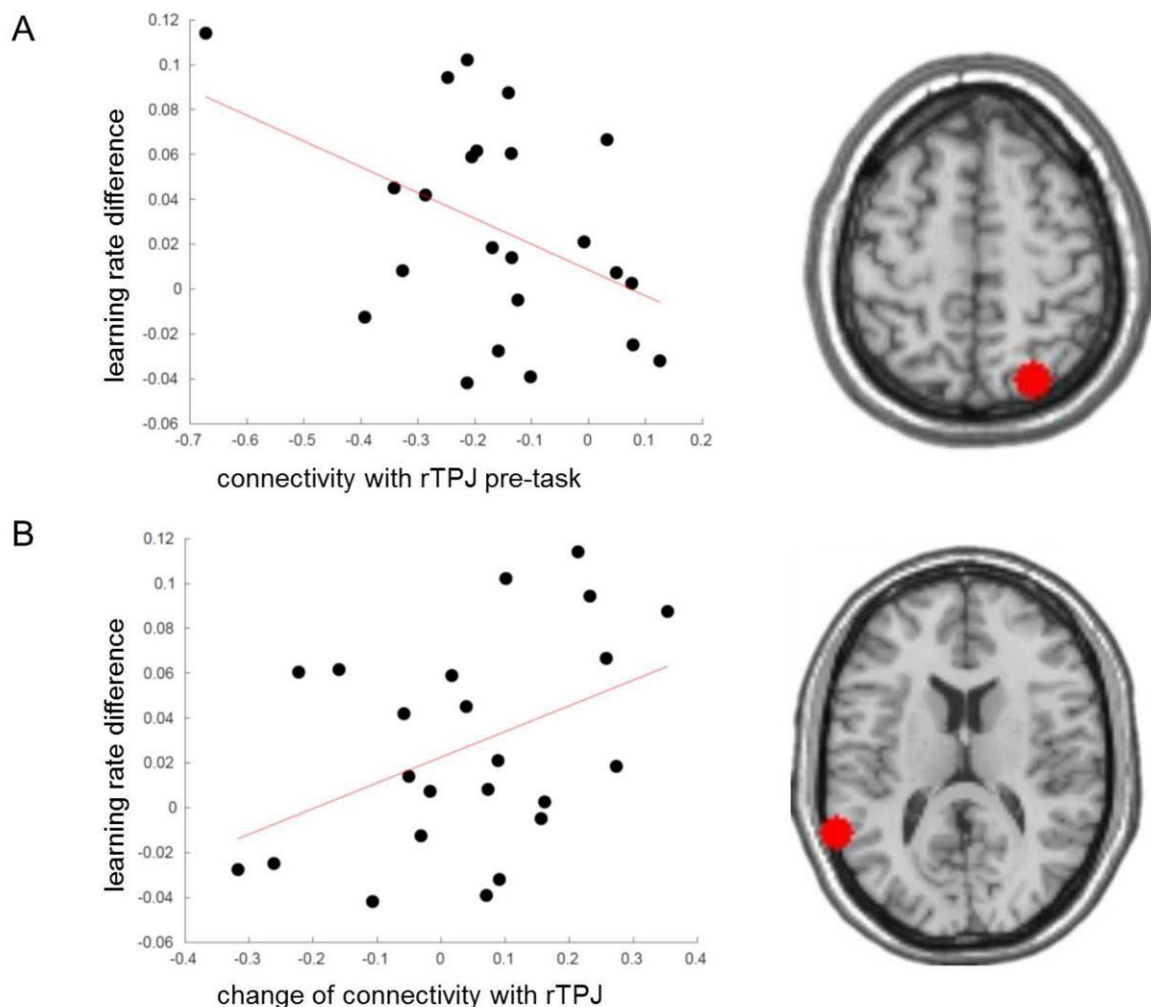


Figure 2.4 Correlations of belief updating and the rsFC between the rTPJ and the rIPS before the task as well as between the rTPJ and lIPS after (as compared to before) the task.

2. Empirical Section

Regarding rTPJ rsFC after (as compared to before) the task, a significant positive correlation between updating and the change of rsFC between the rTPJ and ITPJ from pre- to post-task was observed ($r=0.43$, $p=0.043$, Figure 2.4 B). Faster updating (in false versus true blocks) was associated with stronger interhemispheric rsFC between left and right TPJ after (as compared to before) the task. This result is in line with the step-wise regression described above, according to which both belief updating and reorienting contributed to the change in rsFC.

Control Analyses

Additional correlation analyses were performed between the rsFC of rTPJ and more general behavioral parameters, i.e., overall RS and accuracy. In none of the six ROIs, these analyses revealed significant effects (all $p>0.05$).

Discussion

This study investigated if the resting-state network architecture of rTPJ with ventral and dorsal attention network nodes is related to belief updating and reorienting. In a modified location-cueing paradigm, block-wise changes of the %CV were implemented, and true and false prior information about the %CV was provided before each block. Higher functional connectivity between rTPJ and rIPS before the task was associated with a smaller difference in learning rates between false and true blocks, i.e., with slower belief updating after false priors. Increases in connectivity between rTPJ and ITPJ after the task were related to both relatively faster belief updating in false blocks and faster reorienting (smaller VEs).

Regarding the behavioral results, we replicated previous findings with the same experimental paradigm (Mengotti et al., 2017). As expected, VEs varied linearly with %CV, and this effect had a reversed direction in false blocks, reflecting learning of the actual %CV. Moreover, participants had a higher learning rate in blocks with false as compared to true prior information (when belief updating was required).

2. Empirical Section

Our results regarding the rsFC pattern of the specific rTPJ coordinate are consistent with previous studies on rsFC of rTPJ (Bzdok et al., 2013; Kucyi et al., 2012; Mars et al., 2012; Shulman et al., 2009), showing positive connectivity between rTPJ and other regions of the ventral attention network, i.e., right IFG. Our positive rsFC pattern especially relates to findings of the rsFC of an anterior cluster of the rTPJ, which has been associated with attentional functions in task-based studies (Bzdok et al., 2013). Furthermore, our findings on the negative rsFC are in line with previous work reporting negative connectivity of rTPJ with frontal regions and the cerebellum, although not all previously described regions showed significant results in this study (Kucyi et al., 2012).

Investigating the association between the rsFC of the rTPJ and the behavioral parameters from the location-cueing paradigm revealed specific relationships for belief updating and reorienting, respectively. As a note of caution, these findings were derived from a correlational approach and thus cannot be interpreted as causal effects. General behavioral parameters such as mean RS and accuracy were not significantly related to the rsFC patterns of rTPJ. Faster belief updating in false versus true blocks was associated with weaker rsFC of rTPJ with rIPS before the task. IPS is regarded as a key region of the dorsal system responsible for top-down control and selection (Corbetta et al., 2000; Hopfinger et al., 2000; Kastner et al., 1999). Hence, the intrahemispheric rIPS-rTPJ connection may reflect the strength of the reliance on top-down information, i.e., in our case, the a priori %CV. Firm reliance on this prior information may then lead to slower updating of %CV, i.e., to a smaller influence of prediction errors on the trial-wise estimation of the probability that the cue will be valid (as parameterized in the learning rate parameter of the RW model). In line with this notion, first evidence exists for an involvement of IPS in contextual updating in a sustained attention task. Here, TMS over IPS suppressed TPJ responses for differentiating targets and non-targets, suggesting that IPS gives input to TPJ to shape stimulus-evoked responses (Leitao et al., 2015).

Regression analysis revealed that rsFC between rTPJ and rIPS was related to belief updating rather than reorienting. This may seem at odds with previous studies showing an

2. Empirical Section

involvement of IPS in reorienting of spatial attention (Chica, Bartolomeo, & Valero-Cabre, 2011; Vossel et al., 2012; Weissman & Prado, 2012; Wen et al., 2012). However, our present results concern the state of the network architecture before the task, rather than connectivity during the task. Hence, the IPS – or connectivity between rTPJ and IPS (see Vossel et al., 2012) - may still play an essential role in online task performance. This, together with the network effects of rTPJ neurostimulation, will be addressed in our future work.

When investigating the interhemispheric connectivity between rTPJ and ITPJ, we found that better behavior (relatively faster updating in false blocks and faster reorienting) was accompanied by an increase in the rsFC between the rTPJ and the ITPJ after (as compared to before) the task. Regression analysis revealed that both reorienting and belief updating contributed to the explanation of interhemispheric rsFC changes between rTPJ and ITPJ. It has been suggested that both ITPJ and rTPJ are vital for updating the statistical contingency between cues and targets, with rTPJ coding mismatches between cues and targets and ITPJ coding with cue-target matches (Doricchi et al., 2010). Moreover, previous task-based fMRI studies on other attentional functions have shown that effective connectivity between ITPJ and rTPJ is related to enhanced filtering of distractors in a partial report paradigm (Vossel et al., 2016). Our results also support and extend findings from patient studies that interhemispheric parietal and temporoparietal interactions are essential for attentional functions (Baldassarre et al., 2014; Carter et al., 2010; He et al., 2007; Siegel et al., 2016). These studies emphasize that a decrease in interhemispheric rsFC, presumably due to an imbalance between both hemispheres after stroke, is related to impaired performance in a location-cueing task and cancellation tests.

Besides, patient studies investigating the effects of non-invasive brain stimulation over parietal cortex for the recovery of neglect symptoms after stroke showed that stimulation protocols could improve impaired behavior (see Salazar et al., 2018 for a review). For instance, both cathodal direct current stimulation of the unlesioned posterior parietal cortex and anodal stimulation of the lesioned homologous region reduced symptoms of neglect

2. Empirical Section

(Sparing et al., 2009). Furthermore, inhibitory TMS on the contralesional left parietal cortex likewise ameliorated neglect (Nyffeler et al., 2019). However, the response rate to the stimulation depended on the integrity of the interhemispheric connections, especially of the corpus callosum connecting homologous parietal regions (Nyffeler et al., 2019). This is in line with findings of healthy participants, where the structural variability within the corpus callosum was a predictor for the individual differences in the effects of inhibitory TMS on the posterior parietal cortex on the allocation of spatial attention (Chechlacz et al., 2015). Consequently, an amelioration of the interhemispheric rsFC between the posterior parietal cortices was found to be associated with the recovery of neglect symptoms (Ramsey et al., 2016), which again emphasizes the importance of intact interhemispheric rsFC for cognitive functions. Here, we show that this is not only relevant for attentional functions, but also the updating of probabilistic beliefs.

However, our present results not only suggest that resting-state connectivity per se is relevant for cognitive functions but also that cognitive processing during a task can change connectivity patterns afterwards in a performance-dependent manner. It has been proposed that the rsFC pattern of a person may be seen as a trait that can be used to predict behavior and disease (Craddock et al., 2009; Khosla et al., 2019). Although our findings are in accord with this notion, they also suggest that the relationship between rsFC and behavior may be more complex, with mutual interactions between cognitive processing and resting-state connectivity architectures.

Conclusions

We have provided resting-state fMRI evidence that rsFC before task and changes in rsFC from pre- to post-task of the rTPJ are related to belief updating and reorienting in a Posner task with uncertain contingencies between cues and targets. Therefore, this study highlights the mutual influence of functional connectivity during rest and behavior. Moreover, it identifies IPS as a crucial network node for rTPJ for the flexible deployment of attention in relation to inferred cue validity.

2. Empirical Section

References

- Baldassarre, A., Ramsey, L. E., Hacker, C. L., Callejas, A., Astafiev, S. V., Metcalf, N. V., Zinn, K., Rengachary, J., Snyder, A. Z., Carter, A. R., Shulman, G. L., & Corbetta, M. (2014). Large-scale changes in network interactions as a physiological signature of spatial neglect. *Brain*, *137*(12), 3267–3283.
- Behzadi, Y., Restom, K., Liu, J., & Liu, T. T. (2007). A component based noise correction method (CompCor) for BOLD and perfusion based fMRI. *NeuroImage*, *37*(1), 90–101.
- Biswal, B., Yetkin, F. Z., Haughton, V. M., & Hyde, J. S. (1995). Functional connectivity in the motor cortex of resting human brain using echo-planar MRI. *Magnetic resonance in medicine*, *34*(4), 537-541.
- Brodersen, K. H., Penny, W. D., Harrison, L. M., Daunizeau, J., Ruff, C. C., Duzel, E., Friston, K. J., & Stephan, K. E. (2008). Integrated Bayesian models of learning and decision making for saccadic eye movements. *Neural Networks*, *21*(9), 1247–1260.
- Bzdok, D., Langner, R., Schilbach, L., Jakobs, O., Roski, C., Caspers, S., Laird, A. R., Fox, P. T., Zilles, K., & Eickhoff, S. B. (2013). Characterization of the temporo-parietal junction by combining data-driven parcellation, complementary connectivity analyses, and functional decoding. *NeuroImage*, *81*, 381–392.
- Carpenter, R. H. S., & Williams, M. L. L. (1995). Neural computation of log likelihood in control of saccadic eye movements. *Nature*, *377*(6544), 59–62.
- Carter, A. R., Astafiev, S. V., Lang, C. E., Connor, L. T., Rengachary, J., Strube, M. J., Pope, D. L. W., Shulman, G. L., & Corbetta, M. (2010). Resting interhemispheric functional magnetic resonance imaging connectivity predicts performance after stroke. *Annals of Neurology*, *67*(3), 365–375.
- Chechlacz, M., Humphreys, G. W., Sotiropoulos, S. N., Kennard, C., & Cazzoli, D. (2015). Structural Organization of the Corpus Callosum Predicts Attentional Shifts after Continuous Theta Burst Stimulation. *The Journal of Neuroscience*, *35*(46), 15353–15368.
- Chica, A. B., Bartolomeo, P., & Valero-Cabre, A. (2011). Dorsal and Ventral Parietal

2. Empirical Section

- Contributions to Spatial Orienting in the Human Brain. *The Journal of Neuroscience*, 31(22), 8143–8149.
- Cook, R. D. (1977). Detection of Influential Observation Linear Regression. *Technometrics*, 19(01), 15–18.
- Corbetta, M., Kincade, M. J., Ollinger, J. M., McAvoy, M. P., & Shulman, G. L. (2000). Voluntary orienting is dissociated from target detection in human posterior parietal cortex. *Nature Neuroscience*, 3(3), 292–297.
- Corbetta, M., Patel, G., & Shulman, G. L. (2008). The Reorienting System of the Human Brain: From Environment to Theory of Mind. *Neuron*, 58(3), 306–324.
- Corbetta, M., Ramsey, L. E., Callejas, A., Baldassarre, A., Hacker, C. D., Siegel, J. S., Astafiev, S. V., Rengachary, J., Zinn, K., Lang, C. E., Connor, L. T., Fucetola, R., Strube, M. J., Carter, A. R., & Shulman, G. L. (2015). Common behavioral clusters and subcortical anatomy in stroke. *Neuron*, 85(5), 927–941.
- Corbetta, M., & Shulman, G. L. (2002). Control of goal-directed and stimulus-driven attention in the brain. *Nature Reviews Neuroscience*, 3(3), 201–215.
- Craddock, R. C., Holtzheimer, P. E., Hu, X. P., & Mayberg, H. S. (2009). Disease state prediction from resting state functional connectivity. *Magnetic Resonance in Medicine*, 62(6), 1619–1628.
- Daunizeau, J., den Ouden, H. E. M., Pessiglione, M., Kiebel, S. J., Stephan, K. E., & Friston, K. J. (2010). Observing the Observer (I): Meta-Bayesian Models of Learning and Decision-Making. *PLOS ONE*, 5(12), e15554.
- Doricchi, F., Macci, E., Silvetti, M., & Macaluso, E. (2010). Neural correlates of the spatial and expectancy components of endogenous and stimulus-driven orienting of attention in the posner task. *Cerebral Cortex*, 20(7), 1574–1585.
- Eickhoff, S. B., Stephan, K. E., Mohlberg, H., Grefkes, C., Fink, G. R., Amunts, K., & Zilles, K. (2005). A new SPM toolbox for combining probabilistic cytoarchitectonic maps and functional imaging data. *NeuroImage*, 25(4), 1325–1335.
- Fox, M. D., Corbetta, M., Snyder, A. Z., Vincent, J. L., & Raichle, M. E. (2006). Spontaneous

2. Empirical Section

- neuronal activity distinguishes human dorsal and ventral attention systems. *Proceedings of the National Academy of Sciences*, 103(26), 10046–10051.
- Fox, M. D., Snyder, A. Z., Vincent, J. L., Corbetta, M., Van Essen, D. C., & Raichle, M. E. (2005). From The Cover: The human brain is intrinsically organized into dynamic, anticorrelated functional networks. *Proceedings of the National Academy of Sciences*, 102(27), 9673–9678.
- Friston, Karl J., Holmes, A. P., Worsley, K. J., Poline, J. B., Frith, C. D., & Frackowiak, R. J. S. (1995). Statistical parametric maps in functional imaging: a general linear approach. *Human Brain Mapping*, 2, 189–210.
- Friston, K. J., Mattout, J., Trujillo-Barreto, N., Ashburner, J., & Penny, W. D. (2007). Variational free energy and the Laplace approximation. *NeuroImage*, 34(1), 220–234.
- Geng, J. J., & Vossel, S. (2013). Re-evaluating the role of TPJ in attentional control: Contextual updating? *Neuroscience and Biobehavioral Reviews*, 37(10), 2608–2620.
- Greicius, M. D., Supekar, K., Menon, V., & Dougherty, R. F. (2009). Resting-state functional connectivity reflects structural connectivity in the default mode network. *Cerebral Cortex*, 19(1), 72–78.
- He, B. J., Snyder, A. Z., Vincent, J. L., Epstein, A., Shulman, G. L., & Corbetta, M. (2007). Breakdown of Functional Connectivity in Frontoparietal Networks Underlies Behavioral Deficits in Spatial Neglect. *Neuron*, 53(6), 905–918.
- Hoffstaedter, F., Grefkes, C., Caspers, S., Roski, C., Palomero-Gallagher, N., Laird, A. R., Fox, P. T., & Eickhoff, S. B. (2014). The role of anterior midcingulate cortex in cognitive motor control. *Human Brain Mapping*, 35(6), 2741–2753.
- Honey, C. J., Sporns, O., Cammoun, L., Gigandet, X., Thiran, J. P., Meuli, R., & Hagmann, P. (2009). Predicting human resting-state functional connectivity - Appendix. *Proceedings of the National Academy of Sciences*, 106(6), 2035–2040.
- Hopfinger, J. B., Buonocore, M. H., & Mangun, G. R. (2000). The neural mechanisms of attentional control. *Nature Neuroscience*, 3(3), 284–291.
- Igelström, K. M., & Graziano, M. S. A. (2017). The inferior parietal lobule and

2. Empirical Section

- temporoparietal junction: A network perspective. *Neuropsychologia*, *105*, 70–83.
- Iglesias, S., Mathys, C., Brodersen, K. H., Kasper, L., Piccirelli, M., den Ouden, H. E. M., & Stephan, K. E. (2013). Hierarchical Prediction Errors in Midbrain and Basal Forebrain during Sensory Learning. *Neuron*, *80*(2), 519–530.
- Kastner, S., Pinsk, M. A., De Weerd, P., Desimone, R., & Ungerleider, L. G. (1999). Increased Activity in Human Visual Cortex during Directed Attention in the Absence of Visual Stimulation. *Neuron*, *22*(4), 751–761.
- Khosla, M., Jamison, K., Ngo, G. H., Kuceyeski, A., & Sabuncu, M. R. (2019). Machine learning in resting-state fMRI analysis. *Magnetic Resonance Imaging*, *64*, 101-121.
- Krall, S. C., Volz, L. J., Oberwelland, E., Grefkes, C., Fink, G. R., & Konrad, K. (2016). The right temporoparietal junction in attention and social interaction: A transcranial magnetic stimulation study. *Human Brain Mapping*, *37*(2), 796–807.
- Kucyi, A., Hodaie, M., & Davis, K. D. (2012). Lateralization in intrinsic functional connectivity of the temporoparietal junction with salience- and attention-related brain networks. *Journal of Neurophysiology*, *108*(12), 3382–3392.
- Leitao, J., Thielscher, A., Tunnerhoff, J., & Noppeney, U. (2015). Concurrent TMS-fMRI Reveals Interactions between Dorsal and Ventral Attentional Systems. *Journal of Neuroscience*, *35*(32), 11445–11457.
- Mars, R. B., Sallet, J., Schüffelgen, U., Jbabdi, S., Toni, I., & Rushworth, M. F. S. (2012). Connectivity-based subdivisions of the human right “temporoparietal junction area”: Evidence for different areas participating in different cortical networks. *Cerebral Cortex*, *22*(8), 1894–1903.
- Mengotti, P., Dombert, P. L., Fink, G. R., & Vossel, S. (2017). Disruption of the Right Temporoparietal Junction Impairs Probabilistic Belief Updating. *The Journal of Neuroscience*, *37*(22), 5419–5428.
- Nyffeler, T., Vanbellingen, T., Kaufmann, B. C., Pflugshaupt, T., Bauer, D., Frey, J., Chechlac, M., Bohlhalter, S., Müri, R. M., Nef, T., & Cazzoli, D. (2019). Theta burst stimulation in neglect after stroke: functional outcome and response variability origins.

2. Empirical Section

Brain, 142, 992–1008.

- Oldfield, R. C. C. (1971). The assessment and analysis of handedness: The Edinburgh inventory. *Neuropsychologia*, 9(1), 97–113.
- Posner, M. I. (1980). Orienting of attention. *The Quarterly Journal of Experimental Psychology*, 32(1), 3–25.
- Ramsey, L. E., Siegel, J. S., Baldassarre, A., Metcalfe, N. V., Zinn, K., Shulman, G. L., & Corbetta, M. (2016). Normalization of network connectivity in hemispatial neglect recovery. *Annals of Neurology*, 80(1), 127–141.
- Rushworth, M. F. S., & Behrens, T. E. (2008). Choice, uncertainty and value in prefrontal and cingulate cortex. *Nature Neuroscience*, 11(4), 389–397.
- Salazar, A. P. S., Vaz, P. G., Marchese, R. R., Stein, C., Pinto, C., & Pagnussat, A. S. (2018). Noninvasive Brain Stimulation Improves Hemispatial Neglect After Stroke: A Systematic Review and Meta-Analysis. *Archives of Physical Medicine and Rehabilitation*, 99(2), 355–366.
- Shulman, G. L., Astafiev, S. V., Franke, D., Pope, D. L. W., Snyder, A. Z., McAvoy, M. P., & Corbetta, M. (2009). Interaction of Stimulus-Driven Reorienting and Expectation in Ventral and Dorsal Frontoparietal and Basal Ganglia-Cortical Networks. *The Journal of Neuroscience*, 29(14), 4392–4407.
- Siegel, J. S., Ramsey, L. E., Snyder, A. Z., Metcalfe, N. V., Chacko, R. V., Weinberger, K., Baldassarre, A., Hacker, C. D., Shulman, G. L., & Corbetta, M. (2016). Disruptions of network connectivity predict impairment in multiple behavioral domains after stroke. *Proceedings of the National Academy of Sciences*, 113(30), 4367–4376.
- Silvetti, M., Lasaponara, S., Lecce, F., Dragone, A., Macaluso, E., & Doricchi, F. (2016). The Response of the Left Ventral Attentional System to Invalid Targets and its Implication for the Spatial Neglect Syndrome: a Multivariate fMRI Investigation. *Cerebral Cortex*, 26(12), 4551–4562.
- Sparing, R., Thimm, M., Hesse, M. D., Küst, J., Karbe, H., & Fink, G. R. (2009). Bidirectional alterations of interhemispheric parietal balance by non-invasive cortical stimulation.

2. Empirical Section

Brain, 132(11), 3011–3020.

Stevens, J. (1996). *Applied multivariate statistics for the social sciences* (6th edition).

Mahwah, NJ: Lawrence Erlbaum Associates.

Vossel, S., Mathys, C., Daunizeau, J., Bauer, M., Driver, J., Friston, K. J., & Stephan, K. E.

(2014). Spatial attention, precision, and bayesian inference: A study of saccadic response speed. *Cerebral Cortex*, 24(6), 1436–1450.

Vossel, S., Mathys, C., Stephan, K. E., & Friston, K. J. (2015). Cortical Coupling Reflects

Bayesian Belief Updating in the Deployment of Spatial Attention. *The Journal of Neuroscience*, 35(33), 11532–11542.

Vossel, S., Weidner, R., Driver, J., Friston, K. J., & Fink, G. R. (2012). Deconstructing the

Architecture of Dorsal and Ventral Attention Systems with Dynamic Causal Modeling. *The Journal of Neuroscience*, 32(31), 10637–10648.

Vossel, S., Weidner, R., Moos, K., & Fink, G. R. (2016). Individual attentional selection

capacities are reflected in interhemispheric connectivity of the parietal cortex. *NeuroImage*, 129, 148–158.

Weissman, D. H., & Prado, J. (2012). Heightened activity in a key region of the ventral

attention network is linked to reduced activity in a key region of the dorsal attention network during unexpected shifts of covert visual spatial attention. *NeuroImage*, 61(4), 798–804.

Wen, X., Yao, L., Liu, Y., & Ding, M. (2012). Causal Interactions in Attention Networks

Predict Behavioral Performance. *The Journal of Neuroscience*, 32(4), 1284–1292.

Whitfield-Gabrieli, S., & Nieto-Castanon, A. (2012). *Conn*: A Functional Connectivity

Toolbox for Correlated and Anticorrelated Brain Networks. *Brain Connectivity*, 2(3), 125–141.

Yeo, B. T. T., Krienen, F. M., Sepulcre, J., Sabuncu, M. R., Lashkari, D., Hollinshead, M.,

Roffman, J. L., Smoller, J. W., Zöllei, L., Polimeni, J. R., Fischl, B., Liu, H., & Buckner, R. L. (2011). The organization of the human cerebral cortex estimated by intrinsic functional connectivity. *Journal of Neurophysiology*, 106(3), 1125–1165.

2.3 Experiment 2a: Behavioral Experiment and Lesion Mapping - Investigating Probabilistic Inference in the Domain of Spatial Attention and its Relation to Spatial Neglect in Stroke Patients

Introduction

Visuospatial neglect is a heterogeneous syndrome observed after focal brain damage such as stroke and is characterized by different impairments of spatial cognition (Li & Malhotra, 2015). The main deficit is the neglect of contralesional stimuli (Bisiach et al., 1986; Husain & Rorden, 2003; Robertson & Halligan, 1999). Depending on the type of spatial bias and reference frame, various subtypes of neglect have been described (e.g. sensory-attentional, motor-intentional and representational neglect, ego- and allocentric neglect, personal, peri- and extra personal neglect; Rode et al., 2017). Despite the fact that neglect is more frequently observed and more severe after right hemispheric (RH) lesions (Karnath & Rorden, 2012), it can also occur after left hemispheric (LH) lesions (Beume et al., 2017). Furthermore, it was shown that neglect adversely affects recovery after stroke (Barker-Collo et al., 2010; Rengachary et al., 2011).

Various studies have shown that neglect cannot be attributed to one critical lesion location (Chechlacz et al., 2012; Molenberghs et al., 2012; Vuilleumier, 2013). Thus, heterogeneous lesion patterns relate to the variety of neglect-related behavioral deficits. Besides cortical lesions of parietal, temporal and frontal areas, subcortical lesions of the basal ganglia and the thalamus are associated with neglect (Karnath & Rorden, 2012; Thiebaut De Schotten et al., 2014; Vuilleumier, 2013). Hence, neglect is thought to arise from dysfunctional networks and structural damage to white matter pathways has been shown to be associated with neglect (Lunven et al., 2015; Lunven & Bartolomeo, 2017; Thiebaut De Schotten et al., 2014).

So far, neglect has mainly been explained by spatial attention deficits (Bartolomeo et al., 2012; Corbetta & Shulman, 2011; Kinsbourne, 1977). Patients with neglect exhibit impaired

2. Empirical Section

exogenous orienting to a cued target as well as deficits in reorienting of spatial attention to invalidly cued targets in the contralesional hemifield (Corbetta & Shulman, 2011; Posner et al., 1984; Rengachary et al., 2011).

However, patients suffering from neglect often also show non-spatial impairments. It was found that they have difficulties in sustaining alertness (Bartolomeo et al., 2012; Husain & Rorden, 2003; Robertson et al., 1998). They exhibit working memory (Danckert & Ferber, 2006; Striemer et al., 2013) and temporal estimation deficits (Danckert et al., 2007; Merrifield et al., 2010). Moreover, spatial priming and statistical learning may be impaired (Shaqiri & Anderson, 2012, 2013).

Therefore, a few studies have challenged the traditional view regarding neglect only as a disorder of spatial attention. More specifically, they argue that the neglect syndrome can be explained by a more general disorder of updating mental models of the environment (Danckert et al., 2012; Filipowicz et al., 2016; Geng & Vossel, 2013; Shaqiri et al., 2013; Stöttinger et al., 2014, 2018).

Some studies have already investigated updating behavior in neglect patients, although the results are still inconclusive. Applying the children's game "rock, paper, scissors" using a computer opponent which covertly altered its strategy, it was found that RH stroke patients performed worse than LH patients (Danckert et al., 2012). However, severe impairment was not associated with the presence of neglect syndrome per se and it was related to lesions of the insula and putamen. In contrast, employing the same task to a different sample of stroke patients revealed a similar impairment of RH and LH patients, although the authors suggested distinct reasons for the deficits (Stöttinger et al., 2014). According to their view, reduced working memory function caused the observed impairments in LH patients, whereas the deficits in RH patients were attributed to an updating deficit. To support their assumption, the authors conducted an additional picture morphing task, in which the subjective perceptual representation of an object needed to be updated and the working memory load was reduced. Here, LH patients performed better than RH patients and deficits in performance were again related to insula damage (Stöttinger et al., 2014, 2018).

2. Empirical Section

It should be mentioned that the updating impairments in the studies described above were not absolute, since patients just needed more resources (e.g. time) to perform the desired response (Stöttinger et al., 2014).

To investigate the neural network underlying updating, the picture morphing task was used in an fMRI study in healthy young participants. Here, a network comprising insula, medial and inferior frontal regions and the inferior parietal cortex was related to updating behavior (Stöttinger et al., 2015). Accordingly, it was suggested that the insula represents the current model of a person, whereas the intraparietal lobe (IPL) compares new information with predictions generated by the model, and the medial prefrontal cortex (PFC), including the anterior cingulate cortex (ACC), explores alternative models (Filipowicz et al., 2016).

Due to the fact that IPL and TPJ overlap and are not easily distinguishable (Igelström & Graziano, 2017), the proposed view fits to existing results of a causal involvement of rTPJ in updating behavior (Mengotti et al., 2017). Further evidence for an involvement of regions of the dorsal and ventral attention network in updating processes has been provided by studies investigating probabilistic inference in the context of spatial attention (i.e. the location-cueing paradigm; Dombert et al., 2016; Vossel et al., 2015). Here, probabilistic inference refers to the ability to infer the changing validity of a spatial cue. To this end, the percentage of cue validity (%CV) (i.e., the proportion of valid and invalid trials) is manipulated over the course of the experiment and the participants have to infer the actual cue validity level (i.e., the probability that the cue will be valid in a given trial). Probabilistic inference can be assessed by parameters of computational learning models, or, alternatively, by assessing the impact of the %CV manipulation on RTs by means of regression analyses. In addition, probabilistic inference can also be assessed by asking participants to explicitly estimate the %CV.

Such paradigms assessing both spatial reorienting and probabilistic inference have not yet been applied to stroke patients. Hence, more systematic investigations in stroke patients are needed to get a better understanding how the lesioned brain performs probabilistic inference and which brain lesions relate to impairments of probabilistic inference.

2. Empirical Section

In the present study, we applied a modified location-cueing paradigm with changing %CV levels in patients with LH and RH stroke as well as healthy elderly controls (HC). Since fMRI and TMS studies in healthy subjects have shown that rTPJ is critically involved in probabilistic inference in such tasks (Dombert, Kuhns, et al., 2016; Käsbauer et al., 2020; Kuhns et al., 2017; Mengotti et al., 2017; Vossel et al., 2015), we hypothesized that deficits should be related to lesions or disconnection of this region. Moreover, since lesions of the ventral attention network comprising rTPJ are often associated with the presence of spatial neglect, we expected a relationship between impaired probabilistic inference and neglect symptoms in neuropsychological tests. Within the patient groups, we correlated measures of probabilistic inference from this task with reorienting as well as with neuropsychological neglect test performance. Furthermore, we employed voxel-based lesion-symptom mapping and lesion-network mapping to investigate the relationship of lesion location and behavior.

2. Empirical Section

Methods

Participants

We screened 106 patients undergoing neurorehabilitation after unilateral stroke. Seventy patients were enrolled and completed the experimental paradigm. Of these patients, 22 LH stroke patients (53.9 (24-77) years old, 165 ± 223 days post-stroke at baseline assessment (20-674), 9 female) and 26 RH stroke patients (58.5 (28-71) years old, 74 ± 103 days post-stroke at baseline assessment (15-469), 12 female) met the final inclusion criteria (first-ever unilateral stroke, age between 18 and 90 years old, written consent, sufficient knowledge of German, no signs of dementia, no alcohol or drug abuse, no previous history of neurological or psychiatric diseases, no global aphasia, no hemianopia). Twenty-two patients were excluded due to a previous history of neurological or psychiatric diseases ($n=4$), unavailable clinical images of the stroke ($n=4$), evidence of periventricular white matter disease grade 3 ($n=4$) (Fazekas et al., 1987) or the presence of an older stroke ($n=10$). Forty-one patients had suffered an ischaemic and seven a haemorrhagic stroke. One LH stroke patient had to be excluded from the final data analyses since he did not have any correct trials in one condition of the experimental paradigm. Therefore, the final sample only comprised 47 stroke patients. In addition, 33 healthy participants (63.4 (51-80) years old; 19 female) without a history of neurological or psychiatric disease participated in the study. All participants have written informed consent prior to participating in the study. The study was carried out following the ethical principles of the World Medical Association (Declaration of Helsinki) and after obtaining approval by the ethics committee of the Medical Faculty in Cologne.

Procedure

Due to the limited attention span of the patients, the neuropsychological assessment and the experimental paradigm were carried out on different days with the neuropsychological

2. Empirical Section

assessment at the first session and the computer task at the second or if needed third and fourth one. Furthermore, two (of the 26) RH stroke patients, who exhibited symptoms of spatial neglect at the behavioral testing, underwent a six months follow-up assessment at home. These single cases were conducted to further investigate the long term effects of the neglect syndrome on attentional reorienting and probabilistic inference.

Neuropsychological Examination

Premorbid handedness was assessed by the Edinburgh Handedness Inventory (Oldfield, 1971). All patients and controls had normal or corrected to normal vision. We used the Mini-Mental State Examination (MMSE, cut-off: <24 of 30 points, Creavin et al., 2016; Folstein & Folstein, 1975) and the short form of the aphasia checklist (ACL-K, cut-off: <12 of 12 points in subtest 2 language comprehension, Kalbe, Reinhold, & Kessler, 2002) to exclude clinically relevant cognitive decline and aphasia. To screen for depression, the Geriatric Depression Scale (GDS, cut-off for depression: > 5 of 15 points, Greenberg, 2007) was administered. To also quantify apraxia in the patient population, the Cologne Apraxia Screening was applied (KAS, cut-off: > 76 of 80 points, Weiss, Kalbe, & Kessler, 2013). For RH patients, the KAS-R (Wirth et al., 2016) was used.

All patients were examined for extinction and neglect. Visual fields were assessed by standardized neurological bedside examination. The following tests were used to assess extinction and neglect:

Visual Extinction

The presence of extinction was tested clinically by wiggling fingers for 2 sec in one or both visual fields while controlling central gaze fixation. Fifteen trials were given in a fixed pseudo-randomized sequence including 10 unilateral trials (five on each side) and five simultaneous bilateral trials. Extinction was considered if a patient failed to report at least two

2. Empirical Section

contralesional stimuli during bilateral simultaneous presentation, while accurately detecting unilateral stimuli (Beis et al., 2004).

Neglect

All patients performed standardized paper-and-pencil tests of visuospatial neglect in the peripersonal space selected from the Neglect Test (Fels & Geissner, 1997), an adapted version of the Behavioural Inattention Test (Wilson et al., 1987). Furthermore, the Mesulam Weintraub Cancellation task (Mesulam, 1985) and the Landmark-M Task (Bisiach et al., 1998) were conducted. Given the lack of specific cut-off criteria for most of the tests employed, we defined neglect-specific (i.e. laterality-based) cut-off scores for the individual tests, which were, however, inferred from existing studies or test scoring systems (Eschenbeck et al., 2010). All tests were performed on white DIN A4 (210×297mm) paper. Each sheet of paper was centered upon the patient's midsagittal. Patients were not allowed to relocate the stimulus sheet.

Letter Cancellation Test

Patients were presented with five rows of different letters, consisting of 34 letters per row. The task was to cancel the letters 'E' and 'R', which were randomly distributed among other irrelevant letters that represented distractors. A laterality index was calculated according to the following formula: $LI = (\text{"hits contralesional"} - \text{"hits ipsilesional"}) / (\text{"hits contralesional"} + \text{"hits ipsilesional"})$ (Bartolomeo & Chokron, 1999; Marshall et al., 1975). Note that this laterality index can vary between -1 and +1. While a score of -1 reflects a complete omission of all letters in the contralesional hemifield, a score of +1 reflects a complete omission of all letters in the ipsilesional hemifield, and a score of 0 indicates an equal amount of cancelled letters in both hemispaces. The cut-off for the presence of neglect was set to $LI \leq -0.2$ (Eschenbeck et al., 2010).

2. Empirical Section

Star Cancellation Test

The target stimuli in this test are 56 small stars, which are interspersed between distracters (large stars, letters and short words). The task was to cross out the small stars. For the calculation of the laterality index, the two central stars were discarded. The interpretation of the results was the same as in the letter cancellation test.

Copying of Figures

Three figures were presented to the patients (a four cornered star, a rhomb and a flower), which were drawn on the left half of the sheet. The task was to copy the figures on the right half of the sheet. Each drawing was rated for contralesional omissions or size distortions of contralesional elements. A score of ≥ 3 omissions or distortions for all drawings combined was regarded to indicate neglect.

Reading

The patient was prompted to read a short text, which was set out in three columns (46, 47 and 46 words in the left, central and right columns, respectively). The number of words read was assessed. Neglect was regarded to be present if the left words were ignored by the patient in at least two different lines.

Clock Drawing

Patients were asked to draw the face of a clock including contour, digits and clock hands on a blank sheet of paper. They were instructed to set the clock hands to the time "11:10". The drawn clock was rated according to the following criteria: (1) contralesional omissions/savings of space in the contour, (2) contralesional omissions of numbers, (3) contralesional omissions or ipsilesional misplacement of the clock hands, and (4) ipsi- or contralesional compression of the numbers. Neglect was indicated if at least one of these criteria was fulfilled.

2. Empirical Section

Mesulam and Weintraub Cancellation Task

Patients were presented with random arrays of nonverbal stimuli, containing 60 targets, with 15 targets in each quadrant of the sheet. They were asked to mark every open circle crossed by a single slanted line and to work as quickly and accurately as possible. A laterality index was calculated following the same procedure as for the cancellation tasks described above.

Landmark-M Task

To differentially assess neglect-related perceptual and response bias, the Landmark-M task was used. Patients were presented with nine different prebisected lines (180mm long and 1mm thick) and were asked according to a forced-choice procedure to manually point with their ipsilesional hand to the longer or shorter segment in different blocks of trials presented in a predefined trial order. The (180mm long) lines were either bisected in the centre of the line or at 5, 15, 30 or 60mm distance from the center (displaced to the left or right side, respectively). Accordingly, the length of the left line segment amounted to 30, 60, 75, 85, 90, 95, 105, 120 and 150mm for lines 1–9. An index for perceptual bias (PB) was calculated on the basis of the relative frequency of contralesional shorter and ipsilesional longer responses ($PB = [\% \text{ contralesional shorter responses} + \% \text{ ipsilesional longer responses}]/2$), since patients with a perceptual bias are supposed to consistently underestimate the length of the contralesional segment. Response bias (RB) was instead measured by the relative frequency of ipsilesional longer and shorter responses ($RB = [\% \text{ ipsilesional longer responses} + \% \text{ ipsilesional shorter responses}]/2$), since a response bias would lead to consistent choices of ipsilesional rather than contralesional segments due to an impairment in directing the hand movement towards contralesional space (i.e., in case of RH patients to the left line segments). For both indices, the absence of any bias is indicated by a value of

2. Empirical Section

50. PB-scores > 60.15 and RB-scores > 51.74 were regarded to signal contralesional perceptual and motor/intentional neglect.

Table 2 summarizes the demographic and neuropsychological data of the 47 stroke patients.

Table 2 Demographic and neuropsychological data of the stroke patients

	LH patients	RH patients	Statistical parameters of the group comparisons
Age (years) (21LH/26RH)	53.7 (±11)	58.5 (±10)	t(45)=-1.579, p=.121
Gender (f/m) (21LH/26RH)	10/11	11/15	X ² (1)=.133, p=.716
Handedness(right/left/bi) (21LH/26RH)	20/0/1	21/2/3	X ² (2)=2.521, p=.284
Time post stroke (days) (21LH/26RH)	150.3 (±216.9)	74.3 (±103.6)	t(27.3)=1.476, p=.151
Lesion volume (voxels) (21LH/26RH)	22174 (±27447)	37887 (±100775)	t(45)=-0.693, p=.492
MMSE (max. 30) (21LH/26RH)	29 (±1.1)	28.8 (±1.4)	t(45)=.504, p=.617
ACL-K (max. 40) (18LH/26RH)	35.9 (±4.1)	37.7 (±2.5)	t(25.3)=-1.656, p=.110
GDS score (max. 15) (21LH/26RH)	3 (±2.1)	3.6 (±2.9)	t(45)=-.807, p=.424
KAS (max. 80) (20LH/26RH)	78.7 (±2.1)	78.4 (±2.1)	t(44)=.564, p=.576
Letter cancellation LI (20LH/26RH)	.004 (±0.01)	-.013 (±0.54)	t(28.2)=1.494, p=.146
Star cancellation LI (20LH/26RH)	.001 (±0.01)	-.001 (±0.02)	t(31.8)=.460, p=.649
MWCT LI (20LH/26RH)	.000 (±0.01)	-.036 (±0.11)	t(24.3)=1.636, p=.115
Figure copying (max. 9) (20LH/26RH)	8.5 (±0.6)	8.2 (±0.9)	t(44)=1.206, p=.234
Reading (max. 140) (20LH/24RH)	136 (±6.7)	138 (±1.9)	t(42)=-1.067, p=.292
Clock drawing (max. 3) (20LH/26RH)	2.9 (±0.3)	2.9 (±0.3)	t(44)=.263, p=.794
Landmark PB (21LH/26RH)	50.0 (±3.9)	54.3 (±5.8)	t(45)=-2.920, p=.005
Landmark RB (21LH/26RH)	50.0 (±1.9)	50.1 (±2.5)	t(45)=-0.175, p=.862
Extinction (yes/no) (18LH/23RH)	0/18	4/19	X ² (1)=3.469, p=.063

Mean and standard deviations from the mean (in parenthesis; if not stated differently) of the demographic and neuropsychological data. Because some variables showed mild violations from normality, we also used nonparametric Mann-Whitney U tests as control analyses. The results of the t-

2. Empirical Section

tests were confirmed by the nonparametric tests; therefore, only the former will be presented. LH left hemisphere, RH right hemisphere, MMSE Mini Mental State Examination, ACL-K Aphasia Check List-short version, GDS Geriatric Depression Scale, KAS Cologne Apraxia Screening, LI Lateralisation Index, MWCT Mesulam Weintraub Cancellation task, PB perceptual bias, RB response bias.

Experimental Paradigm

We used a modified version of a location-cueing paradigm with central cueing (Posner, 1980) to assess attentional reorienting and belief updating/probabilistic inference about cue validity (%CV). As a fixation point during the total duration of the task, a central diamond on a grey background was presented. To verify that participants followed the instructions to maintain fixation, eye movements were monitored by the experimenter during the experimental session. For patients, either a portable Tobii X1 Light or a portable Tobii pro X3 eyetracker with sampling rates of 30 and 120 Hz was used. For healthy controls, eye movements were recorded with the Eye-Link® 1000 (SR Research) eye tracking system with a sampling rate of 500 Hz. In each trial, a spatial cue, consisting of an arrowhead pointing to either the left or right side, appeared for 800 ms to indicate in which hemifield the target would appear. After a 1000 ms stimulus onset asynchrony (SOA), two stimuli, a triangle (the target) and a diamond (distractor), appeared for 1000 ms on the left and right side of the fixation point (7.6° eccentric in each visual field). Patients had to press a button with the index or middle finger of their ipsilesional hand (for healthy controls the used hand was counterbalanced) to indicate if the triangle was pointing up- or downwards. The response mapping was counterbalanced across participants. Trials were separated by a response period of 1500 ms (see Figure 2.5). During the experimental session, participants performed three blocks. Each block comprised 80 trials, resulting in a total of 240 trials. The percentage of %CV, i.e., the ratio of valid and invalid trials, was manipulated between blocks but was kept constant within each block. %CV within each block amounted to 80%, 60% or 40%, respectively. In the 40% CV blocks, the cue was counter-predictive, as the majority of trials were invalid. No information about the %CV was given. Participants were instructed to

2. Empirical Section

use the spatial cues and to estimate the true %CV. At the end of each block, participants had to explicitly state their estimated %CV using a vertical 9 point scale ranging from 10% to 90%. A vertical scale instead of a horizontal one was used to avoid spatial biases. For the main trials, RTs and accuracy of the target discrimination were measured. Each participant completed a short practice before the experimental session consisting of one block with constant 75%CV. However, here was also no information about the %CV provided. Each participant was presented with the same sequence of trials within each block and same sequence of blocks (80%CV, 40%CV and 60%CV). The duration of the paradigm was around 16 minutes with two breaks between the blocks.

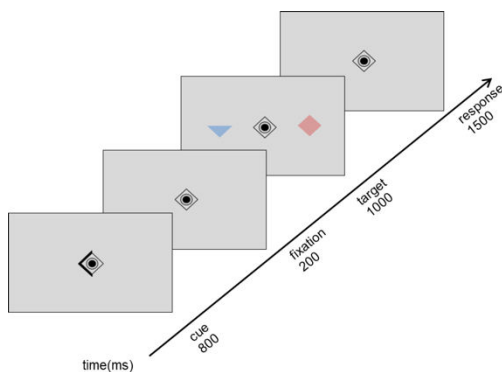


Figure 2.5 Experimental paradigm with one example trial (valid trial). On each trial, participants indicated whether the target triangle was pointing up- or downwards. The participants were asked to maintain central fixation throughout the experiment.

Behavioral Data Analysis

Reaction Times and Validity Effects

Reaction times (RTs) were measured for each trial. Anticipations (RT <100 ms), misses, and incorrect responses were excluded from the analyses, and mean RT was computed separately for left and right valid and invalid trials.

The validity effect (VE) is the difference in RTs between invalid and valid trials and reflects the time necessary to reorient attention from an expected to an unexpected location (Posner, 1980). To test if the VE was affected by the different %CV levels (i.e., if the participants

2. Empirical Section

inferred the actual %CV in the different blocks), the VE was calculated separately for each %CV block (see Figure 2.6).

For the group-level analyses, averaged accuracy scores expressed in percentage of correct responses were used in a 2 x 3 ANOVA with the within-participant factor *validity* (valid, invalid) and the between-participant factor *group* (LH, RH, HC). Because both conditions showed mild violations from normality, we also used nonparametric Kruskal-Wallis test as control analysis. The results of the ANOVA were confirmed by the nonparametric test; therefore, only the former will be presented.

Since the manipulation of %CV was expected to mainly influence the speed of responding, mean RTs in each %CV block were subjected to a 3 x 2 x 3 ANOVA with the within-participant factors %CV (80%CV, 60%CV, 40%CV) and *validity* (valid, invalid) and the between-participant factor *group* (LH, RH, HC). Two conditions showed mild violations from normality, so we added nonparametric Kruskal-Wallis tests as control analyses. The results of the ANOVA were confirmed by the nonparametric tests; therefore, only the former will be presented.

To account for the generally slower responses in patients revealed by the ANOVA on raw RT, RTs were normalized to the mean RT of all trials and the analyses of the VEs were calculated on the basis of normalized RT.

Block-wise VEs were then analyzed with 3 x 3 ANOVA on the normalized VE (RT difference between invalid and valid trials) with the within-participant factor %CV (80%CV, 60%CV, 40%CV) and the between-participant factor *group* (LH, RH, HC). Here, we expected to find a significant linear trend for the %CV effect, since this would reflect the adaptation of behavior to %CV, i.e., inference of the actual %CV levels by the participants. One condition showed a mild violation from normality, so we added nonparametric Kruskal-Wallis tests as control analyses. The results of the ANOVA were confirmed by the nonparametric tests; therefore, only the former will be presented.

To compare deviations of the patient performance from healthy controls, the patient data was z-transformed by subtracting the mean of the healthy controls from the individual patient

2. Empirical Section

value and dividing this by the standard deviation of the healthy controls. This was done separately for the contra- and ipsilesional side of target appearance. We calculated a 2 x 2 x 2 ANOVA with the within-participant factors *side* (ipsilesional, contralesional) and *validity* (valid, invalid) and the between-participant factor *group* (LH, RH) on the z-standardized accuracy scores. Moreover, we calculated a 2 x 2 x 2 ANOVA with the within-participant factors *side* (ipsilesional, contralesional), and *validity* (valid, invalid) and the between-participant factor *group* (LH, RH) on the z-standardized RT, as well as a 2 x 2 ANOVA with the within-participant factor *side* (ipsilesional, contralesional) and the between-participant factor *group* (LH, RH) on the z-standardized normalized VE averaged over all %CV blocks. Note that, when averaging across the %CV-blocks, the sign for the counterpredictive 40%CV block was not flipped. This was due to the observation that the validity effects were not reversed in this block, owing to the fact that the participants were not informed about the %CV levels and had to infer them from trial-to-trial observations. Since the 40% block was preceded by the 80% block, it is very likely that the subjective %CV estimates would not fall below 50%.

In additional analyses, the factor *used hand* was included as a between-participant factor in all the ANOVAs. Moreover, since the data were acquired in a more complex study design where different versions of the experimental paradigm probing also feature-based and motor attention were as well assessed, we investigated the influence of version order on the relevant effects. Hence, in additional analyses, the factor *order* with three levels (first, middle, last) was included as a between-participant factor in all the ANOVAs examining if the position when participants did the spatial version had an effect.

All group-level analyses (also the probabilistic inference ones) were performed with SPSS (SPSS Statistics for Windows, version 25.0, IBM). Results from these analyses are reported at a significance level of $p < 0.05$ after Greenhouse–Geisser correction where applicable. Paired-sample and two-sample t-tests (with Bonferroni correction) were computed to interpret interaction effects.

2. Empirical Section

Probabilistic Inference

To quantify the influence of %CV on RTs in valid and invalid trials (i.e. to assess probabilistic inference) we calculated linear regressions applying a model with intercept on the raw RTs in left and right valid and invalid trials with the regressor %CV for each participant using MATLAB (R2017b, The MathWorks, Inc., Natick, Massachusetts, United States). The resulting regression weights of %CV were subjected to a 2 x 3 ANOVA with the within-participant factor *validity* (valid, invalid) and the between-participant factor *group* (LH, RH, HC). Furthermore, the regression weights were tested for normality (skewness and kurtosis within ± 2 (George & Mallery, 2010) and in cases of violation from normality, nonparametric Kruskal-Wallis tests were further calculated as control analyses.

To compare deviations of the patient performance from healthy controls the regression weight for %CV was z-standardized. The z-transformed regression weights were then analyzed with a 2 x 2 x 2 ANOVA with the within-participant factors *side* (ipsilesional, contralesional) and *validity* (valid, invalid) and the between-participant factor *group* (LH, RH). Again, we also included the factor *used hand* and *order* as additional factors in the above mentioned ANOVAs. There were no deviations from normality for the regression weights for %CV, so no further tests were computed.

Mean scores of the explicit evaluation of %CV, as given by the patients and healthy controls at the end of each block, were tested for normality and analyzed with an ANOVA with the within-participant factor %CV (80%CV, 60%CV, 40%CV) and the between-participant factor *group* (LH, RH, HC). There were no deviations from normality for the explicit evaluations and thus, no further non-parametric test needed. Moreover, the influence of *order* on the relevant main and interaction effects was analyzed. Two-sample t-tests (with Bonferroni correction) were computed to interpret interaction effects.

Since RH patients showed by trend deficits in probabilistic inference indicated by a reduced modulation of RTs by %CV in invalid contralesional trials and issues in estimating the explicit %CV, we conducted an exploratory correlation of these parameters (invalid contralesional

2. Empirical Section

%CV regression weight & averaged explicit %CV estimate) using Spearman's rho correlation coefficient to further explore their relationship.

Relationship of Neuropsychological Data and Task Behavior

To examine the relationship between probabilistic inference in the location-cueing task and neglect-related symptoms, correlations between the %CV regression weight, the averaged explicit %CV, contralesional reorienting and neuropsychological neglect test performance were analyzed. Since the data analyses described above showed (by trend) the strongest deviations of the regression weight for invalid contralesional trials, the correlation analyses were restricted to this measure.

The results from the figure copying, clock drawing and reading test were not analyzed due to a lack of patients showing neglect symptoms (figure n=1; reading n=1; clock n=0). For the three cancellation tests, a mean lateralization index (LI) was calculated.

The Spearman's rank correlation coefficients between the z-standardized invalid contralesional %CV regression weight, the averaged explicit %CV across blocks, the z-standardized contralesional VE averaged over all %CV blocks, and the neuropsychological scores of the mean LI as well as the PB and RB of the Landmark-M task were calculated. To check if outliers drove the correlations, we calculated Cook's distance (Cook, 1977). If Cook's distance values were > 1 (Stevens, 1996) for a given patient, the correlations were recalculated without this patient to check if the significant relationship persisted. All correlations were further calculated for RH and LH separately.

Lesion Analyses

Voxel-based Lesion-symptom Mapping

Lesion mapping was based on clinical imaging by computed tomography (CT) (n=8) or MRI (n=39). A semi-automated lesion delineation approach using the Clusterize toolbox (Clas et

2. Empirical Section

al., 2012; De Haan et al., 2015) was applied. Normalization of CT or MRI scans and the corresponding lesions to MNI space with $1 \times 1 \times 1 \text{ mm}^3$ resolution was performed by using the Clinical Toolbox (Rorden et al., 2012) under SPM12 (Statistical Parametric Mapping software, the Wellcome Department of Imaging Neuroscience, London, UK, www.fil.ion.ucl.ac.uk/spm), which provides age-specific templates in MNI space for both CT and MRI scans and uses lesion cost function masking (Brett et al., 2001). The lesion mapping was double-checked by another investigator; both investigators had to agree on lesion location and extent.

Since some patients under- and others overestimated the averaged explicit %CV, the absolute values of the z-transformed patient data was used as a parameter for impairments in explicitly estimating the %CV for the VLSM.

Voxel-based lesion-symptom mapping (VLSM) was carried out using the non-parametric mapping (NPM) program (Rorden et al., 2007) (distributed with MRICron, <https://people.cas.sc.edu/rorden/mricron/index.html>). Lesion-symptom associations for the z-standardized invalid contralesional %CV regression weight, the absolute values of the z-standardized averaged explicit %CV across blocks, the z-standardized contralesional VE, and the neuropsychological scores of the mean LI as well as the PB and RB of the Landmark-M task were assessed. In VLSM, *t*-tests on the behavioral scores are performed at each voxel, with groups defined by the presence or absence of damage in each voxel (Bates et al., 2003). Thereby, voxels in which damage is associated with a task deficit can be identified. Only voxels damaged in at least 2 of the 47 patients ($n = 2$) were included in the analysis. The statistical threshold was set to $p < .05$ (corrected by FDR to control for multiple comparisons) with a minimum cluster size of 10 voxels. Furthermore, analyses were also conducted for RH and LH patients separately. For variables of main interest, the threshold was lowered to an uncorrected threshold of $p < 0.05$ if no significant findings were obtained at a corrected threshold to look for trends in the results.

The results were localized anatomically using the Automatic Anatomical Labelling atlas for grey matter brain regions (AAL; Tzourio-Mazoyer et al., 2002) distributed with MRICron

2. Empirical Section

(Rorden et al., 2007; www.nitrc.org/projects/mricron). The localization of white matter fiber tracts damaged by the lesion was based on the “JHU-atlas” (Hua et al., 2008) and the atlas provided by Rojkova et al. (2016).

Lesion-network Mapping

In order to assess the relevance of disconnected white matter tracts, lesions from each patient were mapped onto tractography reconstructions of white matter pathways obtained from a group of healthy controls (Rojkova et al., 2016) using the BCBtoolkit (Foulon et al., 2018; <http://www.toolkit.bcblab.com>). Furthermore, disconnectome maps were calculated using the BCBtoolkit (Foulon et al., 2018). This approach uses a set of 10 healthy controls (Rojkova et al., 2016) diffusion weighted imaging datasets to track fibers passing through each lesion. For each participant tractography were estimated as indicated in Thiebaut de Schotten et al. (2011). Patients' lesions in the MNI152 space were registered to each control native space using affine and diffeomorphic deformations (Avants et al., 2011; Klein et al., 2009) and subsequently used as seed for the tractography in Trackvis (Wang & Benner, 2007). Tractographies from the lesions were transformed in visitation maps (Thiebaut de Schotten, Ffytche, et al., 2011), binarised and brought to the MNI152 space using the inverse of precedent deformations. Finally, a percentage overlap map was produced by summing at each point in MNI space the normalized visitation map of each healthy participant. Hence, in the resulting disconnectome map, the value in each voxel takes into account the interindividual variability of tract reconstructions in controls, and indicates a probability of disconnection from 0 to 100% for a given lesion (Thiebaut de Schotten et al., 2015). For the disconnectomes of our patients, the default threshold of >50% probability of disconnection was chosen. Additionally, the severity of the disconnection was quantified by measuring the probability of the tract to be disconnected using Tractotron software as part of the BCBtoolkit (Thiebaut De Schotten et al., 2014; Foulon et al., 2018). In the subsequent statistical analyses using SPSS, the impact of white matter tract disconnection on behavioral

2. Empirical Section

parameters, i.e. the z-standardized invalid contralesional %CV regression weight, the averaged explicit %CV across blocks, the z-standardized contralesional VE, and the neuropsychological scores of the mean LI as well as the PB and RB of the Landmark-M task, was analyzed by dividing patients into those whose lesions spared a particular tract and those whose lesions disconnected the tract with at least 50% probability. Then, the scores in the different behavioral test parameters were compared between these groups using Mann-Whitney U tests (see Machner, Könemund, von der Gablentz, Bays, & Sprenger, 2018 for a similar approach). Once again, these analyses were also conducted for RH and LH groups separately.

Furthermore, due to our a priori hypothesis of an involvement of rTPJ in probabilistic inference, it was evaluated if the disconnection maps of the patients affected the rTPJ (ROI from experiment 1 with an 8 mm radius sphere centered at $x = 56$, $y = -44$, $z = 12$) and the patients were divided into two groups, respectively. Using Mann-Whitney U tests, it was investigated if there were significant differences between these two groups with and without rTPJ involvement in the behavioral parameters.

Single Case Comparison

To investigate the long term effects of the neglect syndrome on attentional reorienting and probabilistic inference, two RH patients exhibiting spatial neglect were reassessed with the same experimental task and some of the neuropsychological tests after six months. Only these two were reassessed since they were the only patients showing neglect symptoms who also gave written permission for a six months follow-up assessment. They were again screened for cognitive decline and aphasia (using MMST and ACL-K). Furthermore, they had to complete the letter cancellation test, the star cancellation test, figure copying, clock drawing, MWCT and Landmark-M tests and were assessed for extinction.

2. Empirical Section

Results

Neuropsychological Examination

Table 3 displays the number of patients who fulfilled the criteria for extinction and neglect in the different neuropsychological tests. Regarding the Landmark-M test, the scores can be classified in medium and strong: The RH patient showing a PB had a strong bias ($PB > 63.91$). In case of the RB, two RH and two LH patients exhibited a medium bias ($RB > 51.74$), whereas four RH and two LH patients had a strong bias ($RB > 52.84$).

Table 3 Overview of patients fulfilling the criteria for extinction and neglect.

Neuropsychological test	LH (yes/no)	RH (yes/no)
Letter cancellation (n=46)	0/21	1/25
Star cancellation (n=46)	0/21	0/25
MWCT (n=46)	0/21	2/23
Figure copying (n=46)	0/21	1/25
Reading (n=44)	0/20	1/23
Clock drawing (n=46)	0/21	0/25
PB (n=47)	0/21	1/25
RB (n=47)	4/17	6/20
Extinction (n=41)	0/18	4/19

Behavioral Results

Reaction Times and Validity Effects

Overall, the average accuracy amounted to 94% (± 0.70 SEM). The ANOVA on accuracy scores with the between-participant factor *group* (LH, RH, HC), and the within-participant factor *validity* (valid, invalid) revealed a main effect of *validity* ($F(1,77)=37.737$, $p= 3.31 \times 10^{-8}$, $\eta_p^2=0.329$) with higher accuracy in valid trials. The factor *group* and the interaction did not reach significance.

The ANOVA on mean RT with the within-participant factors %CV (80%CV, 60%CV, 40%CV), and *validity* (valid, invalid) and the between-participant factor *group* (LH,RH, HC) revealed a main effect of *group* ($F(2,77) = 4.7$, $p=0.012$, $\eta_p^2=0.109$), a main effect of *validity* ($F(1,77) = 42.8$, $p= 6.05 \times 10^{-9}$, $\eta_p^2=0.357$) with higher RTs in invalid trials, as well as a

2. Empirical Section

significant $\%CV \times validity$ interaction ($F(2,154) = 21.7, p = 4.87 \times 10^{-9}, \eta_p^2=0.220$). Pairwise comparisons (Bonferroni corrected threshold $p=0.016$) showed that RH patients had significantly higher RTs compared to healthy controls ($t(57)=2.9, p=0.005$; significant after Bonferroni correction). HC and LH patients ($t(52)=2.1, p=0.04$; not significant after Bonferroni correction) and the two patient groups did not show any significant differences ($t(45)=-0.8, p=0.408$). The factor $\%CV$ and all other interactions did not reach significance.

To further interpret the $\%CV \times validity$ interaction and to consider the difference in overall response times between the different groups, we subjected the normalized difference in RTs between invalid and valid trials, i.e., the normalized block-wise VE, to a 3×3 ANOVA with the within-participant factor $\%CV$ (80%CV, 60%CV, 40%CV), and the between-participant factor *group* (LH, RH, HC). As expected, the linear trend for the $\%CV$ main effect was significant ($F(1,77) = 30.4, p = 4.58 \times 10^{-7}, \eta_p^2=0.283$) (see Figure 2.6). This confirms that the participants inferred the actual $\%CV$ levels in the present paradigm. Neither the main effect of *group* nor the interaction with *group* were significant.

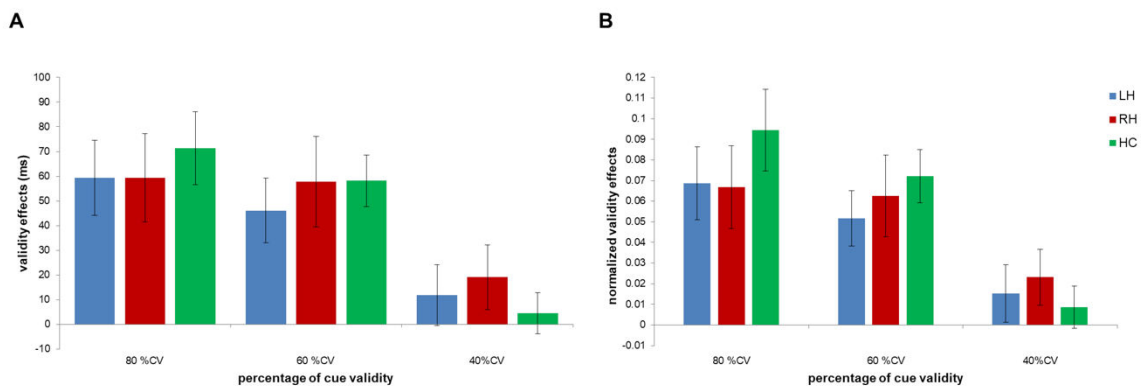


Figure 2.6 A Block-wise validity effects (RT invalid minus RT valid) (mean \pm SEM) for each $\%CV$ block. B Normalized validity effects (RT invalid minus RT valid) (mean \pm SEM) for each $\%CV$ block. The validity effects vary linearly with actual $\%CV$.

To investigate potential performance deviations of the two patient groups from controls and to tests for lateralization effects, z-scores for accuracy and RT were subjected to the same analyses with the additional factor *side* (contralesional, ipsilesional).

2. Empirical Section

For accuracy, the 2 x 2 x 2 ANOVA with the within-participant factors *side* (ipsilesional, contralesional) and *validity* (valid, invalid) and the between-participant factor *group* (LH, RH) did not reveal any significant main effects or interactions (all p-values > 0.163).

Moreover, the 2 x 2 x 2 ANOVA on z-transformed RTs with the within-participant factors *side* (ipsilesional, contralesional), and *validity* (valid, invalid) and the between-participant factor *group* (LH, RH) showed a main effect of *side* ($F(1,45) = 10.0$, $p=0.003$, $\eta_p^2=0.183$), with higher deviations of the RT for the contralesional side. The main effects of *validity* and *group* and all interactions were not significant.

For the 2 x 2 ANOVA on the z-standardized normalized VE averaged over all %CV blocks with the within-participant factor *side* (ipsilesional, contralesional) and the between-participant factor *group* (LH, RH) no significant main or interaction effects were found (all p-values > 0.587).

Furthermore, the additional analyses with the between-participant factor *used hand* did not reveal any significant main effects or interaction effects with this factor (all p-values > 0.331).

The additional analyses with the between-subject factor *order* showed a significant *order* x *group* interaction for the normalized VE ($F(4,71) = 3.2$, $p=0.018$, $\eta_p^2=0.153$). Separate one-way ANOVAS (Bonferroni corrected threshold $p=0.016$) for each group with the factor *order* revealed a trend for a difference in RH patients ($F(2,25) = 3.9$, $p=0.04$; not significant after Bonferroni correction). If RH patients did the spatial task first, they displayed low normalized VEs, whereas if they did the task later, their normalized VEs were positive (see Figure 2.7).

There was no difference for the LH patients ($p=0.465$) or HC ($p=0.341$). Moreover, for the z-standardized RT there was a significant *validity* x *group* x *order* interaction ($F(2,41) = 4.0$, $p=0.026$, $\eta_p^2=0.164$). However, two-sample t-tests (Bonferroni corrected threshold $p=0.016$) for each order separately did not reveal any group differences (all p-values > 0.226).

Furthermore, also for the z-standardized normalized VE averaged over all %CV blocks for each side separately a significant *order* x *group* interaction was discovered ($F(2,41) = 4.0$, $p=0.027$, $\eta_p^2=0.162$). Post-hoc two-sample t-tests (Bonferroni corrected threshold $p=0.016$) revealed a trend for a group difference, with RH patients deviating more negatively (from

2. Empirical Section

HC) than LH patients (who did not deviate from HC) if they did the spatial task first ($t(10)=2.8$, $p=0.02$; not significant after Bonferroni correction). If they did the spatial task later, there were no group differences (middle: $t(19)=-1.4$, $p=0.164$; last: $t(12)=-0.2$, $p=0.867$).

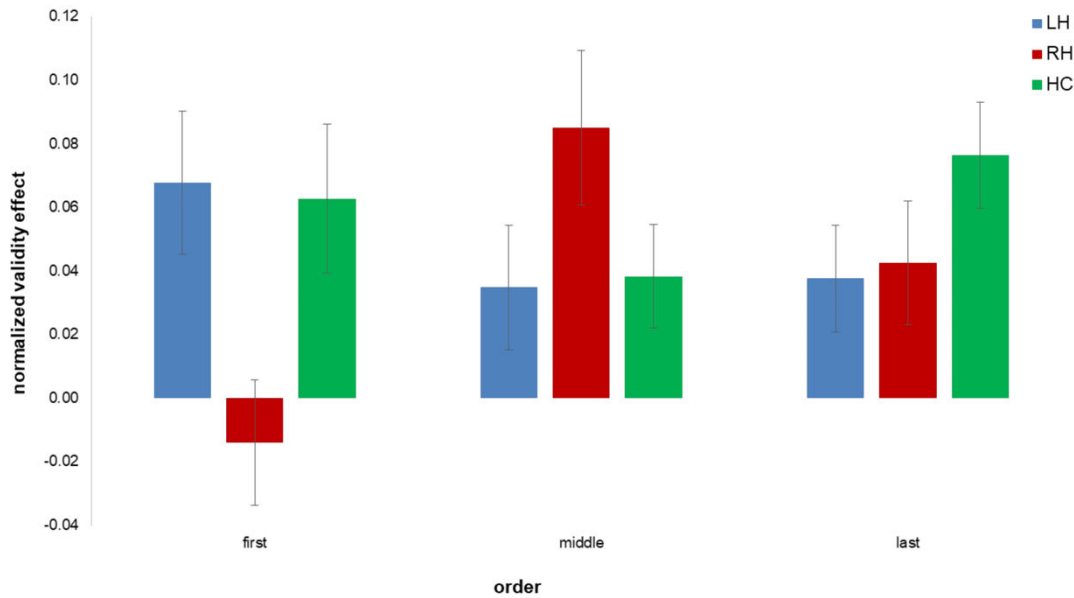


Figure 2.7 Effect of order on the normalized validity effect (mean \pm SEM).

Probabilistic Inference

Regarding probabilistic inference, the regression weights of %CV on mean RT in the different conditions in each participant were compared with a 2 x 3 ANOVA with the within-participant factor *validity* (valid, invalid) and the between-participant factor *group* (LH, RH, HC). A main effect of *validity* ($F(1,77) = 33.6$, $p=1.44 \times 10^{-7}$, $\eta_p^2=0.303$) was found, with higher regression weights of %CV for invalid than for valid RTs. As expected, in healthy controls, regression weights were negative for valid and positive for invalid trials (see Figure 2.8 A), reflecting a decrease of RTs with higher %CV in valid and an increase with higher %CV in invalid trials. Despite this pattern was not consistently observed in patient groups, neither the main effect of *group* nor any interaction with group was significant.

As with the analyses of the parameters of reorienting attention, the analyses were performed on z-transformed regression weights and the additional factor side (contralesional,

2. Empirical Section

ipsilesional). A 2 x 2 x 2 ANOVA with the within-participant factors *side* (ipsilesional, contralesional) and *validity* (valid, invalid) and the between-participant factor *group* (LH, RH) revealed no significant main or interaction effect, although a trend for a *side* x *validity* x *group* interaction was observed ($F(1,45) = 3.2$, $p=0.079$, $\eta_p^2=0.067$; driven by the invalid contralesional condition, see Figure 8B).

Furthermore, the additional analyses with the between-participant factor *used hand* did not yield any significant effects of this factor (all p -values > 0.325).

Moreover, the analyses of the influence of *order* revealed no main or interaction effects regardless of whether the regression weights of %CV (all p -values > 0.233) or the z-standardized version was used (all p -values > 0.138).

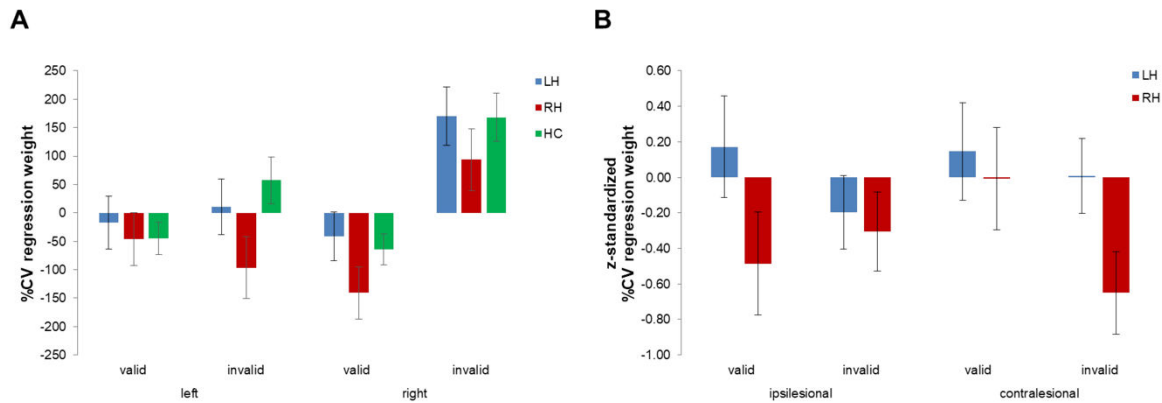


Figure 2.8 A %CV regression weights (mean ± SEM) for each condition for all three groups. RH patients deviated the most in the left invalid condition from HC and LH patients. B z-standardized %CV regression weights (mean ± SEM) for the two patient groups. The RH patients differed the most in the invalid contralesional condition.

The 3 x 3 ANOVA on the mean scores of the explicit evaluation of %CV with the within-participant factor %CV (80%CV, 60%CV, 40%CV) and the between-subject factor *group* (LH, RH, HC) revealed that the linear trend for the %CV main effect was significant ($F(1.9,142.7) = 44.0$, $p= 7.25 \times 10^{-15}$, $\eta_p^2=0.364$), reflecting learning of the actual %CV at an explicit level. The main effect of *group* was not significant ($F(2,77) = 2.5$, $p=0.088$, $\eta_p^2=0.061$), but we observed a significant %CV x *group* interaction ($F(4,154) = 2.5$, $p=0.042$, $\eta_p^2=0.062$). To explore this interaction effect, one-way ANOVAs (Bonferroni corrected

2. Empirical Section

threshold $p=0.016$) for the separate %CV blocks were calculated and revealed a significant group difference only for the 80%CV ($F(2,77) = 6.1$, $p=0.003$, significant after Bonferroni correction; 60%CV: $p=0.637$; 40%CV: $p=0.492$). Further post-hoc two-sample t-tests (Bonferroni corrected threshold $p=0.005$) revealed that RH patients significantly underestimated the actual %CV level compared to HC ($t(57)=3.3$, $p=0.002$; significant after Bonferroni correction). There was a trend that they also underestimated the actual %CV level compared to LH patients ($t(45)=2.6$, $p=0.011$; not significant after Bonferroni correction). There was no significant difference between LH patients and HC ($t(52)=-0.6$, $p=0.957$).

The additional analyses with the between-participant factor *order* revealed no significant main or interaction effects, although there was a trend for a *group* x *order* interaction ($F(4,71) = 2.5$, $p=0.052$, $\eta_p^2=0.122$) indicating that if RH patients did the spatial task first, their mean estimate was close to the true %CV. Otherwise, they tended to underestimate the %CV (see Figure 2.9).

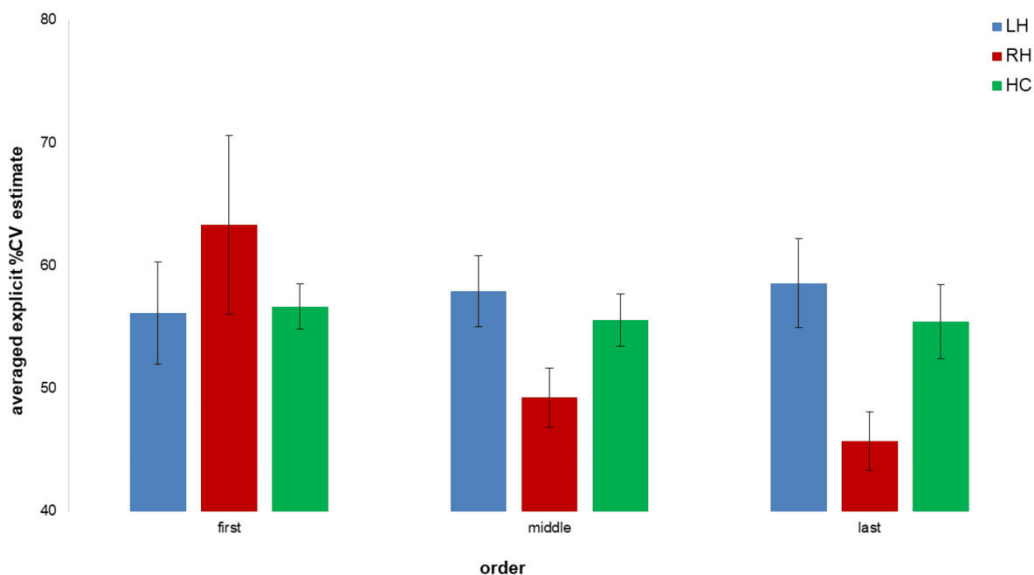


Figure 2.9 Effect of order on the estimation of the explicit %CV (mean \pm SEM).

Furthermore, the exploratory correlation analysis in RH patients of the two probabilistic inference parameters revealed no significant correlation ($r=.152$ $p=.458$, see Figure 2.10).

2. Empirical Section

Hence, the impact of the %CV manipulation on RTs and the participants' explicit estimations of the true %CV levels were not related.

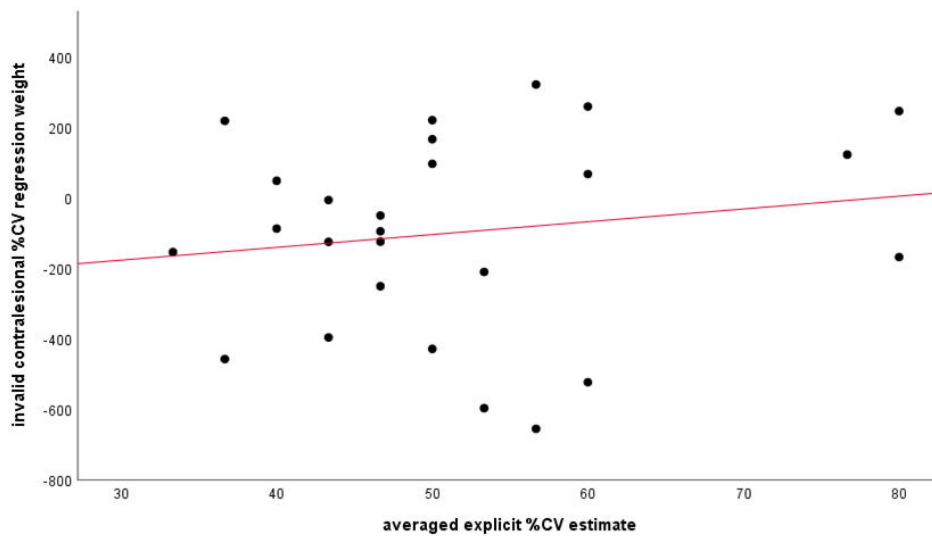


Figure 2.10 Within-group correlation of the two probabilistic inference parameters (invalid contralesional %CV regression weight & averaged explicit %CV estimate) for RH patients only (n=26)

Linking Neuropsychological Deficits to Reorienting and Belief Updating

To examine the relationship between the neglect-related impairments of the patients and reorienting of attention and probabilistic inference in the location-cueing task, respectively, Spearman's rank correlation coefficients between the z-standardized invalid contralesional %CV regression weight, the averaged explicit %CV estimate across blocks, the z-standardized contralesional VE, and the neuropsychological scores of the mean lateralization index as well as the PB and RB of the Landmark-M task were calculated. Correlating these variables in the whole group of patients revealed a significant negative correlation between the RB and the averaged explicit %CV estimate ($r=-.374$, $p=.010$, Figure 2.11 A). Underestimating the %CV was related to higher RB (indicating a tendency towards more frequent responses in ipsilesional space). Furthermore, a significant positive relationship between the z-standardized invalid contralesional %CV regression weight and the RB ($r=0.302$, $p=0.039$, Figure 2.11 B) was revealed. Higher RB-scores were related to

2. Empirical Section

higher %CV regression weights. Moreover, a positive correlation between the z-standardized contralesional VE and the z-standardized invalid contralesional %CV regression weight was found ($r=0.327$, $p=0.025$, Figure 2.11 C) with smaller VEs being related to a smaller influence of true %CV in contralesional invalid trials. The analysis of Cook's distance showed that no outliers drove the correlations (all values <1).

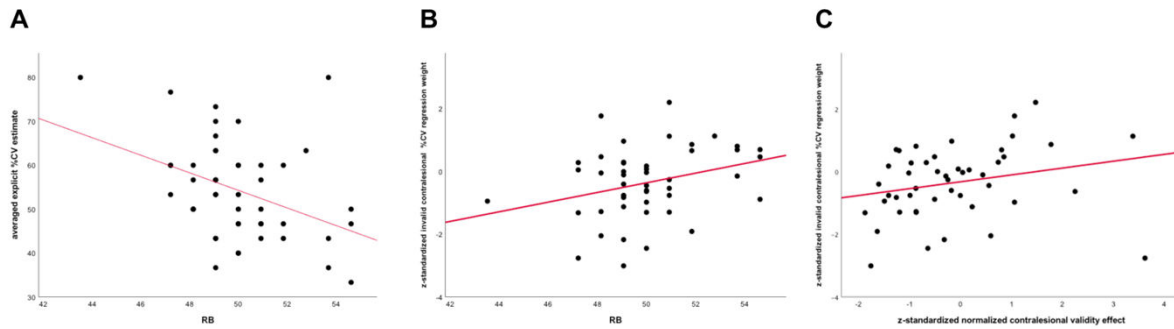


Figure 2.11 Correlations of the neglect and task parameters with all 47 patients.

Within the group of RH patients only, correlations of task behavior with the neglect scores revealed a significant negative correlation of the PB and the normalized VE for contralesional targets ($r=-0.544$, $p=0.004$, Figure 2.12 A). The analysis of Cook's distance indicated that the correlation with the normalized contralesional VE was driven by an outlier, however removing this outlier did not change the result ($r=-0.504$, $p=0.010$). Therefore, higher PB-scores (indicating a neglect of the contralesional line segments) were related to smaller normalized contralesional VEs.

Furthermore, a trend for a positive correlation of the RB and the z-standardized invalid contralesional %CV regression weight ($r=0.379$, $p=0.056$) as well as a trend for a negative correlation of the RB and the averaged explicit %CV estimate ($r=-0.358$, $p=0.073$) were found. Similar to the correlations with all patients, higher RB-scores were related to higher %CV regression weights. Moreover, underestimating the %CV was related to higher RB-scores.

When focusing on LH patients, a positive correlation between the contralesional normalized VE and the z-standardized invalid contralesional %CV regression weight was found ($r=0.496$, $p=0.022$, Figure 2.12 B), which was not driven by any outlier (<1).

2. Empirical Section

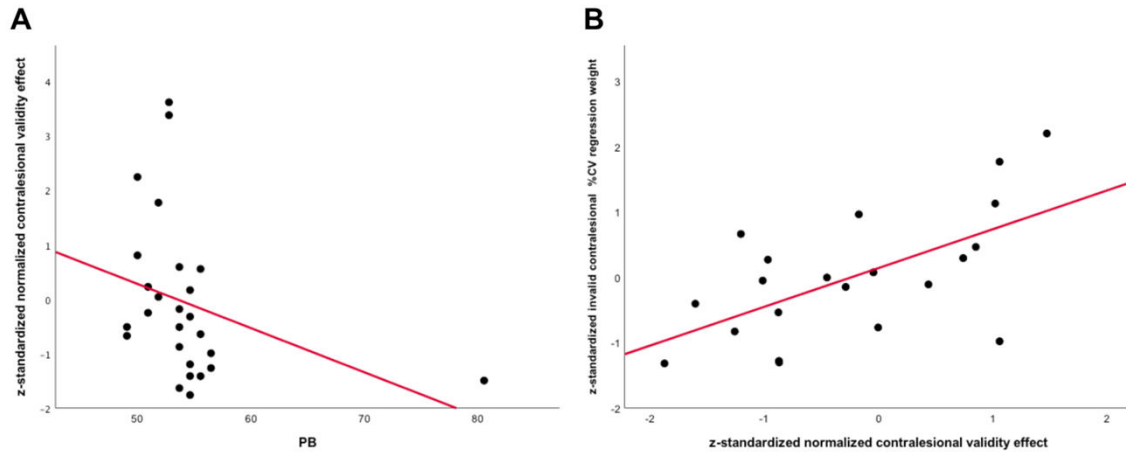


Figure 2.12 Within-group correlations of the neglect and task parameters for A) RH patients only (n=26) and B) LH patients only (n=21).

Voxel-based Lesion-symptom Mapping (VLSM)

Figure 2.13 depicts the lesion distribution of the current sample of 47 stroke patients.

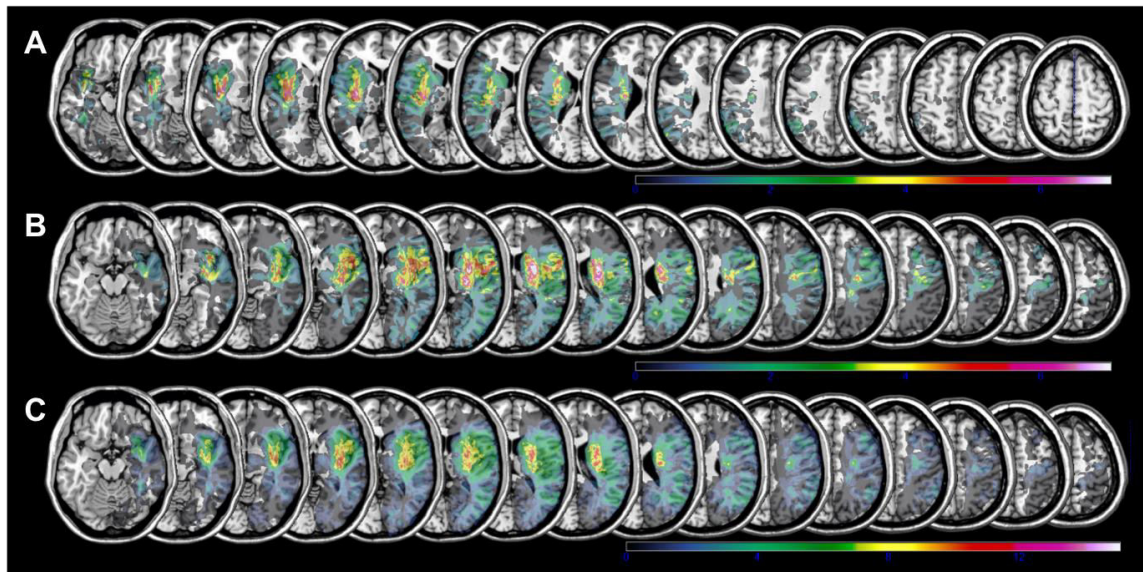


Figure 2.13 Lesion distribution of the current sample of stroke patients (n=47). Color shades represent the number of overlapping lesions. Slices with the MNI-z-coordinates from -16 to 59 are shown. A Lesion overlay of LH patients only (n=21). B Lesion overlay of RH patients only (n=26). C Lesion overlay of all patients flipped on the RH (n=47).

The results of the VLSM with all patients using a threshold of a lesion overlap of a minimum of two patients revealed significant voxels for the parameter of the mean LI (Figure 2.14 A)

2. Empirical Section

and the PB (Figure 2.15 A). Performing the analyses only with RH patients replicated the results (Figure 2.14 B and Figure 2.15 B) and running the VLSM only with LH patients did not lead to any significant voxels surviving the statistical threshold.

Both analyses suggested that omissions in contralesional space (i.e., a negative mean LI) were associated with widespread damage of fronto-parietal, occipital, as well as subcortical areas and white matter tracts, especially the putamen and the superior longitudinal fasciculus. Higher PB-scores were related to similar lesion locations as the mean LI (Figure 2.15).

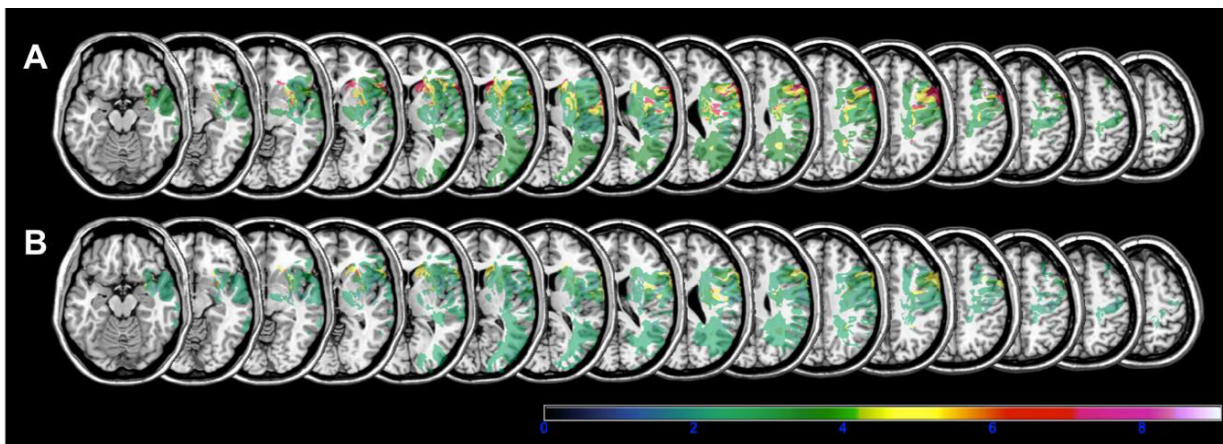


Figure 2.14 VLSM result for mean LI thresholded at FDR $p < 0.05$ A for all patients ($n=46$). B RH patients only ($n=25$). Slices with the MNI-z-coordinates from -16 to 59 are shown.

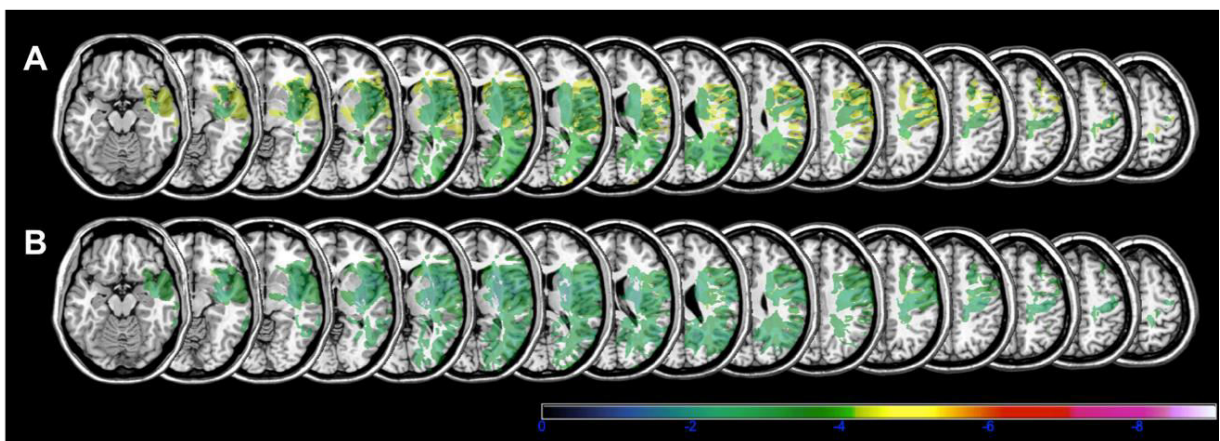


Figure 2.15 VLSM result for PB thresholded at FDR $p < 0.05$ A for all patients ($n=47$). B RH patients only ($n=26$). Slices with the MNI-z-coordinates from -16 to 59 are shown.

2. Empirical Section

The VLSM analyses of the RB scores, the contralesional VE and the signatures of probabilistic inference did not reveal any significant lesion correlates at corrected statistical thresholds. Still, the results of the lesion overlap ($n=2$) are reported at an uncorrected threshold of $p < 0.05$ in the following. VLSMs were only performed for a given variable if patients deviated in the parameters from healthy control (as reflected in a Z-score of ± 1.96).

Since only RH patients deviated in the z-standardized normalized contralesional VE and the z-standardized invalid contralesional %CV regression weight from healthy controls, we only calculated VLSMs for the absolute values of the z-standardized averaged explicit %CV estimate and the RB of the Landmark-M task for all patients. Impairments in estimating the averaged explicit %CV were related to lesions of the basal ganglia, insula, IFG, middle and superior temporal gyrus, Heschl's gyrus, temporal pole, operculum, thalamus and white matter (Figure 2.16 A). Moreover, higher RB-scores were linked to lesions affecting the right putamen and bihemispheric white matter (Figure 2.16 B).

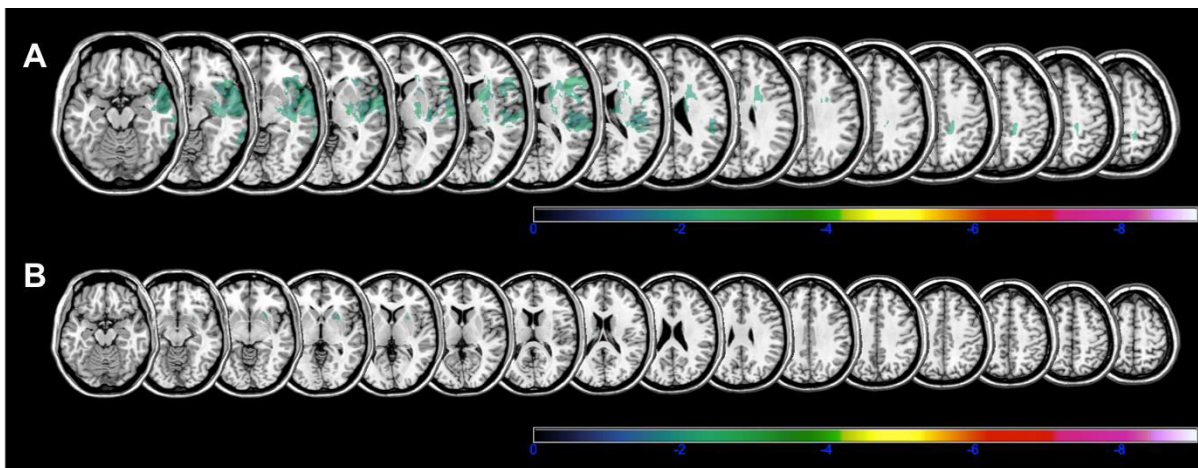


Figure 2.16 VLSM results thresholded at $p < 0.05$ uncorrected ($n=47$) for **A** the absolute values of the z-standardized averaged explicit %CV. **B** higher RB-scores. Slices with the MNI-z-coordinates from -16 to 59 are shown, panel B shows the lesions with a smaller overlap of the two hemispheres.

Performing these analyses for RH patients only, it was revealed that higher z-standardized normalized contralesional VEs were linked to lesions affecting the middle temporal gyrus, including TPJ, and white matter (Figure 2.17 A). Furthermore, lower z-standardized invalid

2. Empirical Section

contralesional %CV regression weights (reflecting a diminished impact of %CV on RTs in this condition) were related to lesion of the insula, temporal pole, thalamus and some white matter pathways (Figure 2.17 B). Impairments in the estimation of the averaged explicit %CV were related to damage of the pallidum, insula, IFG, STG and pole, Heschl's gyrus, operculum, thalamus and white matter (Figure 2.17 C). Furthermore, higher RB-scores (indicating a tendency towards more frequent responses in ipsilesional space) were linked to lesions of the putamen (Figure 2.17 D).

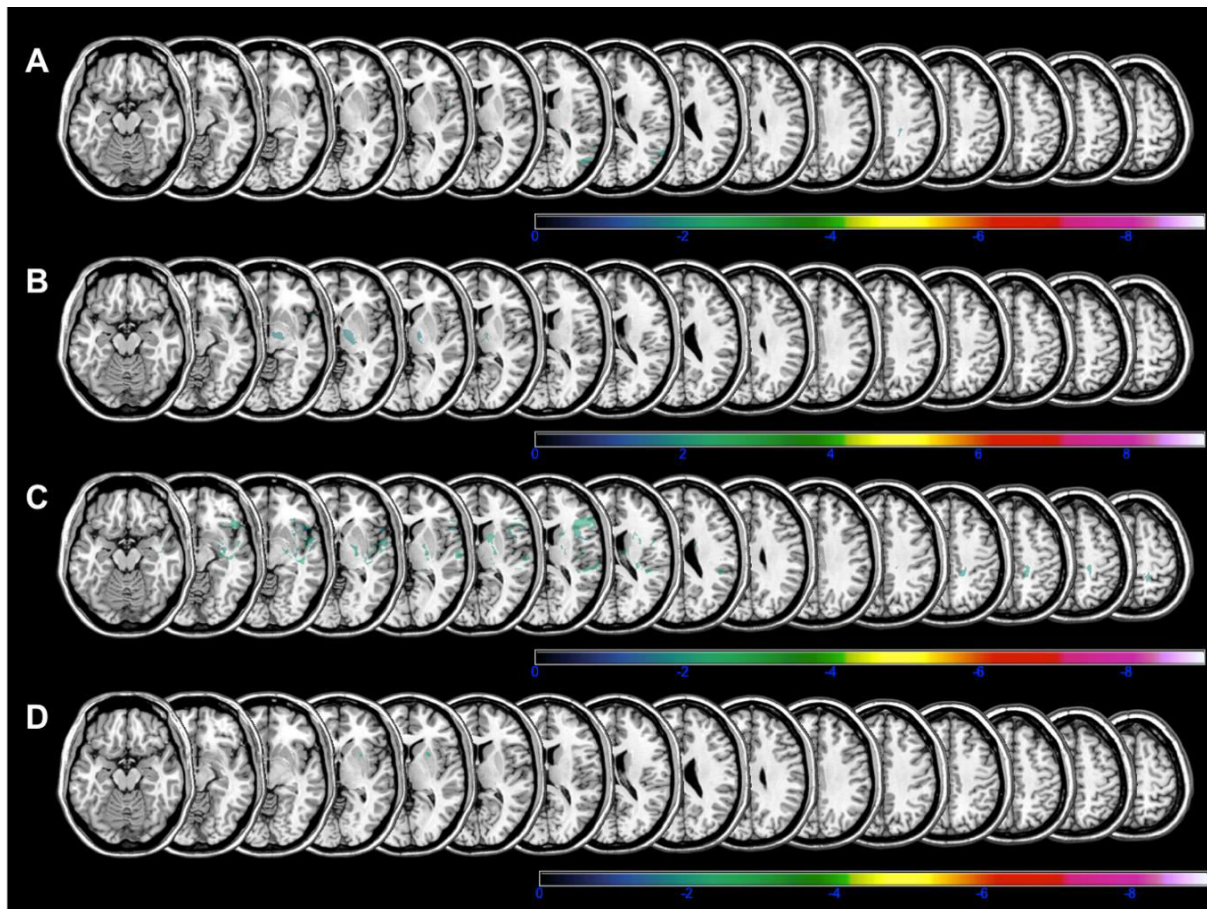


Figure 2.17 VLSM results of RH patients only thresholded at $p < 0.05$ uncorrected ($n=26$) for **A** the z-standardized normalized contralesional VE. **B** the z-standardized invalid contralesional %CV regression weight. **C** the absolute values of the z-standardized averaged explicit %CV. **D** higher RB-scores. Slices with the MNI-z-coordinates from -16 to 59 are shown.

Since LH patients did not exhibit any deficits in the mean LI, PB, z-standardized normalized contralesional VE and the z-standardized invalid contralesional %CV regression weight, we only calculated VLSMs for the absolute values of the z-standardized averaged explicit %CV

2. Empirical Section

estimate and the RB of the Landmark-M task. Estimating the VLSMs with LH patients only, it was found that estimation impairments of the averaged explicit %CV were linked to lesions affecting the left HPC, parahippocampal gyrus, fusiform area, inferior temporal gyrus, cerebellum and white matter pathways including ILF and IFOF (Figure 2.18 A). Moreover, higher RB-scores were linked to lesions affecting the inferior frontal triangular gyrus, the caudate, the superior temporal pole and white matter tracts (Figure 2.18 B).

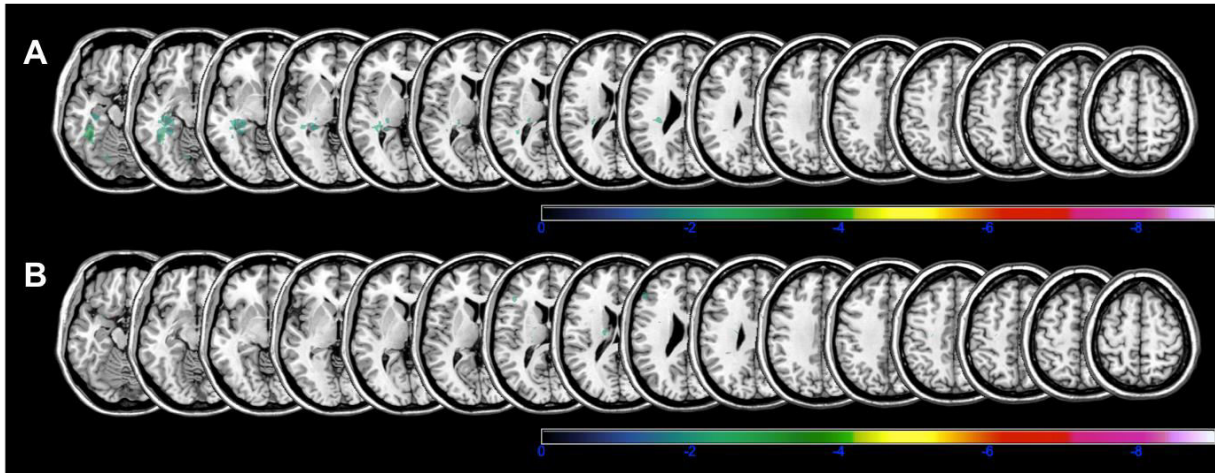


Figure 2.18 VLSM results of LH patients only thresholded at $p < 0.05$ uncorrected ($n=21$) for A the absolute values of the z-standardized averaged explicit %CV. B higher RB-scores. Slices with the MNI-z-coordinates from -16 to 59 are shown.

Lesion-network Mapping

In order to analyze the impact of disconnections of the different white matter tracts for neglect behavior, reorienting of attention and probabilistic inference, we applied the Disconnectome and Tractotron software from the BCB toolkit to the patients' lesion data (see Method section). The disconnectome maps, showing those tracts that are disconnected with a probability of $>50\%$ by the patient's lesion, are visualized as an overlap (Fig. 2.19).

In RH patients, the disconnectome maps indicated severe white matter disconnections for the frontoparietal tracts (arcuate, IFOF, ILF, SLF I-III) in the right hemisphere as well as affection of the corpus callosum (CC). However, the disconnectome maps of LH patients

2. Empirical Section

also comprised these tracts in the respective hemisphere as well as a more pronounced disconnection of the optic radiata.

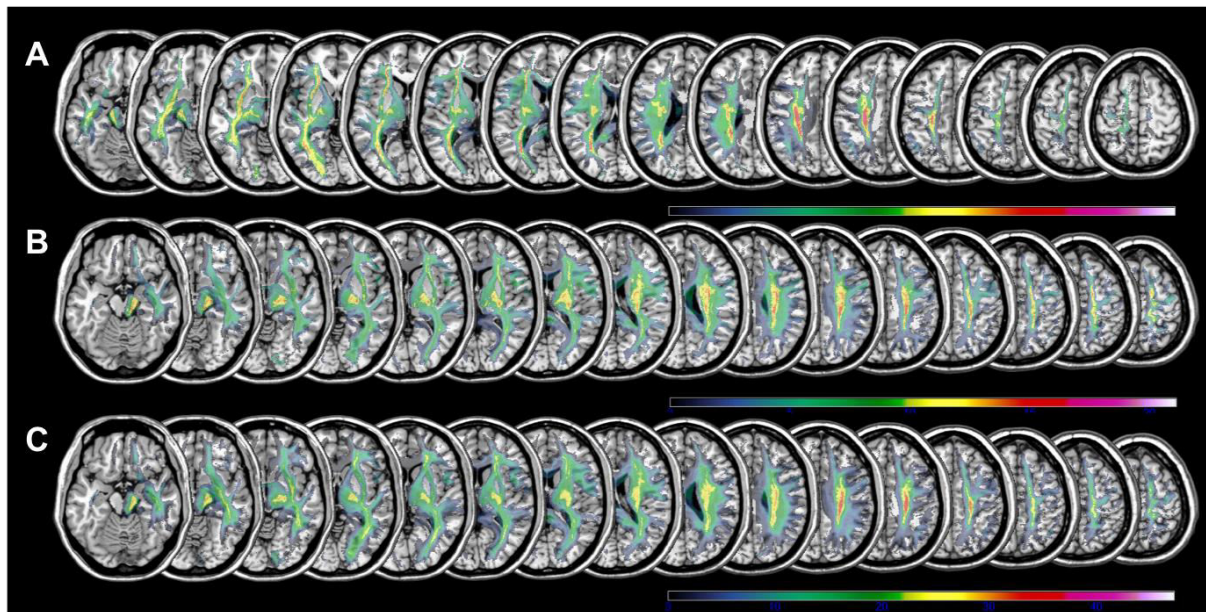


Figure 2.19 Disconnection distribution of the current sample of stroke patients (n=47). Color shades represent the number of overlapping disconnections. Slices with the MNI-z-coordinates from – 16 to 59 are shown. **A** Disconnect overlay of LH patients only (n=21). **B** Disconnect overlay of RH patients only (n=26). **C** Disconnect overlay of all patients flipped on the RH (n=47).

The results of the comparison of the mean results in different behavioral test parameters between patients having relevant tracts spared or disconnected are displayed in Figure 2.20. Since only RH patients exhibited deficits in the mean LI, PB, z-standardized normalized contralesional VE and the z-standardized invalid contralesional %CV regression weight, we only calculated Mann-Whitney U tests for the explicit %CV estimate and the RB of the Landmark-M task as in the VLSMs. Looking at all patients, we did not find any significant differences.

2. Empirical Section

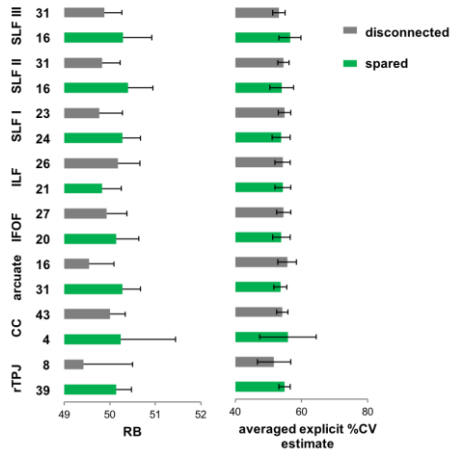


Figure 2.20 Behavioral test performances in relation to white matter tract damage for all patients (n=47). The behavioral test results of the RB of the Landmark-M test and the averaged explicit %CV estimate are depicted as a mean performance of patients without (green) or with (gray) disconnection of different ipsilesional white matter tracts of interest or the rTPJ. The number of patients (n) with or without disconnection of the according tract is provided on the left of the y-axis. Error bars show standard error of the mean.

In RH patients, SLF II damage was related to a smaller mean LI (indicating a higher number of contralesional omissions) ($U=-2.2$, $p=0.026$, see Figure 2.21). Moreover, there were similar trends for SLF I and ILF (both: $U=-1.7$, $p=0.095$).

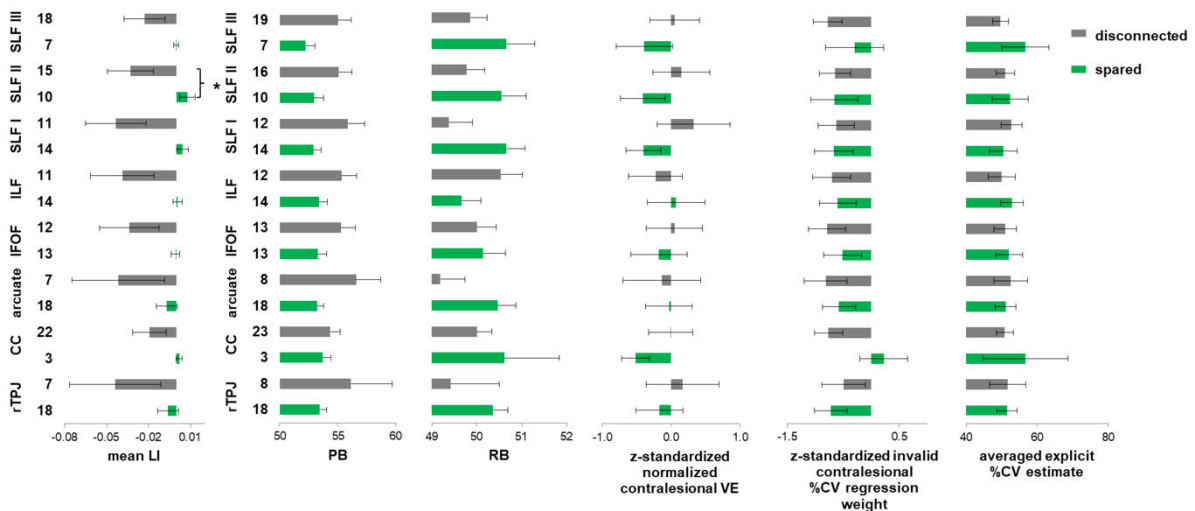


Figure 2.21 Behavioral test performances in relation to white matter tract damage for RH patients (n=25/26). The behavioral test results of the mean LI, the PB and RB of the Landmark-M test, the z-standardized normalized contralesional VE, the z-standardized invalid contralesional %CV regression

2. Empirical Section

weight and the averaged explicit %CV estimate are depicted as a mean performance of patients without (green) or with (gray) disconnection of different white matter tracts of interest or the rTPJ. The number of patients (n) with or without disconnection of the according tract is provided on the left of the y-axis. Error bars show standard error of the mean. * $p < .05$, Mann-Whitney U test.

Since LH patients did not exhibit any deficits in the mean LI, PB, z-standardized normalized contralesional VE and the z-standardized invalid contralesional %CV regression weight, we only calculated Mann-Whitney U tests for the explicit %CV estimate and the RB of the Landmark-M task as in the exploratory VLSMs. There were no significant differences in behavior related to white matter damage (see Figure 2.22).

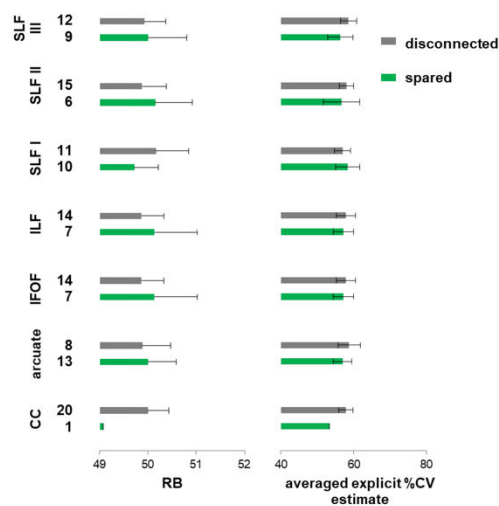


Figure 2.22 Behavioral test performances in relation to white matter tract damage for LH patients (n=21). The behavioral test results of the RB of the Landmark-M test and the averaged explicit %CV estimate are depicted as a mean performance of patients without (green) or with (gray) disconnection of different white matter tracts of interest. The number of patients (n) with or without disconnection of the according tract is provided on the left of the y-axis. Error bars show standard error of the mean.

Furthermore, investigating if there were significant differences in the behavioral parameters between patients having the rTPJ spared or damaged it was found that for RH patients damage of the rTPJ was by trend related to more neglect symptoms as operationalized by the mean LI ($U = -1.8$, $p = 0.074$, see Figure 2.21). However, there was no relation to the other task parameters.

2. Empirical Section

Single Case Comparison

Investigating the long term effects of the neglect syndrome on attentional reorienting and probabilistic inference, two RH patients exhibiting spatial neglect syndrome were assessed with the same experimental task and neuropsychological tests after 6 months. They had to redo the letter cancellation, star cancellation, MWCT and Landmark-M tests. Moreover, they were screened for any signs of depression, dementia and aphasia again. Table 4 displays the values of the comparison. Regarding the screening, the patients' general state had not changed. They did not show any signs of dementia or aphasia, as well as their mood indicated by the GDS seemed constant. However, their neglect symptoms had decreased and their task performance increased. While their general task parameters were constant (mean accuracy and RT), their invalid contralesional %CV regression weight as well as their explicit ratings were better.

Both patients displayed distinct deficit profiles, although both exhibited low normalized validity effects. Patient P1 showed strong neglect symptoms of the contralesional side (as indicated by the mean LI and PB) and he explicitly overestimated the %CV. Patient P2 underestimated the explicit %CV and had a strong negative invalid contralesional %CV regression weight, while his neglect symptoms were only present in the RB and he suffered from visual extinction. Interestingly, recovery of their symptoms led to enhanced task performance in probabilistic inference parameters in both patients. Therefore, it can be assumed that a spatial bias relates to compromised probabilistic inference abilities.

2. Empirical Section

Table 4 Neuropsychological and task parameter data of the two RH neglect patients on their first assessment and six month follow up.

patient	P1		P2	
	1. assessment	6 month follow up	1. assessment	6 month follow up
days since stroke	48	253	20	233
age	51	52	51	52
GDS	4	4	8	8
MMST	27	29	29	29
ACL-K	37	36	40	40
Letter cancellation LI	-0.20	0.05	-0.05	0.00
Star cancellation LI	0.00	0.00	-0.04	0.00
MWCT time (sec)	467	233	311	156
MWCT LI	-0.40	-0.03	0.11	0.00
PB	80.56 PB	53.70 no PB	53.7 no PB	50.93 no PB
RB	43.52 No RB	42.59 No RB	51.85 RB	45.37 No RB
Extinction	no	no	yes	no
Mean accuracy (%)	55.2	49.7	98.3	99.5
Mean RT (ms)	661.23	604.91	955.59	795.46
Normalized ipsilesional VE	-0.13	0.04	0.13	0.06
z-standardized normalized ipsilesional VE	-2.71	-0.42	0.74	-0.16
Normalized contralesional VE	-0.06	0.03	-0.07	0.03
z-standardized normalized contralesional VE	-1.49	-0.22	-1.63	-0.22
Invalid contralesional %CV regression weight	-165.97	200.69	-394.38	34.43
z-standardized invalid contralesional %CV regression weight	-0.94	0.60	-1.91	-0.10
Averaged explicit %CV estimate	80%	60%	43.3%	56.6%
z-standardized averaged explicit %CV estimate	3.12	0.54	-1.62	0.10

2. Empirical Section

Discussion

This study investigated if probabilistic inference abilities are compromised in stroke patients. In a modified location-cueing paradigm, block-wise changes of the %CV were implemented, and probabilistic inference was assessed by analyzing the impact of the %CV manipulation on RTs using linear regressions in individual participants. Moreover, the participants' explicit estimations of the true %CV levels were assessed.

It was found that probabilistic inference abilities were not per se compromised in the tested patients. They were mostly able to learn the probabilities as indicated by the linear pattern of the VEs and the explicit %CV estimates. However, some RH patients had difficulties using their knowledge to adapt their behavior in contralesional space: by trend, the group of RH patients showed a reduced modulation of RTs by %CV in invalid contralesional trials. Furthermore, they had issues when explicitly estimating the true %CV level. However, the correlation of the two parameters revealed no significant relationship between the both, indicating that these parameters characterize different independent components of probabilistic inference. Whereas the impact of the %CV manipulation on RTs represents an implicit process which might not be consciously accessible by the participants, the explicit estimation of the %CV involves a conscious representation of the participants' inferences.

Due to our task design where no information about the %CV was provided, participants had to learn the underlying probabilities without being given prior information. In the explicit evaluation of %CV, a group difference between RH patients and HC was revealed in the first %CV block of 80%. This effect could potentially reflect different prior assumptions about %CV of the patients. If a patient had a low subjective prior (e.g. 30%) and was as well a slow learner, he/she would probably need more time to detect the underlying probabilities and might not adapt his/her prior to 80%, but rather to 50%. Hence, no big difference between the groups might be detected for the other %CV, since in that case the deviation from the internal adapted prior of the first %CV to the 40%CV and 60%CV would be small and slow learning might be sufficient. Furthermore, if a patient displayed a reduced impact of the %CV manipulation on RTs only in contralesional invalid trials, this might not affect his ability to

2. Empirical Section

estimate the explicit %CV. A lateralized adaption deficit should not impair the general learning abilities of the patients. This behavioral independence of the two measures of probabilistic inference fits to our VLSM results which identified distinct lesion patterns for the two parameters.

Regarding our expectation that deficits in probabilistic inference in a spatial attention task were related to lesions of the right TPJ, we did not find strong evidence to prove our assumption when using regression analyses of %CV on RTs as a measure of probabilistic inference. In the whole group of RH patients, deficits in the adaption of responses to %CV were only by trend evident for contralesional invalidly cued targets, so that responses to ipsilesional targets were modulated by %CV. Lesions of the right TPJ were not related to this lateralized adaption deficit. In contrast, the lateralized deficits in probabilistic inference (reduced regression weights for %CV in contralesional invalid trials) were rather related to lesions of anterior insula, thalamus and white matter (SLF I & II). Previous research has postulated that the right anterior insula is crucial for maintaining current mental models of our environment (Filipowicz et al., 2016) and for model updating (Stöttinger et al., 2015; Stöttinger, Aichhorn, et al., 2018; Stöttinger, Filipowicz, Marandi, et al., 2014; Stöttinger, Guay, et al., 2018). However, our results suggest that the insula is rather responsible for adapting behavior based on probabilistic beliefs, rather than for updating per se. Still, the present findings were only observed at a very lenient statistical threshold and need to be interpreted with caution. Furthermore, our experimental paradigm to assess probabilistic inference abilities was based on location-cueing task with a pronounced spatial component whereas the paradigms used by Stöttinger and colleagues (Stöttinger et al., 2014, 2018) relied more on sustained attention. Thus, different neural correlates might be detected in dependence of the used experimental design.

Moreover, the involvement of the insula might reflect the prevalence with which this territory is affected by cerebrovascular diseases (Mah et al., 2014), although it was found in healthy participants that this brain area and connected regions were active in tasks where statistical

2. Empirical Section

and perceptual representations were required (Menon & Uddin, 2010; Stöttinger, Filipowicz, Danckert, et al., 2014).

Furthermore, our findings did not provide strong evidence for impairments of probabilistic inference being related to contralesional neglect. Underestimating the explicit %CV was related to a tendency towards more frequent responses in ipsilesional space as indicated by higher RB-scores of the Landmark-M test. So far, general estimation deficits and their link to the neglect syndrome have only been studied in the domain of time perception, where it was found that the underestimation of time intervals related to neglect (Danckert et al., 2007). However, more studies assessing the estimation abilities of neglect patients in non-spatial domains are needed to draw further conclusions. In addition, the absence of a strong relationship between deficits in probabilistic inference and the neglect syndrome might be caused by our heterogeneous patient sample. We only assessed subacute and chronic patients and only very few patients exhibited neglect symptoms. In these cases, the symptoms were of mild to moderate severity. Thus, our data may be underpowered to detect a strong relationship.

In the present study, higher PB-scores (indicating a neglect of the contralesional line segments) were related to smaller normalized contralesional VEs. This finding is in contrast to previous research showing that neglect patients have difficulties in reorienting to contralesional targets (e.g. Posner et al., 1984; Rengachary et al., 2011). However, our paradigm differed from the original study by Posner. Whereas Posner et al used a constant %CV of 80%, block-wise %CV was manipulated in the present paradigm using both (80% & 60%) and counter-predictive (40%) blocks. Moreover, as noted above, participants were not informed about these %CV levels. Therefore, the further requirement of inferring the actual predictive value of the cue in our task may have contributed to the lack of increased contralesional validity effects in patients with neglect symptoms as reflected in the PB scores. It should also be mentioned that in our study the normalized validity effects were modulated by prior task experience (order effects) in RH patients. Previous studies, investigating probabilistic inference and attentional reorienting in differing attentional

2. Empirical Section

subsystems in healthy participants did not find any effects of order (Dombert, Kuhns, et al., 2016; Kuhns et al., 2017; Mengotti, Kuhns, et al., 2020). In this study, this was replicated for LH patients and healthy controls. However, RH showed low/no validity effects if they did the spatial task first compared to when they were experienced with other versions of the task.

Regarding the neural correlates of neglect-related symptoms, we found that lesions including the rTPJ and frontoparietal white matter pathways were related to contralesional neglect indicated by the mean lateralization index. This is in line with previous studies (Karnath & Rorden, 2012; Thiebaut De Schotten et al., 2014; Lunven & Bartolomeo, 2017; Lunven et al., 2015). Previous research investigating the neural correlates of the parameters of the Landmark-M task found that lesions within middle frontal, inferior parietal and parieto-occipital brain regions were related to the PB score, whereas a RB was associated with subcortical lesions primarily of the caudate, but also of the internal capsule and putamen (Vossel et al., 2010). In line with this, we found lesions of the putamen and white matter to be related to a RB, although our analyses did not replicate the specific relation to the caudate. Similar to previous work a PB related to broader pattern of fronto-parietal lesions.

Impaired reorienting of spatial attention to the contralesional hemifield was linked to lesions affecting the middle temporal gyrus, partially including TPJ, as well as white matter pathways. This is in line with previous research (Friedrich et al., 1998; Rengachary et al., 2011), although we did not find the expected relationship with the ventral frontal cortex (Rengachary et al., 2011) and the lesion-network analysis for the rTPJ did not reach significance.

It should be noted that for many analyses, neglect symptoms or signatures of probabilistic inference could not be associated with specific lesion patterns at corrected statistical thresholds. This can be attributed to the low lesion overlap in cortical areas in our sample. Hence, our lesion data might also be underpowered for conducting conclusive VLSM (Kimberg et al., 2007). Nonetheless, while acknowledging these limitations, our findings may provoke new hypotheses regarding the structure–function relationship of probabilistic inference and the neglect syndrome.

2. Empirical Section

In summary, we have provided evidence that probabilistic inference impairments are not per se linked to the neglect syndrome or RH damage, respectively. The stroke patients in this study were mostly able to perform probabilistic inference, although lateralized adaptation deficits were more related to RH than to LH brain damage. Hence, a better understanding of this cognitive impairment is necessary for advancing our knowledge of post-stroke deficits as well as new therapeutic rehabilitation techniques.

2.4 Experiment 2b: Behavioral Experiment and Lesion Mapping - Investigating Probabilistic Inference during Feature-based Attention and Motor-intention in Stroke Patients

Introduction

To flexibly adapt to our changing environment, predictions about upcoming events based on previous observations play a crucial role in shaping our behavior. It has been shown that similar mechanisms are involved in the modulation of attentional deployment (Vossel et al., 2015; Vossel, Mathys, et al., 2014). By using modifications of the classical location-cueing paradigm (Posner, 1980), reorienting of attention/motor-intention as well as probabilistic inference can be investigated within the same task. In this context, probabilistic inference describes the ability to infer changing probabilities about the predictability of a cue and the updating process of the belief about them. By manipulating the percentage of cue validity (%CV) (i.e., the proportion of valid and invalid trials) over the time course of an experiment, the participants have to infer the actual cue validity level (i.e., the probability that the cue will be valid in a given trial) and probabilistic inference can be assessed. To assess different cognitive subsystems, the cue type can be varied, i.e. predicting the location of a target, a specific feature of it or a required motor-response. Whereas faster responses are induced by validly cued targets, slower responses can be observed in case predictions are violated, i.e. during invalid trials. While reorienting is reflected in the response time (RT) difference between invalid and valid trials, belief updating/probabilistic inference can be investigated by parameters of computational learning models or, alternatively, by assessing the impact of the %CV manipulation on RTs by means of regression analyses. In addition, probabilistic inference can also be assessed by asking participants to explicitly estimate the %CV. Previous studies have already shown that people were sensitive to changes in %CV, although these changes were not explicitly indicated (Dombert, Kuhns, et al., 2016; Kuhns et al., 2017; Vossel, Mathys, et al., 2014).

2. Empirical Section

Furthermore, reorienting of attention, probabilistic inference and their neural correlates in feature-based attention, motor-intention and spatial attention have been already investigated in younger (Dombert, Kuhns, et al., 2016; Kuhns et al., 2017) and older healthy adults (Mengotti, Kuhns, et al., 2020). However, so far there have not been any stroke patient studies addressing how the lesioned brains performs probabilistic inference in various attentional domains.

Investigating reorienting and probabilistic inference in different domains in young participants revealed that feature-based and spatial attention shared neural correlates of the same process, whereas motor-intention and spatial attention did not. Comparing feature-based and spatial attention, it was found that a region located in the left anterior intraparietal sulcus (IPS) was associated with the inferring of the trial-wise %CV both during spatial and feature-based attention (Dombert, Kuhns, et al., 2016). However, different brain regions were related to this process when comparing spatial attention and motor-intention (Kuhns et al., 2017). As in previous research investigating the neural correlates of probabilistic inference, the activity of the rTPJ was modulated by probabilistic inference during spatial attention (Dombert, Kuhns, et al., 2016; Mengotti et al., 2017; Vossel et al., 2015), whereas activity of the left angular gyrus (ANG) and anterior cingulate cortex (ACC) was involved in this process during the motor-intention task (Kuhns et al., 2017). Additional connectivity analyses applying psychophysiological interaction analyses revealed that the right hippocampus (HPC) was associated with cue-predictability-dependent changes of the coupling of all three brain regions.

The comparison of younger and older healthy participants showed that a reduced ability of probabilistic inference was only found for older participants in a difficult version of a motor-intention task (Mengotti, Kuhns, et al., 2020). A general deficit in probabilistic inference for older adults as it has been shown in reward-based probabilistic learning (Eppinger et al., 2011; Nassar et al., 2016) was not observed. This preserved probabilistic inference ability in the domain of attention was in line with studies reporting sustained cueing effects in older adults for endogenous attention (for a review see Staub et al., 2013, e.g. Tales et al., 2002).

2. Empirical Section

It was also explained by the differing neural correlates of probabilistic inference in attention and motor-intention tasks, since the function of the ACC (involved in motor-intention, Kuhns et al. 2017) declines with age (Mann et al., 2011; Pardo et al., 2007).

Nevertheless, it still remains to be investigated how the lesioned brain performs probabilistic inference and which lesion patterns might be responsible for common or distinct deficits of this cognitive process in different domains.

However, two cognitive processes related to probabilistic inference - priming and statistical learning - have already been studied in stroke patients in different domains (Shaqiri et al., 2018; Shaqiri & Anderson, 2012, 2013) suggesting potential effects of the different hemispheres. It has been shown that the neural correlates underlying feature (color) and spatial (position) priming differ (Kristjánsson et al., 2007). While both priming effects were related to activation of regions from the dorsal and ventral attention networks, spatial priming was associated with greater involvement of the right hemisphere than feature priming. Supporting this notion, it was found that color priming was preserved in right-hemispheric (RH) patients, whereas spatial priming was not (Shaqiri & Anderson, 2012). Furthermore, employing a task where deviations from a given probability needed to be detected to perform well, RH patients were more impaired than left-hemispheric (LH) patients (Danckert et al., 2012). However, investigating statistical learning in the auditory domain, impairments were irrelevant of the side of hemispheric damage (Shaqiri et al., 2018).

Hence, it still needs to be explored whether and how probabilistic inference in different domains is affected by damage to the different hemispheres. Based on previous research, we predict that RH patients will show impairments in probabilistic inference of spatial attention (cf. Experiment 2a). Moreover, preserved probabilistic inference abilities of feature-based attention are expected in all patients. Deficits of probabilistic inference in case of motor-intention are predicted in LH patients. To test these assumptions, we conducted three modified versions of a location-cueing task assessing spatial attention, feature-based attention, and motor-intention in LH and RH stroke patients and older healthy controls. Furthermore, by applying voxel-based lesion-symptom mapping and lesion-network

2. Empirical Section

mapping, we investigated the relationship between lesions to the different hemispheres and the cognitive processes of reorienting and probabilistic inference in different attentional domains. In Experiment 2a, we especially addressed whether lesions of the rTPJ link to impairments of probabilistic inference of spatial attention. Here, we investigated if damage of the left IPS relates to deficits in feature-based and spatial probabilistic inference and lesions of the left ANG and ACC to motor-intentional probabilistic inference as well as lesions of the right HPC are associated with deficits in probabilistic inference in spatial attention and motor-intention.

Methods

Participants

We used the same patient and healthy control (HC) sample as in Experiment 2a. One further LH patient had to be excluded, since this patient had only performed the spatial attention task and not the other two versions of the task. Furthermore, one HC had to be excluded due to poor performance in the motor-intention task (mean accuracy score < 50%). Consequently, our sample comprised 32 HC, 20 LH and 26 RH patients. Excluding the LH patient did not lead to significant differences of the demographic and neuropsychological data between the two patient groups (see Table 5), apart from the pre-existing difference in PB.

Table 5 Demographic and neuropsychological data of the stroke population.

	LH patients	RH patients	Statistical parameters of the group comparisons
Age (years) (20LH/26RH)	53.7 (± 11)	58.5 (± 10)	$t(44)=-1.545$, $p=.129$
Gender (f/m) (20LH/26RH)	10/10	11/15	$\chi^2(1)=.270$, $p=.604$
Handedness (right/left/bi) (20LH/26RH)	19/0/1	21/2/3	$\chi^2(2)=2.358$, $p=.308$

2. Empirical Section

Time post stroke (days) (20LH/26RH)	156.8 (±220.5)	74.3 (±103.6)	t(25.4)=1.548, p=.134
Lesion volume (voxels) (20LH/26RH)	23225 (±27723)	37887 (±100775)	t(44)=-.631, p=.531
MMSE (max. 30) (20LH/26RH)	29 (±1.2)	28.8 (±1.4)	t(44)=.492, p=.625
ACL-K (max. 40) (17LH/26RH)	35.7 (±4.1)	37.7 (±2.5)	t(23.5)=-1.837, p=.079
GDS score (max. 15) (20LH/26RH)	3.0 (±2.1)	3.6 (±2.9)	t(44)=-.852, p=.399
KAS (max. 80) (19LH/26RH)	78.7 (±2.1)	78.4 (±2.1)	t(43)=.452, p=.653
Letter cancellation LI (19LH/26RH)	.004 (±0.02)	-.013 (±0.54)	t(28.6)=1.504, p=.144
Star cancellation LI (19LH/26RH)	.001 (±0.01)	-.001 (±0.02)	t(32.5)=.467, p=.644
Figure copying (max. 9) (19LH/26RH)	8.5 (±0.6)	8.2 (±0.9)	t(43)=1.083, p=.285
Reading (max. 140) (19LH/24RH)	136 (±6.8)	138 (±1.9)	t(41)=-1.159, p=.253
Clock drawing (max. 3) (19LH/26RH)	2.9 (±0.3)	2.9 (±0.3)	t(43)=.207, p=.837
MWCT LI (19LH/26RH)	.000 (±0.01)	-.036 (±0.11)	t(24.3)=1.635, p=.115
Landmark PB (20LH/26RH)	49.8 (±4.0)	54.3 (±5.8)	t(44)=-2.952, p=.005
Landmark RB (20LH/26RH)	50.0 (±1.9)	50.1 (±2.5)	t(44)=-.106, p=.916
Extinction (yes/no) (17LH/23RH)	0/17	4/19	X ² (1)=3.285, p=.070

Mean and standard deviations from the mean (in parenthesis; if not stated differently) of the demographic and neuropsychological data. Apart from the difference in PB (p=.005), there were no

2. Empirical Section

further significant differences between the LH and RH patient groups for any other variable (all $p > .070$). Because some variables showed mild violations from normality, we also used nonparametric Mann-Whitney U tests as control analyses. The results of the t-tests were confirmed by the nonparametric tests; therefore, only the former will be presented. *LH* left hemisphere, *RH* right hemisphere, *MMSE* Mini Mental State Examination, *ACL-K* Aphasia Check List-short version, *GDS* Geriatric Depression Scale, *KAS* Cologne Apraxia Screening, *LI* Laterality Index, *MWCT* Mesulam Weintraub Cancellation task, *PB* perceptual bias, *RB* response bias

Experimental Paradigm

We used analogue experimental paradigms as described in Experiment 2a and adapted the cue stimuli to investigate feature-based attention and motor-intention. In the feature-based attention task, a cue indicating the target's color consisting of a two-letter abbreviation of the color word in the center of the fixation diamond (RO for 'red' and BL for 'blue') was used (see Figure 2.23). A previous study has shown that this cue produced the most effective cueing effects when compared to the whole color word or physical color (Dombert, Fink, et al., 2016). For the motor-intention task, the cue comprised a picture of the two response buttons within the fixation diamond, with one being white and the other one being gray (see Figure 2.23). The white button indicated the potential response, so that participants could prepare for the upcoming target. The same cues have been already investigated in a previous study in young and old healthy controls (Mengotti, Kuhns, et al., 2020). However, there the %CV changed over the course of the experiment between levels of 50% and 80%. In this study, we used a block design with three fixed %CV as in Experiment 2a.

The order in which the three different cueing tasks testing spatial attention, feature-based attention and motor-intention were assessed as well as the response mapping of the index and middle finger was counterbalanced across participants.

The duration of the whole experiment was around 45 minutes with two small breaks between the blocks in each task and two long breaks between the tasks. Due to the limited attention

2. Empirical Section

span of the patients, none of them completed the experiment on one day. However, all HC performed the experiment in one run.

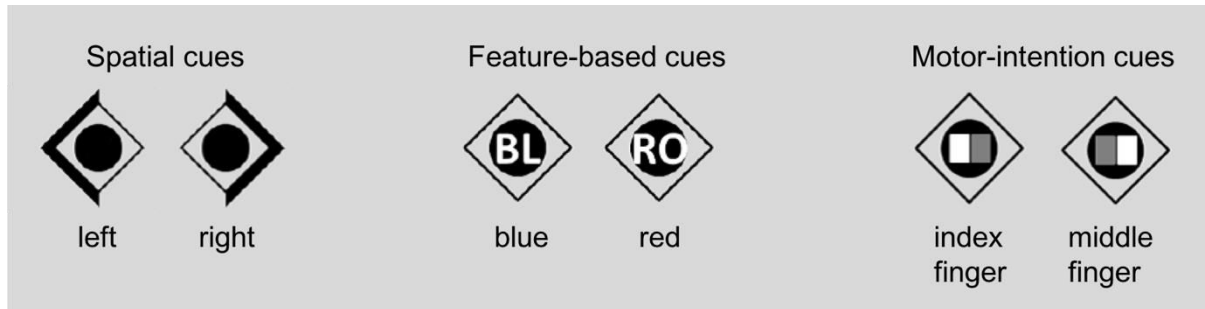


Fig 2.23 Three different cues were used for investigating spatial attention (Experiment 2a), feature-based attention, and motor-intention. The feature cue informed about the color of the target, whereas the motor cue prepared the potential motor response.

Behavioral Data Analysis

The same analyses as in Experiment 2a were performed for each task version separately. Furthermore, we conducted correlations of the parameters governing probabilistic inference of the three task versions (invalid contralesional %CV regression weight and averaged explicit %CV estimate) using Spearman's rho correlation coefficient to explore the relationship of probabilistic inference in different attentional domains.

Lesion Analyses

The same lesion and white matter maps were used from Experiment 2a excluding the one LH patient. Moreover, the same procedures and parameters were used for the voxel-based lesion-symptom mapping and lesion-network mapping.

Furthermore, as in Experiment 2a, due to our a priori hypothesis of an involvement of rTPJ, left IPS, left ANG, left ACC and right HPC in probabilistic inference, it was evaluated if the disconnection maps of the patients affected these ROIs [rTPJ (ROI from Experiment 1 (Käsbauer et al., 2020; Mengotti et al., 2017; Vossel et al., 2015) with an 8 mm radius sphere centered at $x = 56, y = -44, z = 12$), left IPS (ROI from Dombert, Kuhns, et al. (2016)

2. Empirical Section

with an 8 mm radius sphere centered at $x = -32, y = -42, z = 34$), left ANG (ROI from Kuhns et al. (2017) with an 8 mm radius sphere centered at $x = -38, y = -58, z = 42$), left ACC (ROI from Kuhns et al. (2017) with an 8 mm radius sphere centered at $x = -8, y = 36, z = 24$) and the right HPC (ROI from Kuhns et al. (2017) with an 8 mm radius sphere centered at $x = 30, y = -24, z = -4$]. The patients were divided into two groups, respectively. Using Mann-Whitney U tests, it was investigated if there were significant differences in the behavioral parameters between these two groups having ROIs spared or damaged/disconnected.

Results

Behavioral Results

Reaction Times and Validity Effects

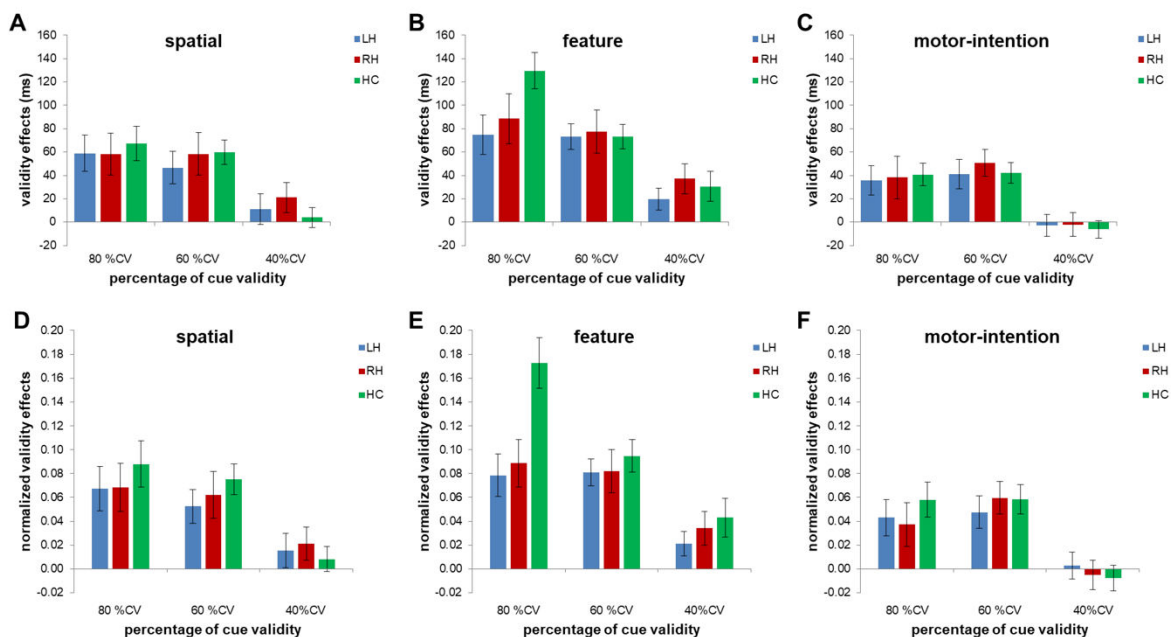


Figure 2.24 Block-wise validity effects (RT invalid minus RT valid) (mean \pm SEM) for each %CV block for **A** the spatial attention task (cf. Experiment 2a). **B** the feature-based attention task. **C** the motor-intention task. Normalized validity effects (RT invalid minus RT valid) (mean \pm SEM) for each %CV block for **D** the spatial attention task. **E** the feature-based attention task. **F** the motor-intention task. The validity effects varied linearly with actual %CV. Data from Experiment 2a are also shown for reasons of comparability.

2. Empirical Section

Spatial Attention

For comparison purposes, the results from Experiment 2a are depicted when reporting the results for the feature-based and motor-intention task. Here, the data from one patient who did not perform all three task versions was excluded.

Feature-based Attention

Overall, the average accuracy amounted to 94% (± 0.72 SEM) in the feature-based attention task. The ANOVA on accuracy scores with the between-participant factor *group* (LH, RH, HC), and the within-participant factor *validity* (valid, invalid) revealed a main effect of *validity* ($F(1,75)=11.974$, $p=0.001$, $\eta_p^2=0.138$) with higher accuracy in valid trials. The factor *group* and the interaction did not reach significance.

The ANOVA on mean RT with the within-participant factors %CV (80%CV, 60%CV, 40%CV) and *validity* (valid, invalid), and the between-participant factor *group* (LH, RH, HC) revealed a main effect of *group* ($F(2,75) = 5.928$, $p=0.004$, $\eta_p^2=0.136$), a main effect of %CV ($F(1.672,125.373) = 15.838$, $p=4 \times 10^{-6}$, $\eta_p^2=0.174$), a main effect of *validity* ($F(1,75) = 87.598$, $p=3.0939 \times 10^{-14}$, $\eta_p^2=0.539$) with higher RTs in invalid trials, as well as a significant %CV \times *validity* interaction ($F(1.738,130.331) = 30.726$, $p=1.1835 \times 10^{-10}$, $\eta_p^2=0.291$). Pairwise comparisons (Bonferroni corrected threshold $p=0.016$) showed that RH and LH patients had significantly higher RTs compared to HC (RH: $t(56)=3.3$, $p=0.003$; significant after Bonferroni correction; LH: $t(50)=2.8$, $p=0.007$; significant after Bonferroni correction). The two patient groups did not show any significant differences ($t(44)=-0.4$, $p=0.658$). Furthermore, pairwise comparisons (Bonferroni corrected threshold $p=0.016$) revealed that RTs decreased over successive %CV blocks, since participants had higher RTs in the 80%CV compared to the 60%CV and 40%V blocks (80%CV versus 60%CV: $t(77)=5.0$, $p=4 \times 10^{-6}$; significant after Bonferroni correction; 80%CV versus 40%: $t(77)=3.5$, $p=0.001$; significant after Bonferroni correction) and RTs were higher for 40%CV than for 60%CV (60%CV versus 40%CV: $t(77)=-3.2$, $p=0.002$; significant after Bonferroni correction). All

2. Empirical Section

other interactions did not reach significance, although there was a trend for a *group* × %CV × *validity* interaction ($F(3.475,130.331) = 2.481, p = 0.055, \eta_p^2=0.062$).

To further interpret the %CV × *validity* interaction and to consider the difference in overall RTs between the different groups, we subjected the normalized difference in RTs between invalid and valid trials, i.e., the normalized block-wise VE, to a 3 × 3 ANOVA with the within-participant factor %CV (80%CV, 60%CV, 40%CV) and the between-participant factor *group* (LH, RH, HC). As expected, the linear trend for the %CV main effect was significant ($F(1,75) = 48.784, p = 9.9262 \times 10^{-10}, \eta_p^2=0.394$) (see Figure 2.24 E). This confirms that the participants inferred the actual %CV levels in the present paradigm. The main effect of *group* was not significant ($F(2,75) = 2.908, p=0.061, \eta_p^2=0.072$), but we observed a significant %CV × *group* interaction ($F(3.643,136.624) = 4.636, p=0.002, \eta_p^2=0.110$). To explore this interaction effect, one-way ANOVAs (Bonferroni corrected threshold $p=0.016$) for the separate %CV-blocks were calculated and revealed a significant group difference only for the 80%CV block ($F(2,75) = 6.748, p=0.002$; 60%CV: $F(2,75) = 0.279, p=0.757$; 40%CV: $F(2,75) = 0.519, p=0.597$). Further post-hoc tests (Bonferroni corrected threshold $p=0.006$) showed that LH patients had smaller normalized VEs than HC in this block ($t(50)=-3.096, p=0.003$; significant after Bonferroni correction). RH patients also tended to have smaller normalized VEs than HC ($t(56)=-2.835, p=0.006$). There was no difference between both patients groups ($t(44)=-0.370, p=0.713$) (see Figure 2.24 E).

To investigate potential performance deviations of the two patient groups from controls and to tests for lateralization effects, z-scores were subjected to the same analyses with the additional factor *side* (contralesional, ipsilesional).

For accuracy, the 2 × 2 × 2 ANOVA with the within-participant factors *side* (ipsilesional, contralesional) and *validity* (valid, invalid) and the between-participant factor *group* (LH, RH) revealed a significant main effect of *validity* ($F(1,44)=10.964, p=0.002, \eta_p^2=0.199$) with higher deviations of accuracy values from controls (i.e. lower accuracy) in valid than in invalid trials. All other main effects or interactions were not significant (all p-values > 0.106).

2. Empirical Section

Moreover, the 2 x 2 x 2 ANOVA with the within-participant factors *side* (ipsilesional, contralesional), *validity* (valid, invalid) and the between-participant factor *group* (LH, RH) on the z-scores of RT showed a main effect of *validity* ($F(1,44) = 5.503$ $p=0.024$, $\eta_p^2=0.111$), with higher deviations from controls (i.e. slower RTs) for valid than for invalid trials. Furthermore, a trend for a main effect of *side* ($F(1,44) = 3.999$ $p=0.052$, $\eta_p^2=0.083$) was revealed, with higher deviations of the RT from controls (i.e. slower RTs) for the contralesional side. The main effect of *group* and all interactions were not significant.

For the 2 x 2 ANOVA on the z-standardized normalized VE averaged over all %CV blocks with the within-participant factor *side* (ipsilesional, contralesional) and the between-participant factor *group* (LH, RH) no significant main or interaction effects were found (all p-values > 0.253).

Furthermore, the additional analyses with the between-participant factor *used hand* revealed no relevant main and interaction effects as well as the additional analyses with the between-subject factor *order* did not reveal any significant main effects or interaction effects with this factor (all p-values > 0.065).

Motor-intention

Overall, the average accuracy amounted to 94% (± 0.71 SEM) in the motor-intention task. The ANOVA on accuracy scores with the between-participant factor *group* (LH, RH, HC), and the within-participant factor *validity* (valid, invalid) did not reveal any significant main effects or interactions (all p-values > 0.128).

The ANOVA on mean RT with the within-participant factors %CV (80%CV, 60%CV, 40%CV), *validity* (valid, invalid) and the between-participant factor *group* (LH, RH, HC) revealed a main effect of *group* ($F(2,75) = 6.857$, $p=0.002$, $\eta_p^2=0.155$), a main effect of *validity* ($F(1,75) = 33.810$, $p= 1.3956 \times 10^{-7}$, $\eta_p^2=0.311$) with higher RTs in invalid trials, as well as a significant %CV \times *validity* interaction ($F(2,150) = 19.405$, $p= 3.1974 \times 10^{-8}$, $\eta_p^2=0.206$). Pairwise comparisons (Bonferroni corrected threshold $p=0.016$) showed that RH and LH patients had significantly higher RTs compared to HC (RH: $t(56)=3.7$, $p=0.000464$;

2. Empirical Section

significant after Bonferroni correction; LH: $t(50)=3.1$, $p=0.004$; significant after Bonferroni correction). The two patient groups did not show any significant differences ($t(44)=-0.5$, $p=0.651$). The factor %CV and all other interactions did not reach significance (all p -values > 0.08).

To further interpret the %CV \times *validity* interaction and to consider the difference in overall RTs between the different groups, we subjected the normalized difference in RTs between invalid and valid trials, i.e., the normalized block-wise VE, to a 3×3 ANOVA with the within-participant factor %CV (80%CV, 60%CV, 40%CV), and the between-participant factor *group* (LH, RH, HC). As expected, the linear trend for the %CV main effect was significant ($F(1,75) = 22.193$, $p= 0.000011$, $\eta_p^2=0.228$) (see Figure 2.24 F). This confirms that the participants inferred the actual %CV levels in the present paradigm. Neither the main effect of *group* nor the interaction with *group* were significant.

To investigate potential performance deviations of the two patient groups from controls and to tests for lateralization effects, z-scores were subjected to the same analyses with the additional factor *side* (contralesional, ipsilesional).

For accuracy, the $2 \times 2 \times 2$ ANOVA with the within-participant factors *side* (ipsilesional, contralesional) and *validity* (valid, invalid) and the between-participant factor *group* (LH, RH) did not reveal any significant main effects or interactions (all p -values > 0.076).

Moreover, the $2 \times 2 \times 2$ ANOVA with the within-participant factors *side* (ipsilesional, contralesional), *validity* (valid, invalid) and the between-participant factor *group* (LH, RH) on the z-scores of RT showed a main effect of *side* ($F(1,44) = 8.107$ $p=0.007$, $\eta_p^2=0.156$), with higher deviations of the RT from controls (slower RTs) for the contralesional side. The main effects of *validity* and *group* were not significant, however, the *side* \times *group* interaction ($F(1,44) = 6.197$ $p=0.017$, $\eta_p^2=0.123$) as well as the *side* \times *validity* \times *group* interaction ($F(1,44) = 13.592$ $p=0.001$, $\eta_p^2=0.236$) reached significance. Post hoc two-sample t-tests (Bonferroni corrected threshold $p=0.0125$) did not reveal any differences between the patient groups for any condition (valid_ipsilesional: $p=0.773$; invalid_ipsilesional: $p=0.582$;

2. Empirical Section

valid_contralesional: $p=0.225$; invalid_contralesional: $p=0.637$). Thus, this interaction was possibly driven by the difference of invalid and valid trials, which was investigated with the subsequent ANOVA on the z-standardized normalized VE.

For the 2 x 2 ANOVA on the z-standardized normalized VE averaged over all %CV blocks with the within-participant factor *side* (ipsilesional, contralesional) and the between-participant factor *group* (LH, RH) there was only a trend for a *side* x *group* interaction ($F(1,44) = 3.690$ $p=0.061$, $\eta_p^2=0.077$), indicating that LH patients deviated negatively (i.e. showed smaller VEs) for the ipsilesional side, whereas RH patients deviated negatively (i.e. showed smaller VEs) for the contralesional side.

Furthermore, the additional analyses with the between-participant factor *used hand* did not reveal any significant main effects or interaction effects with this factor (all p -values > 0.059). The additional analyses with the between-subject factor *order* showed a significant *validity* x *%CV* x *order* x *group* interaction for the RT ($F(8,138) = 2.916$, $p=0.005$, $\eta_p^2=0.145$). To investigate this complex interaction further, we used the validity effect and calculated for each group separately a 3 x 3 ANOVA with the within-participant factor *%CV* and the between-participant factor *order* (Bonferroni corrected threshold $p=0.016$). However, neither the main effect of *order* nor any *%CV* x *order* interaction survived the corrected threshold (all p -values > 0.027). Furthermore, also for the normalized VE a significant *%CV* x *order* x *group* interaction was discovered ($F(8,138) = 2.291$, $p=0.025$, $\eta_p^2=0.117$). A post-hoc 3 x 3 ANOVA for each order separately with the within-participant factor *%CV* and the between-participant factor *group* was calculated (Bonferroni corrected threshold $p=0.016$). It was revealed that only when participants did the motor-intention task first, there was a significant *%CV* x *group* interaction ($F(4,42) = 4.053$, $p=0.007$, $\eta_p^2=0.279$, significant after Bonferroni correction; middle: $F(4,40) = 1.767$, $p=0.155$, $\eta_p^2=0.150$; last: $F(4,56) = 0.155$, $p=0.960$, $\eta_p^2=0.011$, see Figure 2.25). Further one-way ANOVAs for each %CV separately with the factor *group* (Bonferroni corrected threshold $p=0.006$) showed only a trend for the 60%CV ($F(2,21) = 3.643$, $p=0.044$; not significant after Bonferroni correction) with post-hoc paired sample t-test (Bonferroni corrected threshold $p=0.0019$) indicating that LH patients had

2. Empirical Section

smaller normalized VE than RH patients ($p=0.043$; not significant after Bonferroni correction). There were no group differences for the 80%CV ($p=0.712$) and 40%CV ($p=0.168$).

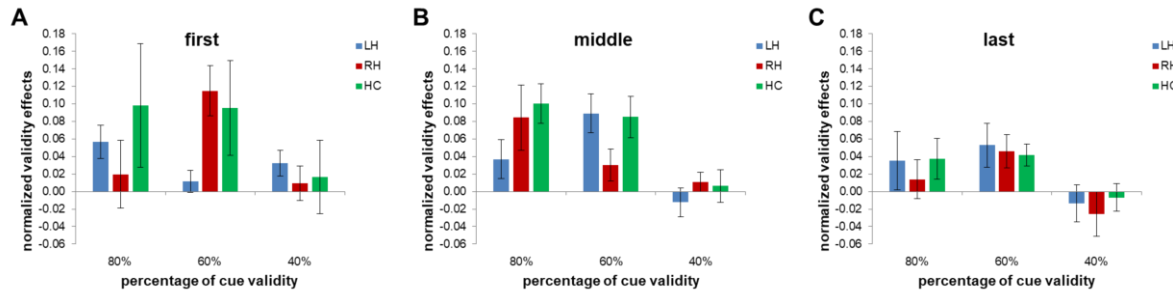


Figure 2.25 Effect of order on the normalized validity effect of the motor-intention task (mean \pm SEM). **A** if they did the task first. **B** if they did the task in the middle. **C** if they did the task last.

Probabilistic Inference

Spatial Attention

Since excluding one LH patient did not change the results, we refrained from listing the results of the spatial attention task again (they can be found in part 2.3 of the thesis), but we show the data in the figures for comparison reasons.

Feature-based Attention

Regarding probabilistic inference, the regression weights of %CV on mean RT in the different conditions were compared with a 2 x 3 ANOVA with the within-participant factor *validity* (valid, invalid) and the between-participant factor *group* (LH, RH, HC). As expected, a main effect of *validity* ($F(1,75) = 42.281$, $p=7.8298 \times 10^{-9}$, $\eta_p^2=0.361$) was found with higher regression weights of %CV for invalid than for valid RTs. Neither the main effect of *group* nor any interaction with group was significant (see Figure 2.26 B).

As with the analyses of the parameters of reorienting attention, the analyses were performed on z-transformed regression weights and the additional factor side (contralesional,

2. Empirical Section

ipsilesional). A 2 x 2 x 2 ANOVA with the within-participant factors *side* (ipsilesional, contralesional) and *validity* (valid, invalid) and the between-participant factor *group* (LH, RH) revealed a main effect of *validity* ($F(1,44) = 9.246$, $p=0.004$, $\eta_p^2=0.174$) with lower z-standardized regression weights of %CV for invalid than for valid RTs. This effect reflects that was more difficult for patients to adapt their behavior in invalid than in valid trials (for both ipsilesional and contralesional targets). No other main effect or any interactions were significant (all p-values > 0.655; see Figure 2.26 E).

Furthermore, the additional analyses with the between-participant factor *used hand* did not yield any significant effects of this factor (all p-values > 0.396).

Moreover, the analyses of the influence of *order* revealed no main or interaction effects regardless of whether the regression weights of %CV (all p-values > 0.355) or the z-standardized version was used (all p-values > 0.304).

The 3 x 3 ANOVA on the mean scores of the explicit evaluation of %CV with the within-participant factor %CV (80%CV, 60%CV, 40%CV) and the between-subject factor *group* (LH, RH, HC) revealed that the linear trend for the %CV main effect was significant ($F(1,75) = 93.845$, $p= 7.4147 \times 10^{-15}$, $\eta_p^2=0.556$) reflecting learning of the actual %CV. Neither the main effect of *group* nor the interaction with *group* was significant (see Figure 2.27 B).

Moreover, the additional analyses with the between-participant factor *order* revealed no significant main or interaction effects (all p-values > 0.612).

Motor-intention

Regarding probabilistic inference, the regression weights of %CV on mean RT in the different conditions were compared with a 2 x 3 ANOVA with the within-participant factor *validity* (valid, invalid) and the between-participant factor *group* (LH, RH, HC). As expected, a main effect of *validity* ($F(1,75) = 22.584$, $p=9 \times 10^{-6}$, $\eta_p^2=0.231$) was found with higher

2. Empirical Section

regression weights of %CV for invalid than for valid RTs. Neither the main effect of *group* nor any interaction with *group* was significant (Figure 2.26 C).

As with the analyses of the parameters of reorienting attention, the analyses were performed on z-transformed regression weights and the additional factor *side* (contralesional, ipsilesional). A 2 x 2 x 2 ANOVA with the within-participant factors *side* (ipsilesional, contralesional) and *validity* (valid, invalid) and the between-participant factor *group* (LH, RH) revealed no significant main or interaction effect (all p-values > 0.275; see Figure 2.26 F).

Furthermore, the additional analyses with the between-participant factor *used hand* did not yield any significant effects of this factor (all p-values > 0.431). Moreover, the analyses of the influence of *order* revealed no main or interaction effects regardless of whether the regression weights of %CV (all p-values > 0.301) or the z-standardized version was used (all p-values > 0.106).

The 3 x 3 ANOVA on the mean scores of the explicit evaluation of %CV with the within-participant factor %CV (80%CV, 60%CV, 40%CV) and the between-subject factor *group* (LH, RH, HC) revealed that the linear trend for the %CV main effect was significant ($F(1,75) = 44.769$, $p = 3.5041 \times 10^{-9}$, $\eta_p^2 = 0.374$) reflecting learning of the actual %CV. Neither the main effect of *group* nor the interaction with *group* was significant (see Figure 2.27 C).

Moreover, the additional analyses with the between-participant factor *order* revealed no significant main or interaction effects (all p-values > 0.7).

2. Empirical Section

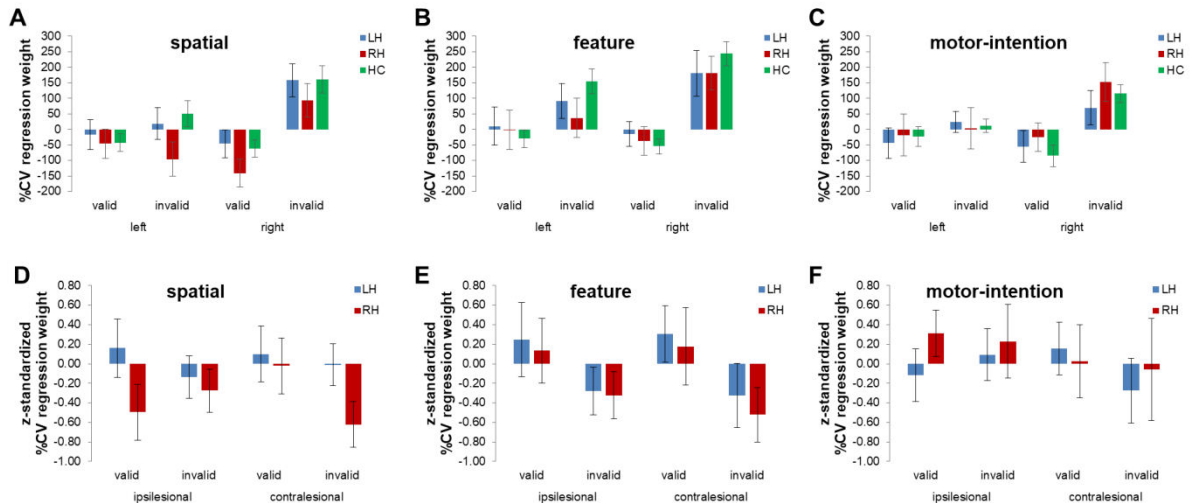


Figure 2.26 %CV regression weights (mean ± SEM) for each condition for all three groups for A the spatial attention task. B the feature-based attention task. C the motor-intention task. z-standardized %CV regression weights (mean ± SEM) for the two patient groups for D the spatial attention task. E the feature-based attention task. F the motor-intention task.

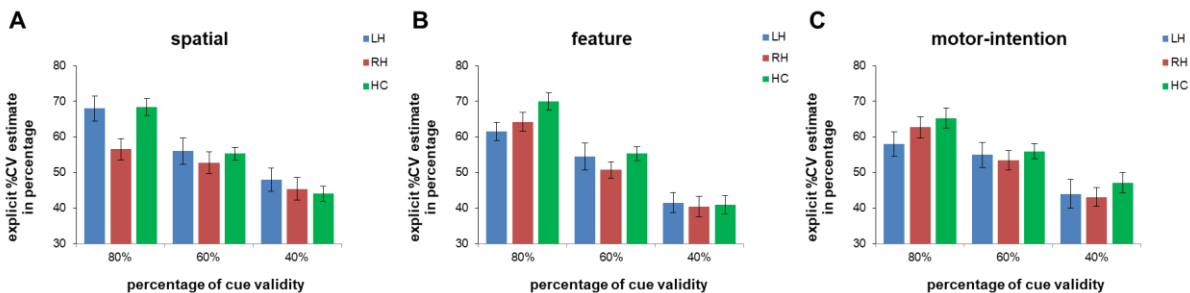


Figure 2.27 Explicit %CV estimates (mean ± SEM) for each %CV block for all three groups for A the spatial attention task. B the feature-based attention task. C the motor-intention task. The explicit %CV estimates varied linearly with actual %CV. Only in the spatial attention task in the 80%CV block RH patients differed from LH patients and HC.

Correlations between Task Versions

The correlation analyses for all patients of the two probabilistic inference parameters of the three task versions revealed a significant positive correlation of the z-standardized contralesional invalid %CV regression weights of the feature and motor-intention version ($r=.441$ $p=.002$, see Figure 2.28 A) as well as a significant positive correlation of the

2. Empirical Section

averaged explicit %CV estimates of the spatial and motor-intention version ($r=.332$ $p=.024$, see Figure 2.28 B). Performing these correlations with RH patients only replicated the results (z-standardized contralesional invalid %CV regression weights: $r=.641$ $p=.000418$; averaged explicit %CV estimates: $r=.557$ $p=.003$). Calculating these correlations with LH patients only did not reveal any significant correlation. No outlier drove any of the correlations (all Cook's distance values <1). As with the two probabilistic inference parameters of the spatial attention version, there was no significant correlation of these parameters within the feature-based attention ($r=.188$ $p=.211$) or the motor-intention version ($r=.059$ $p=.695$). Hence, the impact of the %CV manipulation on RTs and the participants' explicit estimations of the true %CV levels were not related within each task version.

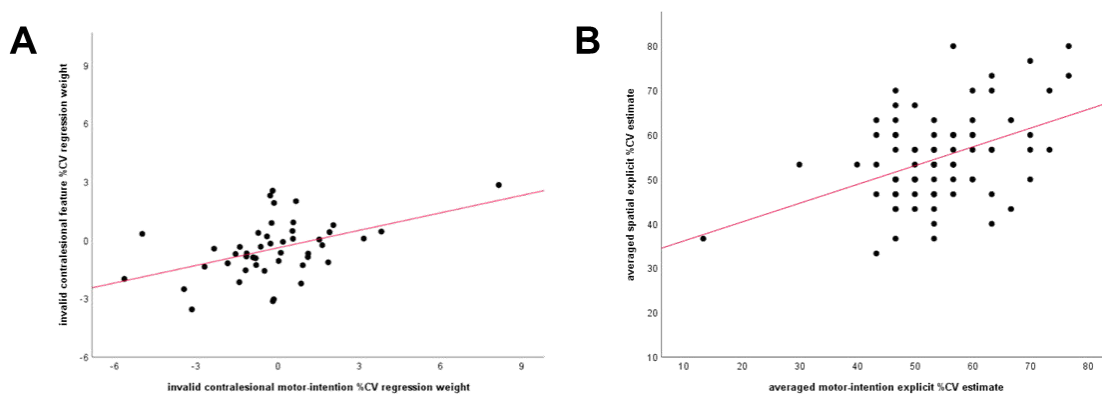


Figure 2.28 Results of the correlations of the two parameters of probabilistic inference across tasks for A the z-standardized contralesional invalid %CV regression weights. B the averaged explicit %CV estimates.

Voxel-based Lesion-symptom Mapping (VLSM)

As in Experiment 2a, VLSMs were only performed for a given variable if patients deviated in the parameters from healthy control. VLSMs in the whole group of patients were only performed in case of performance deviations in both LH and RH groups. If the results did not survive the corrected statistical threshold, the results are shown at a level of $p<.05$ (uncorrected).

2. Empirical Section

Z-standardized Invalid Contralesional %CV Regression Weights

Lower z-standardized invalid contralesional %CV regression weights of the feature task were associated with lesions affecting left amygdala, right basal ganglia, insula, Heschl's gyrus, operculum, pre- and postcentral gyrus and bihemispheric white matter (Figure 2.29 A), whereas lower z-standardized invalid contralesional %CV regression weights of the motor-intention task were linked to lesions affecting left thalamus, HPC, parahippocampal gyrus, fusiform area, inferior temporal gyrus, right pre- and postcentral gyrus, inferior parietal areas, insula, middle and superior occipital areas, operculum, Heschl's gyrus, putamen and bihemispheric white matter (Figure 2.29 B).

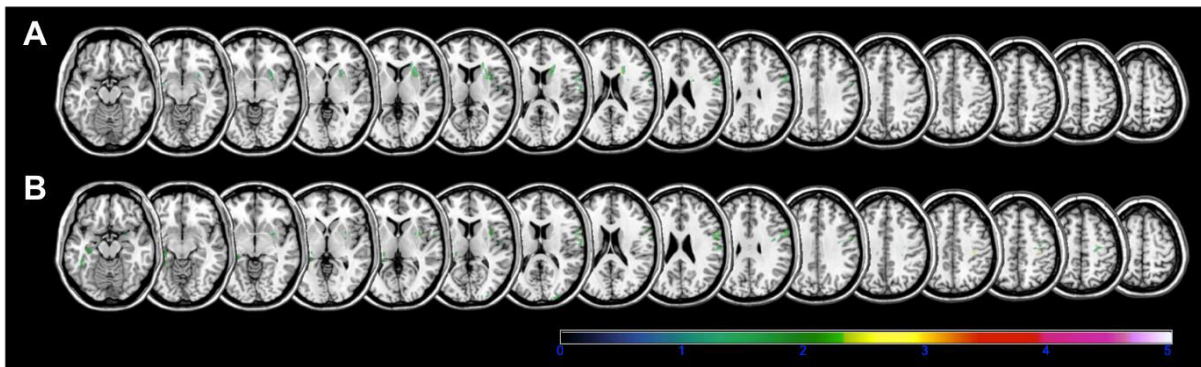


Figure 2.29 VLSM results for the z-standardized invalid contralesional %CV regression weight of all patients (n=46) thresholded at $p < 0.05$ uncorrected for **A** the feature version. **B** the motor-intention version. Slices with the MNI-z-coordinates from -15 to 60 are shown.

In the spatial version (cf. Experiment 2a), the VLSMs in the group of RH patients only revealed that lower z-standardized invalid contralesional %CV regression weights were related to lesions affecting the right insula, STG and pole as well as white matter pathways (Figure 2.30 A). In the feature-based task, lesions of the right pre- and postcentral gyrus, basal ganglia, insula, operculum and surrounding white matter were linked to lower z-standardized invalid contralesional %CV regression weights (Figure 2.30 B), whereas lesions affecting pre- and postcentral gyrus, SMG, putamen, insula, operculum and white matter related to lower values in the motor-intention version (Figure 2.30 C).

2. Empirical Section

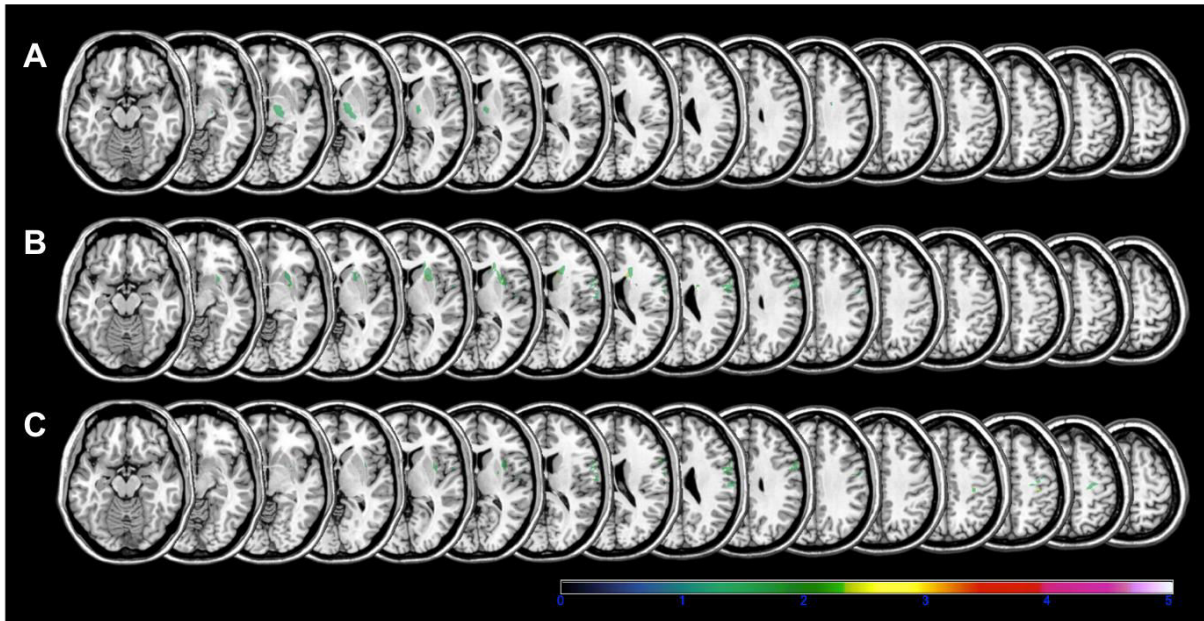


Figure 2.30 VLSM results for the z-standardized invalid contralesional %CV regression weight in RH patients only (n=26) thresholded at $p < 0.05$ uncorrected for A the spatial version. B the feature version. C the motor-intention version. Slices with the MNI-z-coordinates from -15 to 60 are shown.

Conducting the analyses with LH patients only, it was found that lower z-standardized invalid contralesional %CV regression weights of the feature version were related to a few lesioned voxels in the white matter (Figure 2.31 A). Moreover, smaller z-standardized invalid contralesional %CV regression weights of the motor-intention version were linked to lesions affecting the left HPC, parahippocampal gyrus, thalamus, inferior temporal gyrus, fusiform area and white matter pathways in LH patients (Figure 2.31 B).

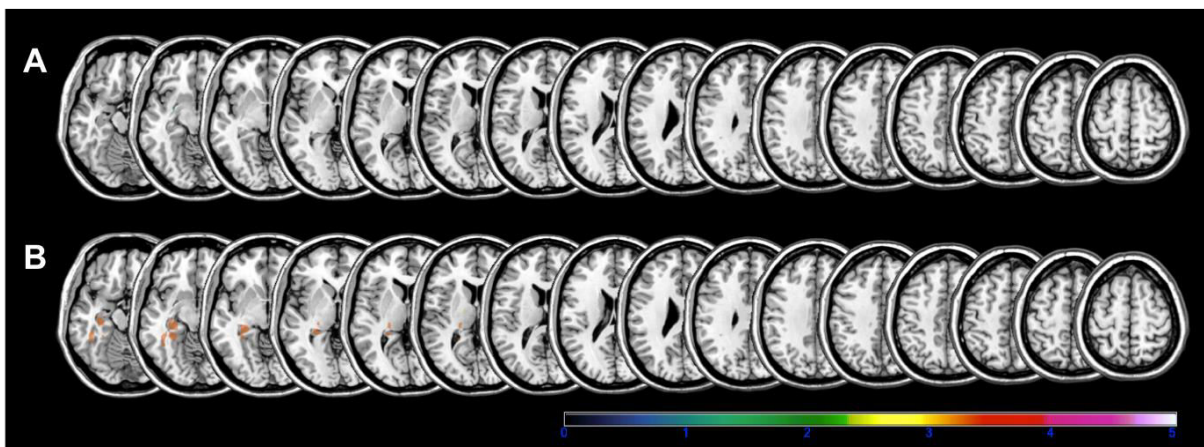


Figure 2.31 VLSM results for the z-standardized invalid contralesional %CV regression weight in LH patients only (n=20) A for the feature version (thresholded at $p < 0.05$ uncorrected). B for the motor-

2. Empirical Section

intention version (thresholded at FDR $p < 0.05$). Slices with the MNI-z-coordinates from -15 to 60 are shown.

Explicit Estimation of %CV

The VLSM results of all patients in Experiment 2a showed that deficits in explicitly estimating the %CV level in the spatial task were related to lesions of the right insula, thalamus, basal ganglia, IFG, middle and superior temporal gyrus, superior temporal pole, operculum, Heschl's gyrus and white matter pathways (Figure 2.32 A). In the feature-based task, impairments in explicitly estimating the averaged %CV were related to lesions affecting the left insula, operculum, IFG, caudate, STG and pole and surrounding white matter (Figure 2.32 B). Deficits in estimating the explicit %CV in the motor-intention version were linked to a similar lesion pattern as in the spatial version including lesions of the right insula, IFG, STG, superior temporal pole, operculum, SMG, Heschl's gyrus and white matter (Figure 2.32 C).

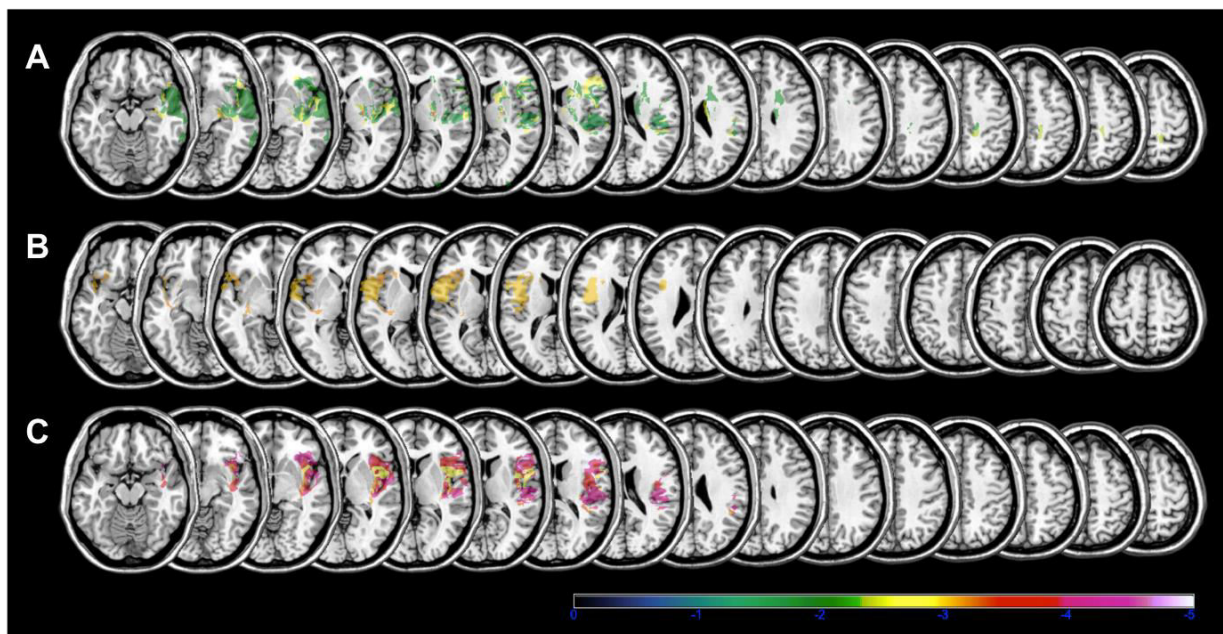


Figure 2.32 VLSM results for the absolute values of the z-standardized averaged explicit %CV of all patients ($n=46$) A for the spatial version (thresholded at $p < 0.05$ uncorrected). B for the feature version (thresholded at FDR $p < 0.05$). C for the motor-intention version (thresholded at FDR $p < 0.05$). Slices with the MNI-z-coordinates from -15 to 60 are shown.

2. Empirical Section

Performing these analyses for RH patients only, it was revealed in Experiment 2a that estimation deficits of the spatial averaged explicit %CV were linked to lesions affecting right superior parietal gyrus, caudate, STG, operculum, IFG, HPC, thalamus and white matter (Figure 2.33 A). In the feature-based task, lesions within right temporal and occipital areas, caudate, cuneus, precuneus, lingual gyrus, calcarine gyrus, ANG and white matter were associated with estimation deficits of explicit %CV (Figure 2.33 B). Furthermore, estimation impairments in the motor-intention version in RH patients replicated the lesion pattern found for all patients (Figure 2.33 C).

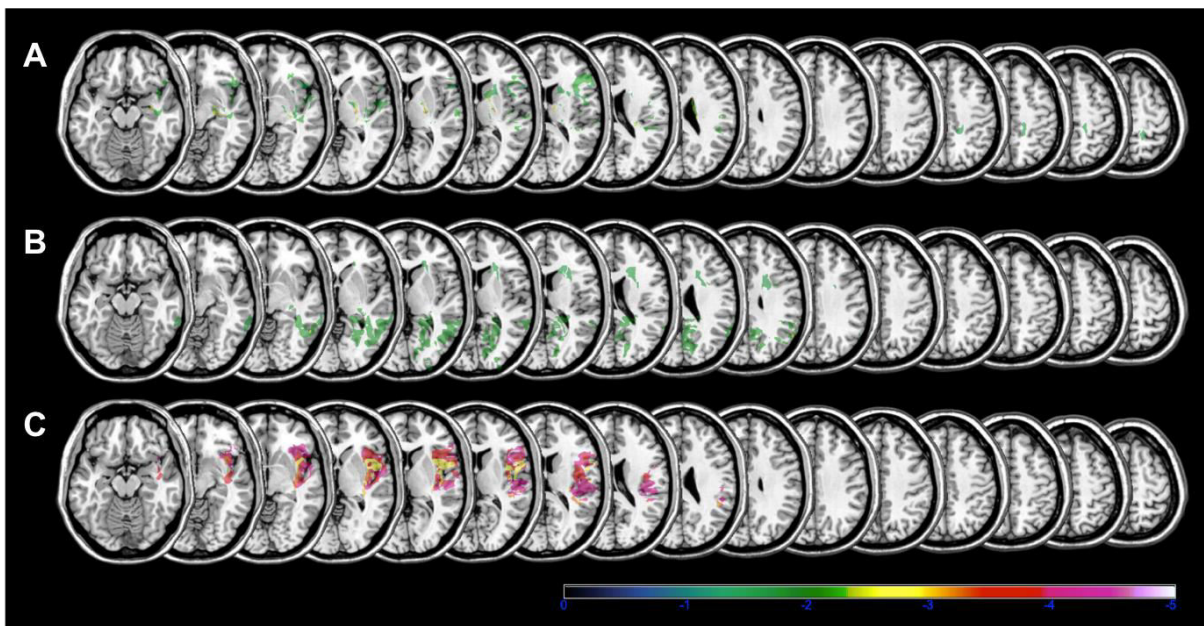


Figure 2.33 VLSM results for the absolute values of the z-standardized averaged explicit %CV in RH patients only (n=26) **A** for the spatial version (thresholded at $p < 0.05$ uncorrected). **B** for the feature version (thresholded at $p < 0.05$ uncorrected). **C** for the motor-intention version (thresholded at FDR $p < 0.05$). Slices with the MNI-z-coordinates from -15 to 60 are shown.

Conducting the analyses with LH patients only revealed that estimation deficits in the spatial version were linked to lesions affecting the cerebellum, the fusiform area, the inferior temporal gyrus, HPC and parahippocampal gyrus, thalamus, insula and white matter pathways (Experiment 2a, Figure 2.34 A). The lesion pattern of the estimation deficits in the feature version of the task from all patients was replicated in LH patients, apart from revealing an additional involvement of the putamen (Figure 2.34 B). Furthermore, it was

2. Empirical Section

found that a few lesioned voxels related to the thalamus were linked to estimation deficits in the motor-intention version of the task (Figure 2.34 C).

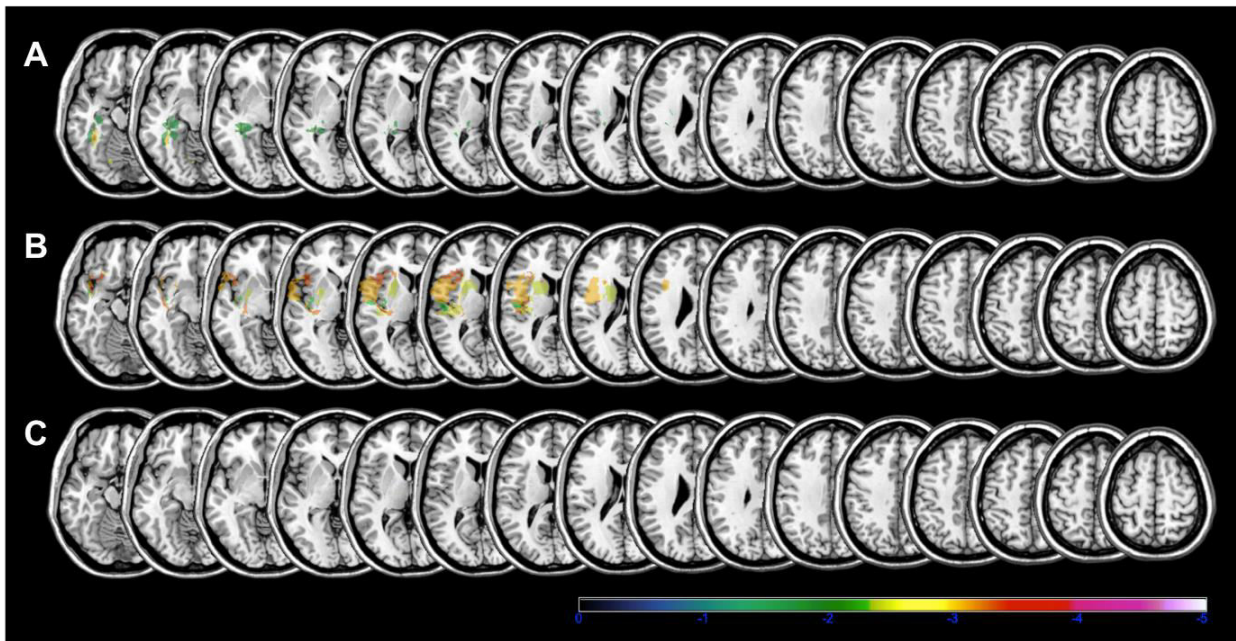


Figure 2.34 VLSM results for the absolute values of the z-standardized averaged explicit %CV in LH patients only (n=20) A for the spatial version (thresholded at $p < 0.05$ uncorrected). B for the feature version (thresholded at FDR $p < 0.05$). C for the motor-intention version (thresholded at $p < 0.05$ uncorrected). Slices with the MNI-z-coordinates from -15 to 60 are shown.

Lesion-network Mapping

The results of the comparison of the mean results in different behavioral test parameters between patients having relevant white matter tracts spared or disconnected revealed no significant differences in any of the task parameters of the feature-based or motor-intention task when looking at all patients.

In RH patients, there was a trend that damage of the IFOF was related to smaller z-standardized invalid contralesional %CV regression weights of the motor-intention task ($U=-1.8$, $p=0.072$), and that damage of the ILF was linked to the underestimation of the averaged explicit %CV of the motor-intention task ($U=-1.8$, $p=0.076$, see Figure 2.35).

2. Empirical Section

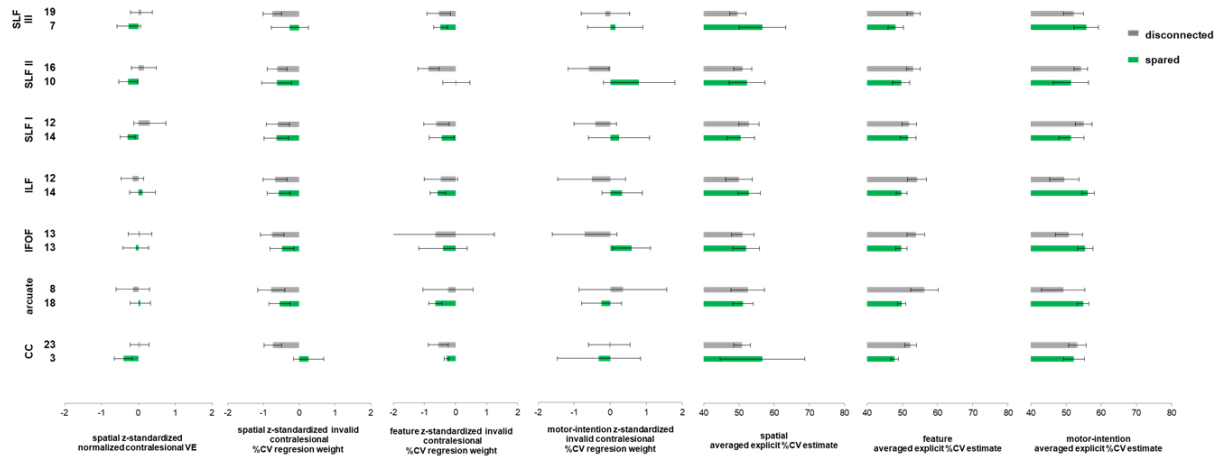


Figure 2.35 Behavioral test performances in relation to white matter tract damage for RH patients (n=26). The behavioral test results of the z-standardized normalized contralesional VE of the spatial task, the z-standardized invalid contralesional %CV regression weights and the averaged explicit %CV estimates of all three task versions are depicted as a mean performance of patients without (green) or with (gray) disconnection of different white matter tracts. The number of patients (n) with or without disconnection of the according tract is provided on the left of the y-axis. Error bars show standard error of the mean.

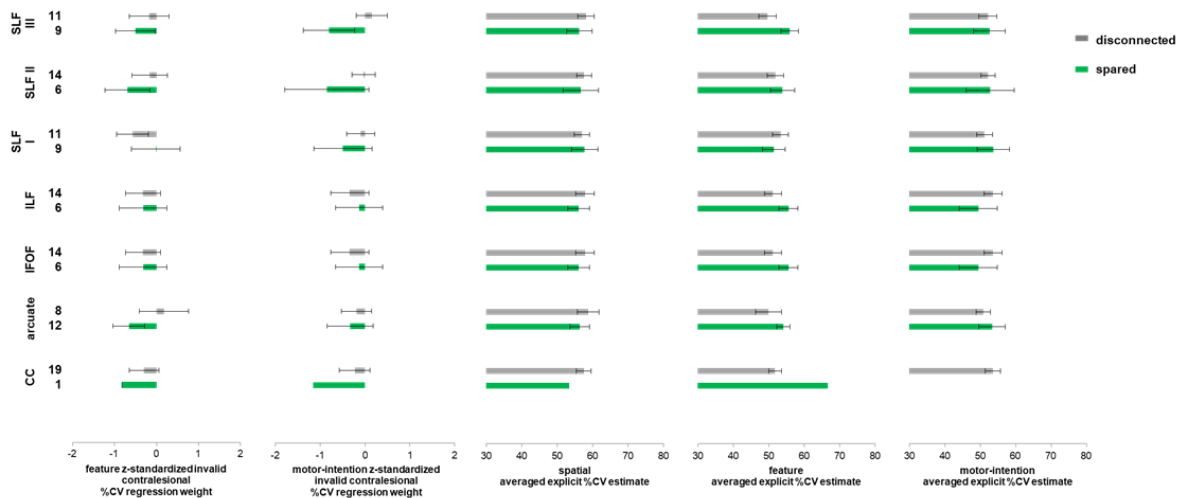


Figure 2.36 Behavioral test performances in relation to white matter tract damage for LH patients (n=20). The behavioral test results of the z-standardized invalid contralesional %CV regression weights of the feature and motor-intention tasks and the averaged explicit %CV estimates of all three tasks are depicted as a mean performance of patients without (green) or with (gray) disconnection of different white matter tracts. The number of patients (n) with or without disconnection of the according tract is provided on the left of the y-axis. Error bars show standard error of the mean.

2. Empirical Section

When looking at LH patients only, there was only a trend for damage of the SLF III being related to underestimation of the averaged explicit %CV of the feature task ($U=-1.8$, $p=0.080$, see Figure 2.36). No relations to other task parameters were found.

A Priori Regions of Interest

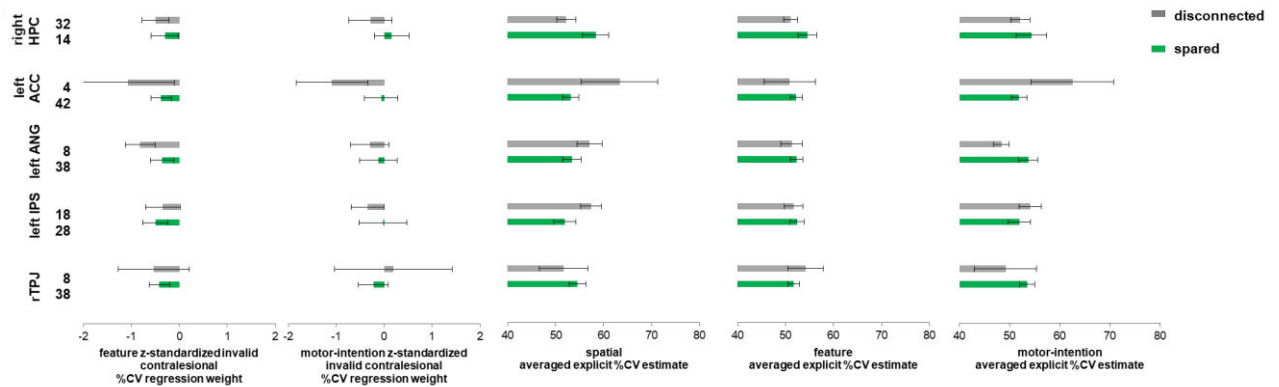


Figure 2.37 Behavioral test performances in relation to region of interest affection for all patients (n=46). The behavioral test results of the z-standardized invalid contralesional %CV regression weights of the feature and motor-intention task and the averaged explicit %CV estimates of all three task versions are depicted as a mean performance of patients without (green) or with (gray) disconnection of different regions of interest (rTPJ, left IPS, left ANG, left ACC, right HPC). The number of patients (n) with or without disconnection of the according tract is provided on the left of the y-axis. Error bars show standard error of the mean.

Investigating if there were significant differences in the behavioral parameters between patients having pre-defined regions of interest (rTPJ, left IPS, left ANG, left ACC, right HPC) spared or damaged, some trends were found when performing the analyses for all patients: Damage of the right HPC was related to the underestimation of the averaged explicit %CV of the spatial version ($U=-1.9$, $p=0.063$, see Figure 2.37). Moreover, damage of the left ANG was associated with the underestimation of the averaged explicit %CV of the motor-intention version ($U=-2.0$, $p=0.053$, see Figure 2.37).

Performing the analyses within patient groups separately (RH or LH only) did not reveal any significant relationship between task parameters and regions of interests.

2. Empirical Section

Discussion

This study investigated if probabilistic inference abilities in different domains are compromised in stroke patients and whether deficits in different domains relate to distinct lesion patterns. In different modified location-cueing paradigms, block-wise changes of the %CV were implemented, and probabilistic inference was assessed by analyzing the impact of the %CV manipulation on RTs using linear regressions as well as by participants' estimations of the true %CV levels.

It was found that in the whole group of patients, probabilistic inference abilities in feature-based attention and motor-intention were not compromised. On average, patient groups and healthy controls were able to learn the underlying probabilities as indicated by the linear pattern of the VEs, the explicit %CV estimates and the absence of any main or interaction effects of the factor group. Thereby, we replicated and extended previous findings of preserved probabilistic inference abilities in the domain of attention for old healthy controls (Mengotti, Kuhns, et al., 2020).

However, in Experiment 2a, it was found that in the spatial attention domain, RH patients had some difficulties in probabilistic inference compared to LH patients and HC. Although only trends were revealed, the group of RH patients showed a reduced modulation of RTs by %CV in invalid contralesional trials and they had issues when estimating the explicit %CV level. However, they still showed the linear variation of the ipsilesional VE and the explicit %CV estimate, which indicates that they were able to learn the underlying pattern of the %CV. It seemed that they had issues to use this knowledge to adapt their behavior in contralesional space (see Experiment 2a for a detailed discussion).

Our finding is thus in line with the notion that deficits in probabilistic inference are domain-specific. This is in accord with previous research on priming and statistical learning (Kristjánsson et al., 2005, 2007; Shaqiri & Anderson, 2012, 2013) stating that feature priming is preserved in RH patients, whereas spatial is not as well as that RH patients are more impaired than LH patients when the ability of detecting probabilities is required (Danckert et al., 2012).

2. Empirical Section

As in the spatial task, the correlations of the two probabilistic inference parameters (RT modulation by %CV and explicit estimation of %CV) within a task version revealed no significant relationship in the feature-based attention and motor-intention task. This finding was in accord with the results of the VLSM indicating distinct lesions patterns.

However, the correlations of the two probabilistic inference parameters across task versions revealed two significant positive correlations. The z-standardized contralesional invalid %CV regression weights in feature-based attention and motor-intention, as well as the averaged explicit %CV estimates in the spatial attention and motor-intention version were related. These links were further supported by the common lesion patterns revealed by the VLSM (discussed in more depth below with regard to the involvement of specific regions of interest). fMRI studies in healthy participants investigating probabilistic inference using computational modelling also found neural commonalities between different domains (Dombert, Kuhns, et al., 2016; Kuhns et al., 2017). However, in these studies, probabilistic inference between spatial and feature-based attention was related, while no significant relationship was found between spatial attention and motor-intention. These opposing results may be due to the different parameters used to operationalize probabilistic inference (computational model parameters for the speed of probabilistic inference versus regression weights for RT modulation). Thus, applying computational modelling to our data would be of high interest to characterize different components of probabilistic inference.

Regarding our expectation of the involvement of specific regions of interest from previous studies (Dombert, Kuhns, et al., 2016; Kuhns et al., 2017; Mengotti et al., 2017) in probabilistic inference of distinct domains, we did not find strong evidence to prove our assumptions when using regression analyses of %CV on RTs. In the group of RH patients, deficits in the adaption of behavioral responses to %CV were only evident for contralesional invalidly cued targets. Lesions of the right TPJ were not related to this lateralized adaption deficit. Since we had a heterogeneous patient sample with only a small number of patients having lesions within rTPJ, a specific involvement could not be detected (see Experiment 2a).

2. Empirical Section

We could also not provide any evidence for the assumption that lesions of the left IPS might be related to deficits in probabilistic inference of feature-based and spatial attention since we did not find any specific link between left IPS lesions and the task parameters.

When investigating the specific involvement of left ANG and ACC in probabilistic inference of motor-intention, it was found that lesions of the left ANG were related to deficits in explicitly estimating the averaged %CV. This is in line with previous research stating that activity of the left ANG was modulated by probabilistic inference (Kuhns et al., 2017). However, we could not replicate this finding for the left ACC. Since the function of the ACC declines with age (Mann et al., 2011; Pardo et al., 2007), it might be that behavior is similarly affected by lesions of this region and general age-dependent decrease and thus, no differences could be detected.

Regarding our last assumption that lesions of the right HPC might particularly be associated with deficits in probabilistic inference in spatial attention and motor-intention, it was revealed that damage to the right HPC led to underestimation of the explicit %CV in the spatial attention task, although no relation to motor-intention was found. However, using correlation analyses and VLSM, it was found that estimating the explicit %CV in the spatial version was related to this process in the motor-intention version, although lesions affecting the right STG, insula, IFG, operculum, Heschl's gyrus and white matter were the common neural structures (and not the HPC).

Furthermore, not finding many relations between the a priori defined regions and the behavioral parameters might be due to again the heterogeneity of the patient sample as well as the used method of defining the ROIs on the disconnection maps of the patients and thus, does not purely reflect the effect of direct lesions of the ROI and related disconnection patterns.

Moreover, a relationship between the regression weights of %CV on RTs in invalid trials of the feature and motor-intention version, as indicated by a positive correlation of these parameters and similar lesion patterns (insula, operculum, pre- and postcentral gyrus, basal ganglia, Heschl's gyrus and white matter), was found (see previous discussion). The neural

2. Empirical Section

mechanisms underlying probabilistic inference of feature-based attention and motor-intention have not been directly compared yet. fMRI studies investigating probabilistic inference of these domains have not reported similar brain structures to be involved in the two processes (Dombert, Kuhns, et al., 2016; Kuhns et al., 2017) and thus, more research is needed to investigate common neural mechanisms.

Nonetheless, the result that patients (assessed at a subacute and chronic stage) and healthy elderly controls did not differ strongly in probabilistic inference might be due to the brain's ability to reorganize with age or damage. Theories of normal aging have postulated general age-related changes of cognitive processes and their underlying neural mechanisms (Cabeza, 2001; Cabeza et al., 2018). In this context, two accounts are existing: The compensation hypothesis proposes recruitment of additional brain regions with increasing age to enable normal task performance (Reuter-Lorenz & Cappell, 2008), whereas the dedifferentiation hypothesis states that brain regions underlying cognitive processes become less functionally differentiated, although more distributed (i.e., *dedifferentiated*) during aging (Park et al., 2004). Thus, according to the dedifferentiation theory, brain lesions might not have such a high impact on broadly distributed cognitive processes (i.e. probabilistic inference). Future fMRI studies assessing probabilistic inference in young and elderly healthy participants as well as in stroke patients might be used to directly investigate the presumed altered neural mechanisms underlying probabilistic inference in the aging and lesioned brain.

Regarding the reorienting of attention, it was found that only RH patients deviated from HC in the spatial attention task. No deviations for other task versions or for LH patients were found. This highlights that, as in the case of probabilistic inference, reorienting of feature-based attention and motor-intention was not impaired in stroke patients. Only spatial reorienting was (by trend) impaired in RH patients and this was related to lesions of the middle temporal gyrus, caudate and white matter as discovered by VLSM. Since our patient sample was very heterogeneous and we chose an easy version of the task, it might be that some impairments of the patients were not discovered as in Mengotti et al. (2020) comparing

2. Empirical Section

younger and older healthy participants. Besides, it should be mentioned that reorienting difficulties in patients were to some extent modulated by their prior task experience (order effects). Previous studies, investigating reorienting of attention and probabilistic inference in differing attentional subsystems in healthy participants did not report any effects of order (Dombert, Kuhns, et al., 2016; Kuhns et al., 2017). In this study, this was replicated for healthy controls who were not affected by any order effects. However, for RH patients in the spatial attention task and for LH patients in the motor-intention task order had an effect. RH patients showed low/no validity effects if they did the spatial task first and had no prior task experience compared to when they were experienced with other versions of the task. In LH patients, task order had the effect that if the patients did the motor-intention task first they showed low/no validity effects compared to RH patients. Our results highlight that task order and prior learning experience should carefully be considered in patient studies, although this might not be the case for healthy participants.

In summary, we have provided evidence that probabilistic inference abilities across domains are not per se impaired in stroke patients. Difficulties were mainly present in RH patients in the spatial attention domain and were not absolute. This highlights the importance of the right hemisphere for spatial processes. Further patient research is needed to validate our findings and to use the knowledge of preserved probabilistic inference abilities in feature-based attention and motor-intention for post-stroke rehabilitation.

3. General Discussion

Defining the neural mechanisms underlying probabilistic interference processes further is not only relevant for a better understanding of post-stroke deficits, in particular the spatial neglect syndrome, but may also prove critical for establishing better therapeutic approaches for its treatment. Previous research has mainly focused on the attentional deficits of spatial neglect and its implications for rehabilitation, although some studies have already postulated that neglect is a more general disorder of updating mental models of our environment (Shaqiri et al., 2013).

Accordingly, the two studies presented in the current thesis aimed at further investigating probabilistic interference processes in the healthy and lesioned brain. For this purpose, parameters of probabilistic inference (derived from a computational learning model (Experiment 1), weights of regression analyses and explicit probability estimations (Experiment 2)) were applied in the context of resting-state fMRI in healthy young participants (Experiment 1) and of lesion analyses in stroke patients (Experiment 2).

In the following, the conducted experiments will be discussed in light of the current literature and possible limitations, but also resulting implications of the obtained findings will be presented.

3.1 Experiment 1

3.1.1 The Relationship between Resting-state Functional Connectivity and Attentional Reorienting as well as Probabilistic Inference

Experiment 1 aimed at investigating the relationship between the resting-state network architecture of the rTPJ with dorsal and ventral attention systems and the two cognitive processes of attentional reorienting and probabilistic belief updating. For this purpose, a modified location-cueing paradigm with block-wise changes of the %CV and true and false prior information about the %CV before each block was employed in healthy young

3. General Discussion

participants. Furthermore, parameters of a Rescorla-Wagner model were estimated on the basis of response times to assess probabilistic inference. Moreover, resting-state fMRI was recorded before and after the task and a seed-based correlation analysis was used to define the rsFC of the rTPJ. Correlations of each behavioral parameter with the rsFC before the task, as well as with changes in rsFC after the task, were assessed in a ROI-based approach.

It was found that higher functional connectivity between rTPJ and rIPS before the task was associated with slower belief updating after false priors. In addition, increased interhemispheric rsFC between rTPJ and lTPJ after the task was related to both relatively faster belief updating in false blocks and faster reorienting of attention. Both findings support previous research and highlight that individual differences in spontaneous cortical activity before a task can predict individual differences in task performance (Baldassarre et al., 2012) as well as task performance can modify spontaneous activity between brain regions possibly engaged by the task (Lewis et al., 2009).

First, our findings contribute to the ongoing discussion about how attentional processes are modulated in the brain by probabilistic context. Previous studies have shown the importance of the dynamic interplay of the dorsal and ventral attention networks for reorienting spatial attention (Vossel et al., 2012; Weissman & Prado, 2012; Wen et al., 2012). Moreover, it was found that the coupling of TPJ (node of the VAN) with FEF (node of the DAN) and putamen relates to probabilistic attentional modulation (Vossel et al., 2015). Our results expand the existing knowledge about the functional mechanisms of probabilistic inference stating that also the resting-state architecture of the TPJ relates to probabilistic belief updating.

Although connectivity between TPJ and IPS may be important during online task performance of reorienting attention (Vossel et al., 2012), the rsFC before the task was rather related to probabilistic belief updating than reorienting. It might be that this was due to the additional component of the task making belief updating more essential for optimal performance and hence shifting the focus on prior information being relevant for updating behavior.

3. General Discussion

Since IPS is seen as pivotal for top-down control of attention (Bowling et al., 2020; Corbetta et al., 2000; Hopfinger et al., 2000) the intrahemispheric rIPS-rTPJ rsFC connection may indicate the strength of the reliance on top-down information. In case of firm reliance on prior information this would result in a smaller influence of prediction errors on the trial-wise estimation of the probability that the cue will be valid. Conforming to this notion, a TMS study on contextual updating in a sustained attention task suggests that IPS affects TPJ to shape stimulus evoked responses (Leitao et al., 2015). In addition, a TMS-fMRI study has revealed that the IPS modulates task-evoked functional connectivity by sending top-down biasing signals (Hwang et al., 2020). Thus, future work should address the effects of pre-task connectivity on task-dependent connectivity in the context of probabilistic inference further.

Both reorienting of attention as well as probabilistic inference were related to the interhemispheric TPJ connectivity. Our results suggest that probabilistic inference activities change the strength of the crosstalk between the two hemispheres in this region. Supporting our finding, it was found that both lTPJ and rTPJ are vital for updating the statistical contingency between cues and targets, with rTPJ coding mismatches between cues and targets and lTPJ coding with cue-target matches (Doricchi et al., 2010). Furthermore, effective connectivity between lTPJ and rTPJ was related to enhanced filtering of distractors in a partial report paradigm indicating interhemispheric communication of TPJ being important for other attentional functions (Vossel et al., 2016). Since the applied paradigm introduced prior information which needed to be validated or updated, lTPJ might be activated by the task as well and thus, future work should investigate the network underlying probabilistic inference in a spatial attention context in more depth.

Second, our findings contribute to the ongoing discussion about how the resting-state network architecture relates to behavior, especially in case of disease e.g. the neglect syndrome and the quest to discover new rehabilitation techniques.

In stroke patient studies it was found that interhemispheric parietal and temporoparietal interactions were crucial for performing attentional functions (Baldassarre et al., 2014; Carter et al., 2010; He et al., 2007; Siegel et al., 2016). Notably, neglect symptoms indicated by

3. General Discussion

impaired performance in a location-cueing task and cancellation tests related to a reduction of the interhemispheric functional connectivity at rest. It has been hypothesized that the weakened connectivity is possibly caused by an imbalance between both hemispheres after stroke (Baldassarre et al., 2014). In line with this notion, successful rehabilitation of neglect symptoms was related to an improved interhemispheric connectivity, in particular of the dorsal attention network (Ramsey et al., 2016; Wåhlin et al., 2019).

Therefore, the underlying imbalance caused by the affected lesioned hemisphere also enables non-invasive brain stimulation techniques as promising rehabilitation techniques. Previous research has already shown that stimulation protocols could improve impaired behavior in patients suffering neglect (see Salazar et al., 2018 for a review). For instance, inhibitory TMS on the contralesional left parietal cortex reduced symptoms of neglect (Nyffeler et al., 2019) as well as tDCS applying both anodal stimulation to the lesioned posterior parietal cortex and cathodal direct current stimulation to the unlesioned homologous area have ameliorated neglect symptoms (Sparing et al., 2009). However, when employing non-invasive neurostimulation techniques it should be considered that the response rate to the stimulation depends on the integrity of the interhemispheric connections (Nyffeler et al., 2019). Supporting this notion, it was found in healthy participants that the structural variability within the corpus callosum predicted individual differences in the effects of inhibitory TMS on the posterior parietal cortex on the allocation of spatial attention (Chechlacz et al., 2015).

Since stroke patients, more precisely patients suffering neglect syndrome, exhibit deficits also in statistical learning (Shaqiri & Anderson, 2012, 2013), a component of probabilistic inference, our results highlight that non-invasive stimulation techniques could also ameliorate these symptoms and not just performance in location-cueing or cancellation tasks. Thus, future patient studies should validate these potential rehabilitation techniques for non-spatial deficits e.g. by applying TMS to the ITPJ (unlesioned hemisphere).

3. General Discussion

3.1.2 Limitations and Implications

There are some limitations to Experiment 1 that will be discussed in the following section.

To investigate the functional connectivity in Experiment 1, we used a seed-based correlation approach. This approach is very common practice and easily interpretable (Smitha et al., 2017; van den Heuvel & Hulshoff Pol, 2010). Nevertheless, the resulting functional connectivity networks depend on the definition of the seed region of interest (ROI) (Cole et al., 2010). Since several ways exist to identify a ROI, this selection is vulnerable to bias. Seeds can be selected by using coordinates of task-based activation studies (Biswal et al., 1995), coordinates derived from meta-analyses (Reid et al., 2017) or anatomical images as reference (Di Martino et al., 2008). The size and borders of a region may underlie interindividual differences. Hence, functional essential voxels could be excluded and/or irrelevant voxels could be included in the analysis.

In case of the right TPJ, the exact definition of the region is still unclear (Igelström & Graziano, 2017). There are several studies proposing a parcellation of this region into subregions (Igelström et al., 2016; Mars et al., 2012). Since there is no consensus about the exact borders of the region, we chose our seed on the basis of a previous activation and neurostimulation study (Mengotti et al., 2017; Vossel et al., 2015). Hence, it could also be interesting to use another seed definition approach (e.g. the meta-analytic approach applying Krall et al., 2015) and compare the results.

Another idea would be to investigate the functional connectivity of a different node of the dorsal and ventral attention network and test how it relates to reorienting and probabilistic inference, respectively. A potential region of interest could be the IPS. In previous task based activation studies, the left anterior IPS was found to be relevant for inferring the trial-wise %CV during both spatial and feature-based attention (Dombert, Kuhns, et al., 2016). The coordinate of this study could be used for a further seed based analysis. Since the results of Experiment 1 revealed an important intrahemispheric connection of TPJ and IPS, investigating this region further could be used to validate and expand our findings.

3.2 Experiment 2

3.2.1 The Relationship between Probabilistic Inference in the Domain of Spatial Attention and the Neglect Syndrome

Two questions were addressed in Experiment 2a. First, it was investigated whether stroke patients exhibited impairments of probabilistic inference in the domain of visuospatial attention. Second, it was examined if the neglect syndrome in particular relates to impairments of spatial probabilistic inference. In order to investigate these aspects, a modified location-cueing paradigm without any prior information with block-wise changes of the %CV was performed by RH and LH patients and HC. Probabilistic inference was assessed by analyzing the impact of the %CV manipulation on RTs using linear regressions as well as explicit probability estimations of the true %CV levels. In addition, patients were screened for the neglect syndrome using a comprehensive neuropsychological test battery and lesion-symptom as well as lesion-network mapping was performed on the relevant behavioral parameters.

The data revealed that probabilistic inference abilities were not per se reduced in the group of stroke patients. They were able to learn the probabilities as indicated by the linear pattern of the VEs and the explicit %CV estimates. However, by trend it was found that some RH patients had difficulties using their knowledge to adapt their behavior in contralesional space as indicated by a reduced modulation of RTs by %CV in invalid contralesional trials and explicit estimation issues. The correlation of the two measures revealed no significant relationship, stating these parameters as independent components of probabilistic inference. This was further supported by the VLSM results.

This study did not reveal strong evidence for impairments of probabilistic inference being related to contralesional neglect. Only underestimating the explicit %CV was related to a tendency towards more frequent responses in ipsilesional space as indicated by higher RB-scores of the Landmark-M test. However, the absence of a strong connection between impaired probabilistic inference and the neglect syndrome might be due to our heterogenous

3. General Discussion

patient sample. Only subacute and chronic patients were assessed with only a few patients exhibiting neglect symptoms of mild to moderate severity. Hence, the data might be underpowered to detect a strong relationship.

Furthermore, functional neuroimaging studies reveal which brain structures and networks are related to a specific cognitive process, whereas brain lesion studies allow the inference which brain regions are necessary for a specific cognitive process (Fellows et al., 2005). Hence, brain regions which have been related a specific cognitive process in fMRI studies might not be revealed as *necessary* for this cognitive process in brain lesion studies given that other brain regions might compensate for the impairment of the lesioned region. Consequently, our results of per se preserved probabilistic inference abilities and no specific association of rTPJ lesions with probabilistic inference impairments in the current stroke sample might reflect functional compensation by intact brain regions.

Additionally, one might argue that the lack of severe deficits in probabilistic inference in the current stroke sample could merely be due to the response strategy (i.e. a compensatory slowing of response times) of the patients to maintain normal task performance. Although no group difference in accuracy was present, it might be that patients benefited in the probabilistic inference parameters by slowing down their responses. Mengotti et al. (2019) found a speed-accuracy trade-off (i.e., responding more slowly in order to perform accurately) and preserved probabilistic inference abilities in old participants. Hence, slow responses of patients might not lead to a benefit of accuracy, but instead to enhanced general learning abilities. Using a paradigm with a shortened period of time to respond might detect impairments in patients which could not have been detected with the current version of our experiment.

Nonetheless, our results contribute to the advanced understanding of the neglect syndrome demonstrating that at a subacute/chronic stage of stroke impairments of probabilistic inference are not per se compromised. Still, our data revealed lateralized adaptation deficits which were related more to RH than to LH brain damage.

3. General Discussion

3.2.2 Limitations and Implications

The following section will discuss the limitations of Experiment 2a and elaborate on possible implications. In Experiment 2a, stroke patients and healthy elderly participants were compared using a spatial cueing paradigm. Among the group of patients, also young patients were included, who were not severely impaired. This might have constrained the comparison with the old healthy controls and have reduced significant differences between the groups. Thus, dividing patients into subgroups, e.g. by the factor age, might unravel undetected group characteristics.

Second, while additional analyses including used hand and order as covariates revealed that these known variables did not explain the reported results, we cannot rule out that there were other unknown variables, which might have contributed to the observed effects. Previous research has stated that especially premorbid brain and cognitive reserve can impact stroke-induced impairment (Umarova, 2017). Further analyses including age, gender, time since stroke and neuropsychological scores as covariates might shed new light onto the reported findings.

Third, in the applied paradigm participants did not receive any information on the level of %CV of each block, not even in the practice. This might explain the absence of severe group differences since it was difficult for all participants to infer the actual %CV. Therefore, another possible approach to assess the updating of probabilistic beliefs/inference would be to expose the participants to information on the level of %CV and manipulate if this information is false or true. This design has already been applied in studies of young healthy participants (see Experiment 1 Käsbaier et al., 2020; Mengotti et al., 2017). In the neurostimulation study, it was discovered that right TPJ is putatively involved in updating probabilistic beliefs. Besides, Experiment 1 revealed a significant relationship of intrahemispheric FC of right TPJ and right IPS and interhemispheric FC of bilateral TPJ with a parameter of probabilistic inference. Hence, it would be interesting to also investigate if patients show impairments of updating false beliefs and if the same lesion patterns

3. General Discussion

especially lesions of white matter pathways connecting nodes of the dorsal and ventral attention systems are related to it.

Generally, it should be noted that the results obtained from the resting-state fMRI study in healthy young participants (Experiment 1) cannot easily be compared to the results of the lesion studies in (neurological) elderly participants (Experiment 2). As mentioned before, both studies varied in their experimental paradigm. Moreover, the samples differed in terms of age. The mean age of the participants in Experiment 1 was 27 years (age range = 20–36 years), whereas the mean age of the healthy controls of Experiment 2 was 63 years (age range = 51–80 years). Theories of normal aging have postulated general age-related changes of cognitive processes and their underlying neural mechanisms (Cabeza, 2001; Cabeza et al., 2018). In this context, two accounts are existing: The compensation hypothesis proposes recruitment of additional brain regions with increasing age to enable normal task performance (Reuter-Lorenz & Cappell, 2008), whereas the dedifferentiation hypothesis states that brain regions underlying cognitive processes become less functionally differentiated, although more distributed (i.e., *dedifferentiated*) during aging (Park et al., 2004). Thus, according to the dedifferentiation theory, brain lesions might not have such a high impact on broadly distributed cognitive processes (i.e. probabilistic inference). Future fMRI studies assessing probabilistic inference in young and elderly healthy participants as well as in stroke patients might be used to directly investigate the presumed altered neural mechanisms underlying probabilistic inference in the aging and lesioned brain.

Furthermore, the applied paradigm of our study focused only on the visual domain. Nevertheless, if the impairment of probabilistic inference is generic, it should be present in other sensory modalities since neglect also results in multimodal impairments (Kerkhoff, 1999). First evidence for a supramodal deficit comes from a study investigating auditory statistical learning (Shaqiri et al., 2018). However, the authors found that stroke patients in general, independent of the damaged hemisphere or the presence of neglect, showed impaired statistical learning in the auditory domain. Thus, more patient studies are needed

3. General Discussion

investigating probabilistic inference in other domains (e.g. auditory and tactile) and its relation to the neglect syndrome.

In addition, there are several general methodological constraints regarding brain lesion studies of stroke patients (Sperber & Karnath, 2018) which need to be taken into account when interpreting our obtained results: First, the functional plasticity of the brain after brain damage might reduce the inferences which can be made (Rorden & Karnath, 2004). Therefore, the time between brain damage (i.e. stroke onset) and examination is critical for potential conclusions. It has been shown that in the (sub)acute phase of a stroke (1–28 days after stroke (Bernhardt et al., 2017)) the causal relationship between a lesion and an impairment of a cognitive process is strong. However, in the chronic stroke phase (> 28 days after stroke) this inference cannot be easily made due to the potential recovery of acute symptoms over time and reorganization of the brain (Karnath & Rennig, 2017). In our study, stroke patients were recruited from the Neurological Rehabilitation Center Godeshöhe, where subacute as well as chronic patients are treated. Thus, our sample is quite heterogenous regarding the time between stroke onset and examination. Notably, time since stroke did not differ significantly between RH and LH patient groups. However, since subacute and chronic patients have been grouped and analyzed together it might be worth to repeat the analyses of subgroups to detect hidden group differences. Still, the neural correlates of chronic dysfunction are of high clinical relevance, as they enable long-term predictions of function based on the acute location of brain damage.

Besides, stroke lesions depend on the affected vascular territory (Ghika et al., 1990) resulting in connected brain regions being jointly impaired, although not inevitably related to the same cognitive process. Since the middle cerebral artery is the most common artery involved in acute stroke (Ng et al., 2007), there might be a potential bias in VLSM studies considering that results are primarily driven by overlapping areas, especially using small patient samples, where statistical power is high (Kimberg et al., 2007).

Moreover, the sample size can affect the results of univariate lesion-behavior mapping. What has been found is that studies with low power due to a small sample size yielded

3. General Discussion

heterogeneous results possibly misjudging the true effect size, whereas studies using higher sample size had the issue of trivial effect sizes becoming significant (Lorca-Puls et al., 2018). Thus, reporting sample as well as effect sizes is important for interpreting the meaningfulness of results.

To improve the anatomical validity of univariate lesion-behavior mapping it is also important to correct for lesion volume and ensure a sufficient minimum lesion overlap (Sperber & Karnath, 2017). Since we only had a small sample size, we did not correct for lesion volume potentially reducing the meaningfulness of our results.

Furthermore, inferences are also limited by the phenomenon of diaschisis, where a focal lesion results in a dysfunction of other structurally intact brain regions (Feeney & Baron, 1986). However, by employing lesion-network mapping techniques, the role of brain connectivity, disconnection, and diaschisis are taken more into account for symptom localization (Fox, 2018). Especially the knowledge of functional networks underlying cognitive functions enables non-invasive brain stimulation as a promising rehabilitation tool. By directly targeting cortical structures or indirectly subcortical areas via the modulation of interconnected cortical areas, amelioration of cognitive processes and behavioral deficits could be achieved.

3.2.3 Probabilistic Inference in Various Cognitive Domains

Experiment 2b investigated whether impairments of probabilistic inference are present in cognitive domains other than spatial attention in stroke patients and whether they can be related to distinct lesion patterns. More precisely, it was aimed to assess if impairments of probabilistic inference are general or domain-specific. For this purpose, three versions of a location-cueing paradigm, where spatial, feature, or motor cues predicted the location, color, or motor response of a target stimulus were performed and lesion-symptom as well as lesion-network mapping was conducted for the relevant behavioral parameters assessing probabilistic inference.

3. General Discussion

The data revealed that probabilistic inference abilities in feature-based attention and motor-intention were not per se compromised. Only in the spatial attention domain, RH patients had by trend some difficulties in probabilistic inference, in particular in adapting their behavior in contralesional space (see Experiment 2a for a detailed discussion). This result promotes the view that deficits in probabilistic inference are domain-specific. Previous research on priming and statistical learning supports this further (Kristjánsson et al., 2005, 2007; Shaqiri & Anderson, 2012, 2013) by stating preserved priming abilities in the feature domain of RH patients, although not in the spatial domain. Moreover, RH patients were found to be more impaired than LH patients in detecting probabilities (Danckert et al., 2012). Regarding our expectation of the involvement of specific regions of interest from previous studies of probabilistic inference of distinct domains in healthy participants (Dombert, Kuhns, et al., 2016; Kuhns et al., 2017; Mengotti et al., 2017), we only found supporting evidence for the left ANG being pivotal for motor-intention and the right HPC being relevant for probabilistic inference of spatial attention.

Furthermore, our results also revealed common mechanisms in probabilistic inference across domains. Two significant positive correlations were found: The z-standardized contralesional invalid %CV regression weights in feature-based attention and motor-intention, as well as the averaged explicit %CV estimates in the spatial attention and motor-intention version were related and shared common lesion patterns as revealed by the VLSM. Reduced modulation of RT by %CV in feature-based attention and motor-intention was associated with lesioned right insula, operculum, pre- and postcentral gyrus, basal ganglia, Heschl's gyrus and white matter pathways. Issues in estimating the explicit %CV in the spatial version as well as in the motor-intention version related to lesions affecting the right STG, insula, IFG, operculum, Heschl's gyrus and white matter pathways. It is important to note that we did not find common lesions or correlations within a parameter across all three cognitive domains.

Previous fMRI studies in healthy participants assessing probabilistic inference by using computational modelling also found neural commonalities between different cognitive

3. General Discussion

domains (Dombert, Kuhns, et al., 2016; Kuhns et al., 2017). In these studies, a common effect for probabilistic inference during spatial and feature-based attention was found in the left IPS and no direct link between spatial attention and motor-intention was detected. It is possible that the opposing results are due to the different parameters used to operationalize probabilistic inference (computational model parameters for the speed of probabilistic inference versus regression weights for RT modulation). Thus, applying computational modelling to our data would be of high interest to compare probabilistic inference in stroke patients with previous research in healthy participants. Moreover, since previous studies investigated young healthy participants, it might be that in our study some differences could not be detected since behavior could have been similarly affected by brain lesions and general age-dependent cognitive decline (e.g. in case of the ACC: Mann et al., 2011; Pardo et al., 2007).

Furthermore, neural structures which have been associated with a cognitive process in fMRI studies might not be revealed by lesion studies, since other brain areas could compensate for the lesioned area (Fellows et al., 2005). Consequently, our results of preserved probabilistic inference abilities in the current subacute/chronic stroke sample might reflect functional compensation by intact brain regions and thus should be validated by further patient studies.

3.2.4 Limitations and Implications

Although some limitations of Experiment 2 and of lesion studies in general have been already discussed in section 3.2.2 of the thesis, there were some more constraints which should be mentioned regarding the use of three different versions of the experimental paradigm.

First, by using modified cueing tasks, each task always contained a spatial component. Although any effects of spatial search should cancel out when comparing valid and invalid RTs (since the spatial component was present in both conditions), other paradigms should

3. General Discussion

be investigated to assess probabilistic inference in various domains and validate our results. The game paper, scissors and rock, where the choice behavior of the opponent was systematically varied, has been already used to investigate statistical learning (Stöttinger et al., 2014, 2018). By introducing a cue to inform about the opponent's choices or adapting it in another similar way to our paradigm could be seen as a first attempt to do so.

Furthermore, by using letters as a cue for the feature-based attention task, a spatial bias towards the right side could have been induced since the processing of letters is strongly linked to reading (Ransley et al., 2018). A previous study has found that the two-letter abbreviation of the color word induces the most robust cueing effects for the whole time course of an experiment, however they did not investigate the factor side in their analyses (Dombert, Fink, et al., 2016). Hence, we cannot rule out a spatial bias in the feature-based attention task, although we controlled for other factors, e.g. excluding patients with aphasia.

Another limitation of the study was that patients and healthy controls performed the whole experiment in a different time frame. Due to the limited attention span of the patients, none of them completed the experiment in one session. However, all healthy controls performed the experiment in one session. This might explain why we did not find many significant differences between elderly HC and patients, since HC could have been fatigued and exhausted. Moreover, the different time frame could also explain the difficulty of estimating the true %CV for some patients, since similarities of the three tasks might not be easily detected if patients did them a week apart instead of in one or two sessions. Therefore, HC and patients who did all the three tasks in one session or only a day apart might have a benefit of repetition and familiarity. This constraint of the experimental procedure can potentially impact on our results, since more severe patients took more time and might also suffer from more comorbidities (e.g. impairments of working memory) making it extremely difficult for them to infer the true %CV. However, we did not find tremendous differences between the groups, indicating that this potential bias might not play a major role in our study. Still, future studies should consider this issue and perform their experiments with a more fixed time schedule of experimental sessions.

3. General Discussion

Finally, it could be of great interest to apply the computational modelling approach of Experiment 1 to the patient data. More precisely, comparing the learning rates derived from the RW model of the distinct versions of the task can provide valuable information about the effect of cue type on individual updating behavior. Since using regression analyses of %CV on RTs as a measure of probabilistic inference only revealed trends for differences between the groups, computational modelling could validate our results or characterize the learning of unknown probabilities in more depth, thereby even detecting group differences. However, in order to reliably estimate these model parameters, the model would need to be considerably adapted (e.g. to account for hemifield-specific effects) and would need to be evaluated if they would be a good fit and applicable for the more variable and hence noisy patient data.

3.3 Future Perspectives and Concluding Remarks

The core research questions of the present thesis concern how the resting-state network architecture of the human brain relates to probabilistic inference as well as how the lesioned brain performs probabilistic inference in different cognitive domains.

The first part of this work was conducted in healthy participants and thus pertains to the field of basic research. It was demonstrated that resting-state functional connectivity before and after a task related to behavioral performance of probabilistic inference. In particular, the importance of interhemispheric (parietal) connectivity for optimal performance was revealed.

The second part of this work was performed with stroke patients, although still belonging to the field of basic research. Here, it was found that stroke patients' probabilistic inference abilities in different domains were not per se impaired and only some RH patients exhibited a lateralized adaption deficit to the probabilistic context in the domain of spatial attention. Furthermore, no significant relation between impairments of probabilistic inference and the neglect syndrome could be shown. However, some behavioral and neural commonalities between probabilistic inference of different domains were revealed.

3. General Discussion

Identifying commonalities or distinctions between probabilistic inference in different domains in patients helps to understand whether the neural computations of probabilistic inference are implemented within a domain general system or whether there are several domain-specific systems. Furthermore, the knowledge of domain general or specific processes is relevant for developing suitable treatment protocols. Our data suggests that the neural implementations for probabilistic inference seem to be dedicated to domain-specific subsystems, which share some common nodes.

Future studies should transfer the gained knowledge from basic research of healthy participants and of patients to a clinical application. By combining the findings of the two studies, new therapeutic strategies for patients should be developed. This could be achieved e.g. by employing the resting-state network pattern of a patient to predict impairments of probabilistic inference as well as therapy outcome. Moreover, the development of suitable treatment protocols for non-invasive brain stimulation techniques improving the interhemispheric connectivity of the lesioned brain or for the behavioral training of preserved probabilistic inference abilities in a cognitive domain to improve performance in other domains are further potential applications.

Thus, the present thesis contributes to an advanced understanding of how probabilistic inference is computed in the healthy and lesioned brain, enabling the development of new clinical treatment techniques.

4. References

- Aguirre, G. K., Zarahn, E., & D'Esposito, M. (1998). The Variability of Human, BOLD Hemodynamic Responses. *NeuroImage*, *8*(4), 360–369.
- Aslin, R. N., & Newport, E. L. (2012). Statistical Learning: From Acquiring Specific Items to Forming General Rules. *Current Directions in Psychological Science*, *21*(3), 170–176.
- Avants, B., Tustison, N. J., Song, G., Cook, P. A., Klein, A., & Gee, J. C. (2011). A reproducible evaluation of ANTs similarity metric performance in brain image registration. *NeuroImage*, *54*(3), 2033–2044.
- Azouvi, P. (2017). The ecological assessment of unilateral neglect. *Annals of Physical and Rehabilitation Medicine*, *60*(3), 186–190.
- Azouvi, P., Samuel, C., Louis-Dreyfus, A., Bernati, T., Bartolomeo, P., Beis, J.-M., Chokron, S., Leclercq, M., Marchal, F., Martin, Y., de Montety, G., Olivier, S., Perennou, D., Pradat-Diehl, P., Prairial, C., Rode, G., Siéroff, E., Wiart, L., & Rousseaux, M. (2002). Sensitivity of clinical and behavioural tests of spatial neglect after right hemisphere stroke. *Journal of Neurology, Neurosurgery, and Psychiatry*, *73*(2), 160-166.
- Baldassarre, A., Lewis, C. M., Committeri, G., Snyder, A. Z., Romani, G. L., & Corbetta, M. (2012). Individual variability in functional connectivity predicts performance of a perceptual task. *Proceedings of the National Academy of Sciences*, *109*(9), 3516–3521.
- Baldassarre, A., Ramsey, L. E., Hacker, C. L., Callejas, A., Astafiev, S. V., Metcalf, N. V., Zinn, K., Rengachary, J., Snyder, A. Z., Carter, A. R., Shulman, G. L., & Corbetta, M. (2014). Large-scale changes in network interactions as a physiological signature of spatial neglect. *Brain*, *137*(12), 3267–3283.
- Barker-Collo, S. L., Feigin, V. L., Lawes, C. M. M., Parag, V., & Senior, H. (2010). Attention deficits after incident stroke in the acute period: frequency across types of attention and relationships to patient characteristics and functional outcomes. *Topics in Stroke Rehabilitation*, *17*(6), 463–476.
- Bartolomeo, P. (2011). The quest for the 'critical lesion site' in cognitive deficits: problems

4. References

- and perspectives. *Cortex*, 47(8), 1010-1012.
- Bartolomeo, P., & Chokron, S. (1999). Egocentric frame of reference: Its role in spatial bias after right hemisphere lesions. *Neuropsychologia*, 37(8), 881–894.
- Bartolomeo, P., Thiebaut de Schotten, M., & Chica, A. B. (2012). Brain networks of visuospatial attention and their disruption in visual neglect. *Frontiers in Human Neuroscience*, 6, 1–10.
- Bartolomeo, P., & Seidel Malkinson, T. (2019). Hemispheric lateralization of attention processes in the human brain. *Current Opinion in Psychology*, 29, 90–96.
- Bates, E., Wilson, S. M., Saygin, A. P., Dick, F., Sereno, M. I., Knight, R. T., & Dronker, N. F. (2003). Voxel-based lesion-symptom mapping. *Nature Neuroscience*, 6(5), 448–450.
- Behrens, T. E., Woolrich, M. W., Walton, M. E., & Rushworth, M. F. S. (2007). Learning the value of information in an uncertain world. *Nature Neuroscience*, 10(9), 1214–1221.
- Behzadi, Y., Restom, K., Liu, J., & Liu, T. T. (2007). A component based noise correction method (CompCor) for BOLD and perfusion based fMRI. *NeuroImage*, 37(1), 90–101.
- Beis, J.-M., Keller, C., Morin, N., Bartolomeo, P., Bernati, T., Chokron, S., Leclercq, M., Louis-Dreyfus, A., Marchal, F., Martin, Y., Perennou, D., Pradat-Diehl, P., Prairial, C., Rode, G., Rousseaux, M., Samuel, C., Sieroff, E., Wiart, L., & Azouvi, P. (2004). Right spatial neglect after left hemisphere stroke. *Neurology*, 63(9), 1600–1605.
- Bernhardt, J., Hayward, K. S., Kwakkel, G., Ward, N. S., Wolf, S. L., Borschmann, K., Krakauer, J. W., Boyd, L. A., Carmichael, S. T., Corbett, D., & Cramer, S. C. (2017). Agreed definitions and a shared vision for new standards in stroke recovery research: The Stroke Recovery and Rehabilitation Roundtable taskforce. *International Journal of Stroke*, 12(5), 444–450.
- Beume, L., Martin, M., Kaller, C. P., Klöppel, S., Schmidt, C. S. M., Urbach, H., Egger, K., Rijntjes, M., Weiller, C., & Umarova, R. M. (2017). Visual neglect after left-hemispheric lesions: a voxel-based lesion–symptom mapping study in 121 acute stroke patients. *Experimental Brain Research*, 235(1), 83–95.
- Bisiach, E., & Luzzatti, C. (1978). Unilateral Neglect of Representational Space. *Cortex*,

4. References

- 14(1), 129–133.
- Bisiach, E., Perani, D., Vallar, G., & Berti, A. (1986). Unilateral neglect: personal and extra-personal. *Neuropsychologia*, 24(6), 759–767.
- Bisiach, E., Ricci, R., Lualdi, M., & Colombo, M. R. (1998). Perceptual and response bias in unilateral neglect: Two modified versions of the Milner Landmark task. *Brain and Cognition*, 37(3), 369–386.
- Biswal, B. (2012). Resting state fMRI: A personal history. *NeuroImage*, 62(2), 938–944.
- Biswal, B., Yetkin, F. Z., Haughton, V. M., & Hyde, J. S. (1995). Functional connectivity in the motor cortex of resting human brain using echo-planar MRI. *Magnetic resonance in medicine*, 34(4), 537-541.
- Boes, A. D., Prasad, S., Liu, H., Liu, Q., Pascual-Leone, A., Caviness, V. S., & Fox, M. D. (2015). Network localization of neurological symptoms from focal brain lesions. *Brain*, 138(10), 3061–3075.
- Boorman, E. D., Rajendran, V. G., O'Reilly, J. X., & Behrens, T. E. (2016). Two Anatomically and Computationally Distinct Learning Signals Predict Changes to Stimulus–Outcome Associations in Hippocampus. *Neuron*, 89(6), 1343–1354.
- Bowling, J. T., Friston, K. J., & Hopfinger, J. B. (2020). Top-down versus bottom-up attention differentially modulate frontal–parietal connectivity. *Human Brain Mapping*, 41(4), 928–942.
- Brett, M., Leff, A. P., Rorden, C., & Ashburner, J. (2001). Spatial normalization of brain images with focal lesions using cost function masking. *NeuroImage*, 14(2), 486–500.
- Broca, P. (1861). Remarques sur le siège de la faculté du langage articulé, suivies d'une observation d'aphémie (perte de la parole). *Bulletin et Memoires de La Societe Anatomique de Paris*, 6, 330–357.
- Brodersen, K. H., Penny, W. D., Harrison, L. M., Daunizeau, J., Ruff, C. C., Duzel, E., Friston, K. J., & Stephan, K. E. (2008). Integrated Bayesian models of learning and decision making for saccadic eye movements. *Neural Networks*, 21(9), 1247–1260.
- Büki, A., & Povlishock, J. T. (2006). All roads lead to disconnection?—Traumatic axonal injury

4. References

- revisited. *Acta Neurochirurgica*, *148*(2), 181–194.
- Bzdok, D., Langner, R., Schilbach, L., Jakobs, O., Roski, C., Caspers, S., Laird, A. R., Fox, P. T., Zilles, K., & Eickhoff, S. B. (2013). Characterization of the temporo-parietal junction by combining data-driven parcellation, complementary connectivity analyses, and functional decoding. *NeuroImage*, *81*, 381–392.
- Cabeza, R. (2001). Cognitive neuroscience of aging: contributions of functional neuroimaging. *Scandinavian Journal of Psychology*, *42*(3), 277–286.
- Cabeza, R., Albert, M., Belleville, S., Craik, F. I. M., Duarte, A., Grady, C. L., Lindenberger, U., Nyberg, L., Park, D. C., Reuter-Lorenz, P. A., Rugg, M. D., Steffener, J., & Rajah, M. N. (2018). Maintenance, reserve and compensation: the cognitive neuroscience of healthy ageing. *Nature Reviews Neuroscience*, *19*(11), 701–710.
- Carpenter, R. H. S., & Williams, M. L. L. (1995). Neural computation of log likelihood in control of saccadic eye movements. *Nature*, *377*(6544), 59–62.
- Carter, A. R., Astafiev, S. V., Lang, C. E., Connor, L. T., Rengachary, J., Strube, M. J., Pope, D. L. W., Shulman, G. L., & Corbetta, M. (2010). Resting interhemispheric functional magnetic resonance imaging connectivity predicts performance after stroke. *Annals of Neurology*, *67*(3), 365–375.
- Carter, A. R., McAvoy, M. P., Siegel, J. S., Hong, X., Astafiev, S. V., Rengachary, J., Zinn, K., Metcalf, N. V., Shulman, G. L., & Corbetta, M. (2017). Differential white matter involvement associated with distinct visuospatial deficits after right hemisphere stroke. *Cortex*, *88*, 81–97.
- Catani, M., Robertsson, N., Beyh, A., Huynh, V., de Santiago Requejo, F., Howells, H., Barrett, R. L. C., Aiello, M., Cavaliere, C., Dyrby, T. B., Krug, K., Ptito, M., D’Arceuil, H., Forkel, S. J., & Dell’Acqua, F. (2017). Short parietal lobe connections of the human and monkey brain. *Cortex*, *97*, 339–357.
- Chechlac, M., Humphreys, G. W., Sotiropoulos, S. N., Kennard, C., & Cazzoli, D. (2015). Structural Organization of the Corpus Callosum Predicts Attentional Shifts after Continuous Theta Burst Stimulation. *The Journal of Neuroscience*, *35*(46), 15353–

4. References

15368.

- Chechlacz, M., Rotshtein, P., & Humphreys, G. W. (2012). Neuroanatomical Dissections of Unilateral Visual Neglect Symptoms: ALE Meta-Analysis of Lesion-Symptom Mapping. *Frontiers in Human Neuroscience*, *6*, 230.
- Chica, A. B., Bartolomeo, P., & Valero-Cabre, A. (2011). Dorsal and Ventral Parietal Contributions to Spatial Orienting in the Human Brain. *The Journal of Neuroscience*, *31*(22), 8143–8149.
- Clark, A. (2013). Whatever next? Predictive brains, situated agents, and the future of cognitive science. *The Behavioral and Brain Sciences*, *36*(3), 181–204.
- Clas, P., Groeschel, S., & Wilke, M. (2012). A semi-automatic algorithm for determining the demyelination load in metachromatic leukodystrophy. *Academic Radiology*, *19*(1), 26–34.
- Cole, D. M., Smith, S. M., & Beckmann, C. F. (2010). Advances and pitfalls in the analysis and interpretation of resting-state fMRI data. *Frontiers in Systems Neuroscience*, *4*, 8.
- Cook, R. D. (1977). Detection of Influential Observation Linear Regression. *Technometrics*, *19*(1), 15–18.
- Corbetta, M., Kincade, M. J., Lewis, C., Snyder, A. Z., & Sapir, A. (2005). Neural basis and recovery of spatial attention deficits in spatial neglect. *Nature Neuroscience*, *8*(11), 1603–1610.
- Corbetta, M., Kincade, M. J., Ollinger, J. M., McAvoy, M. P., & Shulman, G. L. (2000). Voluntary orienting is dissociated from target detection in human posterior parietal cortex. *Nature Neuroscience*, *3*(3), 292–297.
- Corbetta, M., Patel, G., & Shulman, G. L. (2008). The Reorienting System of the Human Brain: From Environment to Theory of Mind. *Neuron*, *58*(3), 306–324.
- Corbetta, M., Ramsey, L. E., Callejas, A., Baldassarre, A., Hacker, C. D., Siegel, J. S., Astafiev, S. V., Rengachary, J., Zinn, K., Lang, C. E., Connor, L. T., Fucetola, R., Strube, M. J., Carter, A. R., & Shulman, G. L. (2015). Common behavioral clusters and subcortical anatomy in stroke. *Neuron*, *85*(5), 927–941.

4. References

- Corbetta, M., & Shulman, G. L. (2002). Control of goal-directed and stimulus-driven attention in the brain. *Nature Reviews Neuroscience*, 3(3), 201–215.
- Corbetta, M., & Shulman, G. L. (2011). Spatial neglect and attention networks. *Annual Review of Neuroscience*, 34(3), 569–599.
- Craddock, R. C., Holtzheimer, P. E., Hu, X. P., & Mayberg, H. S. (2009). Disease state prediction from resting state functional connectivity. *Magnetic Resonance in Medicine*, 62(6), 1619–1628.
- Creavin, S. T., Wisniewski, S., Noel-Storr, A. H., Trevelyan, C. M., Hampton, T., Rayment, D., Thom, V. M., Nash, K. J. E., & Elhamoui, H. (2016). Mini-Mental State Examination (MMSE) for the detection of dementia in people aged over 65. *Cochrane Database of Systematic Reviews*, 1, 1–185.
- Danckert, J., & Ferber, S. (2006). Revisiting unilateral neglect. *Neuropsychologia*, 44(6), 987–1006.
- Danckert, J., Ferber, S., Pun, C., Broderick, C., Striemer, C., Rock, S., & Stewart, D. (2007). Neglected time: impaired temporal perception of multisecond intervals in unilateral neglect. *Journal of Cognitive Neuroscience*, 19(10), 1706–1720.
- Danckert, J., Stöttinger, E., Quehl, N., & Anderson, B. (2012). Right hemisphere brain damage impairs strategy updating. *Cerebral Cortex*, 22(12), 2745–2760.
- Daunizeau, J., den Ouden, H. E. M., Pessiglione, M., Kiebel, S. J., Friston, K. J., & Stephan, K. E. (2010). Observing the observer (II): Deciding when to decide. *PLoS ONE*, 5(12), e15555.
- Daunizeau, J., den Ouden, H. E. M., Pessiglione, M., Kiebel, S. J., Stephan, K. E., & Friston, K. J. (2010). Observing the Observer (I): Meta-Bayesian Models of Learning and Decision-Making. *PLoS ONE*, 5(12), e15554.
- De Haan, B., Clas, P., Juenger, H., Wilke, M., & Karnath, H.-O. (2015). Fast semi-automated lesion demarcation in stroke. *NeuroImage: Clinical*, 9, 69–74.
- De Haan, B., & Karnath, H.-O. (2018). A hitchhiker's guide to lesion-behaviour mapping. *Neuropsychologia*, 115, 5–16.

4. References

- De Lange, F. P., Heilbron, M., & Kok, P. (2018). How Do Expectations Shape Perception? *Trends in Cognitive Sciences*, 22(9), 764–779.
- Den Ouden, H. E. M., Daunizeau, J., Roiser, J., Friston, K. J., & Stephan, K. E. (2010). Striatal prediction error modulates cortical coupling. *Journal of Neuroscience*, 30(9), 3210–3219.
- Deubel, H. (2008). The time course of presaccadic attention shifts. *Psychological Research*, 72(6), 630–640.
- Di Martino, A., Scheres, A., Margulies, D. S., Kelly, A. M. C., Uddin, L. Q., Shehzad, Z., Biswal, B., Walters, J. R., Castellanos, F. X., & Milham, M. P. (2008). Functional Connectivity of Human Striatum: A Resting State fMRI Study. *Cerebral Cortex*, 18(12), 2735–2747.
- Dombert, P. L., Fink, G. R., & Vossel, S. (2016). The impact of probabilistic feature cueing depends on the level of cue abstraction. *Experimental Brain Research*, 234(3), 685–694.
- Dombert, P. L., Kuhns, A. B., Mengotti, P., Fink, G. R., & Vossel, S. (2016). Functional mechanisms of probabilistic inference in feature- and space-based attentional systems. *NeuroImage*, 142, 553–564.
- Doricchi, F., Macci, E., Silvetti, M., & Macaluso, E. (2010). Neural correlates of the spatial and expectancy components of endogenous and stimulus-driven orienting of attention in the posner task. *Cerebral Cortex*, 20(7), 1574–1585.
- Egner, T., Monti, J. M. P., Trittschuh, E. H., Wieneke, C. A., Hirsch, J., & Mesulam, M. M. (2008). Neural Integration of Top-Down Spatial and Feature-Based Information in Visual Search. *The Journal of Neuroscience*, 28(24), 6141–6151.
- Eickhoff, S. B., Stephan, K. E., Mohlberg, H., Grefkes, C., Fink, G. R., Amunts, K., & Zilles, K. (2005). A new SPM toolbox for combining probabilistic cytoarchitectonic maps and functional imaging data. *NeuroImage*, 25(4), 1325–1335.
- Eppinger, B., Hämmerer, D., & Li, S.-C. (2011). Neuromodulation of reward-based learning and decision making in human aging. *Annals of the New York Academy of Sciences*,

4. References

1235, 1–17.

- Eschenbeck, P., Vossel, S., Weiss, P. H., Saliger, J., Karbe, H., & Fink, G. R. (2010). Testing for neglect in right-hemispheric stroke patients using a new assessment battery based upon standardized activities of daily living (ADL). *Neuropsychologia*, *48*(12), 3488–3496.
- Fazekas, F., Chawluk, J. B., Alavi, A., Hurtig, H. I., & Zimmerman, R. A. (1987). MR signal abnormalities at 1.5 T in Alzheimer's dementia and normal aging. *American Journal of Roentgenology*, *149*(2), 351–356.
- Feeney, D. M., & Baron, J. C. (1986). Diaschisis. *Stroke*, *17*(5), 817–830.
- Feldman, H., & Friston, K. J. (2010). Attention, uncertainty, and free-energy. *Frontiers in Human Neuroscience*, *4*, 215.
- Fellows, L. K., Heberlein, A. S., Morales, D. A., Shivde, G., Waller, S., & Wu, D. H. (2005). Method Matters: An Empirical Study of Impact in Cognitive Neuroscience. *Journal of Cognitive Neuroscience* *17*(6), 850–858.
- Fels, M., & Geissner, E. (1997). *Neglect-Test (NET): ein Verfahren zur Erfassung visueller Neglectphänomene ; deutsche überarbeitete Adaption des Behavioural Inattention Test (Wilson, Cockburn & Halligan, 1987)*. Göttingen: Hogrefe.
- Filipowicz, A., Anderson, B., & Danckert, J. (2016). Adapting to change: The role of the right hemisphere in mental model building and updating. *Canadian Journal of Experimental Psychology = Revue Canadienne de Psychologie Experimentale*, *70*(3), 201–218.
- Fisicaro, R. A., Jost, E., Shaw, K., Brennan, N. P., Peck, K. K., & Holodny, A. I. (2016). Cortical Plasticity in the Setting of Brain Tumors. *Topics in Magnetic Resonance Imaging: TMRI*, *25*(1), 25–30.
- Folstein, M. F., & Folstein, S. E. (1975). "Mini-mental state": a practical method for grading the cognitive state of patients for the clinician. *Journal of Psychiatric Research*, *12*(3), 189–198.
- Foulon, C., Cerliani, L., Kinkingnéhun, S., Levy, R., Rosso, C., Urbanski, M., Volle, E., & Thiebaut de Schotten, M. (2018). Advanced lesion symptom mapping analyses and

4. References

- implementation as BCBtoolkit. *GigaScience*, 7(3), giy004.
- Fox, M. D. (2018). Mapping symptoms to brain networks with the human connectome. *New England Journal of Medicine*, 379(23), 2237–2245.
- Fox, M. D., Corbetta, M., Snyder, A. Z., Vincent, J. L., & Raichle, M. E. (2006). Spontaneous neuronal activity distinguishes human dorsal and ventral attention systems. *Proceedings of the National Academy of Sciences*, 103(26), 10046–10051.
- Fox, M. D., Snyder, A. Z., Vincent, J. L., Corbetta, M., Van Essen, D. C., & Raichle, M. E. (2005). The human brain is intrinsically organized into dynamic, anticorrelated functional networks. *Proceedings of the National Academy of Sciences*, 102(27), 9673–9678.
- Friedrich, F. J., Egly, R., Rafal, R. D., & Beck, D. (1998). Spatial attention deficits in humans: a comparison of superior parietal and temporal-parietal junction lesions. *Neuropsychology*, 12(2), 193–207.
- Friston, K. J., Holmes, A. P., Worsley, K. J., Poline, J. B., Frith, C. D., & Frackowiak, R. J. S. (1995). Statistical parametric maps in functional imaging: a general linear approach. *Human Brain Mapping*, 2(4), 189–210.
- Friston, K. J. (2005). A theory of cortical responses. *Philosophical Transactions of the Royal Society of London. Series B, Biological Sciences*, 360(1456), 815–836.
- Friston, K. J. (2011). Functional and Effective Connectivity: A Review. *Brain Connectivity*, 1(1), 13–36.
- Friston, K. J., & Kiebel, S. J. (2009). Predictive coding under the free-energy principle. *Philosophical Transactions of the Royal Society of London. Series B, Biological Sciences*, 364(1521), 1211–1221.
- Friston, K. J., Mattout, J., Trujillo-Barreto, N., Ashburner, J., & Penny, W. D. (2007). Variational free energy and the Laplace approximation. *NeuroImage*, 34(1), 220–234.
- Geng, J. J., & Behrmann, M. (2002). Probability Cuing of Target Location Facilitates Visual Search Implicitly in Normal Participants and Patients with Hemispatial Neglect. *Psychological Science*, 13(6), 520–525.

4. References

- Geng, J. J., & Behrmann, M. (2006). Competition between simultaneous stimuli modulated by location probability in hemispatial neglect. *Neuropsychologia*, *44*(7), 1050–1060.
- Geng, J. J., & Vossel, S. (2013). Re-evaluating the role of TPJ in attentional control: Contextual updating? *Neuroscience and Biobehavioral Reviews*, *37*(10), 2608–2620.
- George, D., & Mallery, P. (2010). *SPSS for Windows step by step. A simple study guide and reference (10th edition)*. Boston, MA: Pearson.
- Gershman, S. J., & Beck, J. M. (2017). Complex Probabilistic Inference. *Computational Models of Brain and Behavior* (ed A. Moustafa). Hoboken, NJ: Wiley-Blackwell.
- Ghika, J. A., Bogousslavsky, J., & Regli, F. (1990). Deep Perforators From the Carotid System: Template of the Vascular Territories. *Archives of Neurology*, *47*(10), 1097–1100.
- Gillebert, C. R., Mantini, D., Thijs, V., Sunaert, S., Dupont, P., & Vandenberghe, R. (2011). Lesion evidence for the critical role of the intraparietal sulcus in spatial attention. *Brain*, *134*(6), 1694–1709.
- Greenberg, S. A. (2007). The geriatric depression scale: Short form. *American Journal of Nursing*, *107*(10), 60–69.
- Greicius, M. D., Supekar, K., Menon, V., & Dougherty, R. F. (2009). Resting-state functional connectivity reflects structural connectivity in the default mode network. *Cerebral Cortex*, *19*(1), 72–78.
- Gusnard, D. A., & Raichle, M. E. (2001). Searching for a baseline: Functional imaging and the resting human brain. *Nature Reviews Neuroscience*, *2*(10), 685–694.
- Hampson, M., Driesen, N. R., Skudlarski, P., Gore, J. C., & Constable, R. T. (2006). Brain Connectivity Related to Working Memory Performance. *The Journal of Neuroscience*, *26*(51), 13338–13343.
- He, B. J., Snyder, A. Z., Vincent, J. L., Epstein, A., Shulman, G. L., & Corbetta, M. (2007). Breakdown of Functional Connectivity in Frontoparietal Networks Underlies Behavioral Deficits in Spatial Neglect. *Neuron*, *53*(6), 905–918.
- Heilman, K. M., & Van Den Abell, T. (1980). Right hemisphere dominance for attention: the

4. References

- mechanism underlying hemispheric asymmetries of inattention (neglect). *Neurology*, 30(3), 327–330.
- Heilman, K. M., & Watson, R. T. (1977). Mechanisms underlying the unilateral neglect syndrome. *Advances in Neurology*, 18, 93–106.
- Herbet, G., Yordanova, Y. N., & Duffau, H. (2017). Left Spatial Neglect Evoked by Electrostimulation of the Right Inferior Fronto-occipital Fasciculus. *Brain Topography*, 30(6), 747–756.
- Hoffstaedter, F., Grefkes, C., Caspers, S., Roski, C., Palomero-Gallagher, N., Laird, A. R., Fox, P. T., & Eickhoff, S. B. (2014). The role of anterior midcingulate cortex in cognitive motor control. *Human Brain Mapping*, 35(6), 2741–2753.
- Honey, C. J., Sporns, O., Cammoun, L., Gigandet, X., Thiran, J. P., Meuli, R., & Hagmann, P. (2009). Predicting human resting-state functional connectivity from structural connectivity. *Proceedings of the National Academy of Sciences*, 106(6), 2035–2040.
- Hopfinger, J. B., Buonocore, M. H., & Mangun, G. R. (2000). The neural mechanisms of attentional control. *Nature Neuroscience*, 3(3), 284–291.
- Horowitz, A. L. (1995). *MRI Physics for Radiologists* (3rd edition). New York, NY: Springer.
- Hua, K., Zhang, J., Wakana, S., Jiang, H., Li, X., Reich, D. S., Calabresi, P. A., Pekar, J. J., van Zijl, P. C. M., & Mori, S. (2008). Tract probability maps in stereotaxic spaces: analyses of white matter anatomy and tract-specific quantification. *NeuroImage*, 39(1), 336–347.
- Husain, M., & Rorden, C. (2003). Non-spatially lateralized mechanisms in hemispatial neglect. *Nature Reviews Neuroscience*, 4(1), 26–36.
- Husain, M., Shapiro, K. L., Martin, J., & Kennard, C. (1997). Abnormal temporal dynamics of visual attention in spatial neglect patients. *Nature*, 385(6612), 154–156.
- Hwang, K., Shine, J. M., Cellier, D., & D'Esposito, M. (2020). The Human Intraparietal Sulcus Modulates Task-Evoked Functional Connectivity. *Cerebral Cortex*, 30(3), 875–887.
- Igelström, K. M., & Graziano, M. S. A. (2017). The inferior parietal lobule and

4. References

- temporoparietal junction: A network perspective. *Neuropsychologia*, *105*, 70–83.
- Igelström, K. M., Webb, T. W., Kelly, Y. T., & Graziano, M. S. A. (2016). Topographical organization of attentional, social, and memory processes in the human temporoparietal cortex. *ENeuro*, *3*(2), 1363–1377.
- Iglesias, S., Mathys, C., Brodersen, K. H., Kasper, L., Piccirelli, M., den Ouden, H. E. M., & Stephan, K. E. (2013). Hierarchical Prediction Errors in Midbrain and Basal Forebrain during Sensory Learning. *Neuron*, *80*(2), 519–530.
- Jezzard, P., & Clare, S. (2001). Principles of nuclear magnetic resonance and MRI. *Functional MRI: An Introduction to Methods* (ed P. Jezzard, P. M. Matthews, and S. M. Smith). Oxford: Oxford University Press.
- Kalbe, E., Reinhold, N., & Kessler, J. (2002). *Kurze Aphasie-Check-Liste (ACL-K)*. Kerpen: UCB-Pharma GmbH.
- Karnath, H.-O., & Rennig, J. (2017). Investigating structure and function in the healthy human brain: validity of acute versus chronic lesion-symptom mapping. *Brain Structure and Function*, *222*(5), 2059–2070.
- Karnath, H.-O., & Rorden, C. (2012). The anatomy of spatial neglect. *Neuropsychologia*, *50*(6), 1010–1017.
- Karnath, H.-O., Sperber, C., & Rorden, C. (2018). Mapping human brain lesions and their functional consequences. *NeuroImage*, *165*, 180–189.
- Käsbauer, A.-S., Mengotti, P., Fink, G. R., & Vossel, S. (2020). Resting-state Functional Connectivity of the Right Temporoparietal Junction Relates to Belief Updating and Reorienting during Spatial Attention. *Journal of Cognitive Neuroscience*, *32*(6), 1130–1141.
- Kastner, S., Pinsk, M. A., De Weerd, P., Desimone, R., & Ungerleider, L. G. (1999). Increased Activity in Human Visual Cortex during Directed Attention in the Absence of Visual Stimulation. *Neuron*, *22*(4), 751–761.
- Kerkhoff, G. (1999). Multimodal spatial orientation deficits in left-sided visual neglect. *Neuropsychologia*, *37*(12), 1387–1405.

4. References

- Khosla, M., Jamison, K., Ngo, G. H., Kuceyeski, A., & Sabuncu, M. R. (2019). Machine learning in resting-state fMRI analysis. *Magnetic Resonance Imaging*, *64*, 101-121.
- Kim, S.-G., & Ogawa, S. (2012). Biophysical and Physiological Origins of Blood Oxygenation Level-Dependent fMRI Signals. *Journal of Cerebral Blood Flow & Metabolism*, *32*(7), 1188–1206.
- Kimberg, D. Y., Coslett, H. B., & Schwartz, M. F. (2007). Power in voxel-based lesion-symptom mapping. *Journal of Cognitive Neuroscience*, *19*(7), 1067–1080.
- Kinsbourne, M. (1977). Hemi-neglect and hemisphere rivalry. *Advances in Neurology* (ed R. P. Weinstein & E. A. Friedland) New York: Raven Press
- Klein, A., Andersson, J., Ardekani, B. A., Ashburner, J., Avants, B., Chiang, M.-C., Christensen, G. E., Collins, D. L., Gee, J. C., Hellier, P., Song, J. H., Jenkinson, M., Lepage, C., Rueckert, D., Thompson, P., Vercauteren, T., Woods, R. P., Mann, J. J., & Parsey, R. V. (2009). Evaluation of 14 nonlinear deformation algorithms applied to human brain MRI registration. *NeuroImage*, *46*(3), 786–802.
- Krall, S. C., Rottschy, C., Oberwelland, E., Bzdok, D., Fox, P. T., Eickhoff, S. B., Fink, G. R., & Konrad, K. (2015). The role of the right temporoparietal junction in attention and social interaction as revealed by ALE meta-analysis. *Brain Structure and Function*, *220*(2), 587–604.
- Krall, S. C., Volz, L. J., Oberwelland, E., Grefkes, C., Fink, G. R., & Konrad, K. (2016). The right temporoparietal junction in attention and social interaction: A transcranial magnetic stimulation study. *Human Brain Mapping*, *37*(2), 796–807.
- Kristjánsson, Á., Vuilleumier, P., Malhotra, P. A., Husain, M., & Driver, J. (2005). Priming of Color and Position during Visual Search in Unilateral Spatial Neglect. *Journal of Cognitive Neuroscience*, *17*(6), 859–873.
- Kristjánsson, Á., Vuilleumier, P., Schwartz, S., MacAluso, E., & Driver, J. (2007). Neural basis for priming of pop-out during visual search revealed with fMRI. *Cerebral Cortex*, *17*(7), 1612–1624.
- Kucyi, A., Hodaie, M., & Davis, K. D. (2012). Lateralization in intrinsic functional connectivity

4. References

- of the temporoparietal junction with salience- and attention-related brain networks. *Journal of Neurophysiology*, *108*(12), 3382–3392.
- Kuhns, A. B., Dombert, P. L., Mengotti, P., Fink, G. R., & Vossel, S. (2017). Spatial Attention, Motor Intention, and Bayesian Cue Predictability in the Human Brain. *The Journal of Neuroscience*, *37*(21), 5334–5344.
- Kwong, K. K., Belliveau, J. W., Chesler, D. A., Goldberg, I. E., Weisskoff, R. M., Poncelet, B. P., Kennedy, D. N., Hoppel, B. E., Cohen, M. S., & Turner, R. (1992). Dynamic magnetic resonance imaging of human brain activity during primary sensory stimulation. *Proceedings of the National Academy of Sciences*, *89*(12), 5675–5679.
- Lasaponara, S., Chica, A. B., Lecce, F., Lupiáñez, J., & Doricchi, F. (2011). ERP evidence for selective drop in attentional costs in uncertain environments: Challenging a purely premotor account of covert orienting of attention. *Neuropsychologia*, *49*(9), 2648–2657.
- Lauterbur, P. C. (1973). Image Formation by Induced Local Interactions: Examples Employing Nuclear Magnetic Resonance. *Nature*, *242*(5394), 190–191.
- Leitao, J., Thielscher, A., Tunnerhoff, J., & Noppeney, U. (2015). Concurrent TMS-fMRI Reveals Interactions between Dorsal and Ventral Attentional Systems. *Journal of Neuroscience*, *35*(32), 11445–11457.
- Lewis, C. M., Baldassarre, A., Committeri, G., Romani, G. L., & Corbetta, M. (2009). Learning sculpts the spontaneous activity of the resting human brain. *Proceedings of the National Academy of Sciences*, *106*(41), 17558–17563.
- Li, K., & Malhotra, P. A. (2015). Spatial neglect. *Practical Neurology*, *15*(5), 333–339.
- Logothetis, N. K. (2002). The neural basis of the blood–oxygen–level–dependent functional magnetic resonance imaging signal. *Philosophical Transactions of the Royal Society of London. Series B: Biological Sciences*, *357*(1424), 1003–1037.
- Logothetis, N. K., & Pfeuffer, J. (2004). On the nature of the BOLD fMRI contrast mechanism. *Magnetic Resonance Imaging*, *22*(10), 1517–1531.
- Lorca-Puls, D. L., Gajardo-Vidal, A., White, J., Seghier, M. L., Leff, A. P., Green, D. W., Crinion, J. T., Ludersdorfer, P., Hope, T. M. H., Bowman, H., & Price, C. J. (2018). The

4. References

- impact of sample size on the reproducibility of voxel-based lesion-deficit mappings. *Neuropsychologia*, 115, 101–111.
- Lunven, M., & Bartolomeo, P. (2017). Attention and spatial cognition: Neural and anatomical substrates of visual neglect. *Annals of Physical and Rehabilitation Medicine*, 60(3), 124–129.
- Lunven, M., Thiebaut De Schotten, M., Boursillon, C., Duret, C., Migliaccio, R., Rode, G., & Bartolomeo, P. (2015). White matter lesional predictors of chronic visual neglect: a longitudinal study. *Brain*, 138(3), 746–760.
- Macaluso, E. (2010). Orienting of spatial attention and the interplay between the senses. *Cortex*, 46(3), 282–297.
- Machner, B., Könemund, I., von der Gablentz, J., Bays, P. M., & Sprenger, A. (2018). The ipsilesional attention bias in right-hemisphere stroke patients as revealed by a realistic visual search task: Neuroanatomical correlates and functional relevance. *Neuropsychology*, 32 (7), 850–865.
- Madden, D. J. (1992). Selective attention and visual search: Revision of an allocation model and application to age differences. *Journal of Experimental Psychology: Human Perception and Performance*, 18(3), 821.
- Mah, Y. H., Husain, M., Rees, G., & Nachev, P. (2014). Human brain lesion-deficit inference remapped. *Brain*, 137(9), 2522–2531.
- Mann, S. L., Hazlett, E. A., Byne, W., Hof, P. R., Buchsbaum, M. S., Cohen, B. H., Goldstein, K. E., Haznedar, M. M., Mitsis, E. M., Siever, L. J., & Chu, K.-W. (2011). Anterior and posterior cingulate cortex volume in healthy adults: effects of aging and gender differences. *Brain Research*, 1401, 18–29.
- Mars, R. B., Sallet, J., Schüffelgen, U., Jbabdi, S., Toni, I., & Rushworth, M. F. S. (2012). Connectivity-based subdivisions of the human right “temporoparietal junction area”: Evidence for different areas participating in different cortical networks. *Cerebral Cortex*, 22(8), 1894–1903.
- Marshall, J. C., Caplan, D., & Holmes, J. M. (1975). The measure of laterality.

4. References

- Neuropsychologia*, 13 (3), 315–321.
- Mathys, C., Daunizeau, J., Friston, K. J., & Stephan, K. E. (2011). A Bayesian foundation for individual learning under uncertainty. *Frontiers in Human Neuroscience*, 5, 39.
- Mengotti, P., Dombert, P. L., Fink, G. R., & Vossel, S. (2017). Disruption of the Right Temporoparietal Junction Impairs Probabilistic Belief Updating. *The Journal of Neuroscience*, 37(22), 5419–5428.
- Mengotti, P., Käsbauer, A.-S., Fink, G. R., & Vossel, S. (2020). Lateralization, functional specialization, and dysfunction of attentional networks. *Cortex*, 132, 206–222.
- Mengotti, P., Kuhns, A. B., Fink, G. R., & Vossel, S. (2020). Age-related changes in Bayesian belief updating during attentional deployment and motor intention. *Psychological Research*, 84(5), 1387–1399.
- Merrifield, C., Hurwitz, M., & Danckert, J. (2010). Multimodal temporal perception deficits in a patient with left spatial neglect. *Cognitive Neuroscience*, 1(4), 244–253.
- Mesulam, M. M. (1981). A cortical network for directed attention and unilateral neglect. *Annals of Neurology*, 10(4), 309–325.
- Mesulam, M. M. (1985). *Principles of behavioral neurology*. Oxford: Oxford University Press.
- Mirman, D., Landrigan, J. F., Kokolis, S., Verillo, S., Ferrara, C., & Pustina, D. (2018). Corrections for multiple comparisons in voxel-based lesion-symptom mapping. *Neuropsychologia*, 115, 112–123.
- Molenberghs, P., Sale, M. V., & Mattingley, J. B. (2012). Is there a critical lesion site for unilateral spatial neglect? A meta-analysis using activation likelihood estimation. *Frontiers in Human Neuroscience*, 6, 78.
- Mumford, D. (1992). On the computational architecture of the neocortex. *Biological Cybernetics*, 66(3), 241–251.
- Nassar, M. R., Bruckner, R., Gold, J. I., Li, S.-C., Heekeren, H. R., & Eppinger, B. (2016). Age differences in learning emerge from an insufficient representation of uncertainty in older adults. *Nature Communications*, 7(1), 1–13.
- Ng, Y. S., Stein, J., Ning, M. M., & Black-Schaffer, R. M. (2007). Comparison of clinical

4. References

- characteristics and functional outcomes of ischemic stroke in different vascular territories. *Stroke*, 38(8), 2309–2314.
- Nijboer, T. C. W., Kollen, B. J., & Kwakkel, G. (2013). Time course of visuospatial neglect early after stroke: a longitudinal cohort study. *Cortex*, 49(8), 2021–2027.
- Nyffeler, T., Vanbellingen, T., Kaufmann, B. C., Pflugshaupt, T., Bauer, D., Frey, J., Chechlac, M., Bohlhalter, S., Müri, R. M., Nef, T., & Cazzoli, D. (2019). Theta burst stimulation in neglect after stroke: functional outcome and response variability origins. *Brain*, 142, 992–1008.
- Ogawa, S., Lee, T. M., Kay, A. R., & Tank, D. W. (1990). Brain magnetic resonance imaging with contrast dependent on blood oxygenation. *Proceedings of the National Academy of Sciences*, 87(24), 9868–9872.
- Oldfield, R. C. C. (1971). The assessment and analysis of handedness: The Edinburgh inventory. *Neuropsychologia*, 9(1), 97–113.
- Pardo, J. V., Lee, J. T., Sheikh, S. A., Surerus-Johnson, C., Shah, H., Munch, K. R., Carlis, J. V., Lewis, S. M., Kuskowski, M. A., & Dysken, M. W. (2007). Where the brain grows old: decline in anterior cingulate and medial prefrontal function with normal aging. *NeuroImage*, 35(3), 1231–1237.
- Park, D. C., Polk, T. A., Park, R., Minear, M., Savage, A., & Smith, M. R. (2004). Aging reduces neural specialization in ventral visual cortex. *Proceedings of the National Academy of Sciences*, 101(35), 13091–13095.
- Pedrazzini, E., Schnider, A., & Ptak, R. (2017). A neuroanatomical model of space-based and object-centered processing in spatial neglect. *Brain Structure and Function*, 222(8), 3605–3613.
- Pedroli, E., Serino, S., Cipresso, P., Pallavicini, F., & Riva, G. (2015). Assessment and rehabilitation of neglect using virtual reality: a systematic review. *Frontiers in Behavioral Neuroscience*, 9, 226.
- Pinto, Y., van Gaal, S., de Lange, F. P., Lamme, V. A. F., & Seth, A. K. (2015). Expectations accelerate entry of visual stimuli into awareness. *Journal of Vision*, 15(8), 13.

4. References

- Posner, M. I. (1980). Orienting of attention. *The Quarterly Journal of Experimental Psychology*, 32(1), 3–25.
- Posner, M. I., Walker, J. A., Friedrich, F. J., & Rafal, R. (1984). Effects of parietal injury on conant orienting of attention. *The Journal of Neuroscience*, 4, 1863–1864.
- Pouget, A., Beck, J. M., Ma, W. J., & Latham, P. E. (2013). Probabilistic brains: knowns and unknowns. *Nature Neuroscience*, 16(9), 1170–1178.
- Ptak, R., & Schnider, A. (2010). The Dorsal Attention Network Mediates Orienting toward Behaviorally Relevant Stimuli in Spatial Neglect. *The Journal of Neuroscience*, 30(38), 12557–12565.
- Raichle, M. E. (2003). Functional Brain Imaging and Human Brain Function. *The Journal of Neuroscience*, 23(10), 3959–3962.
- Ramsey, L. E., Siegel, J. S., Baldassarre, A., Metcalfe, N. V., Zinn, K., Shulman, G. L., & Corbetta, M. (2016). Normalization of network connectivity in hemispatial neglect recovery. *Annals of Neurology*, 80(1), 127–141.
- Ramsey, L. E., Siegel, J. S., Lang, C. E., Strube, M. J., Shulman, G. L., & Corbetta, M. (2017). Behavioural clusters and predictors of performance during recovery from stroke. *Nature Human Behaviour*, 1(3), 1–10.
- Ransley, K., Goodbourn, P. T., Nguyen, E. H. L., Moustafa, A. A., & Holcombe, A. O. (2018). Reading direction influences lateral biases in letter processing. *Journal of Experimental Psychology: Learning, Memory, and Cognition*, 44(10), 1678–1686.
- Reid, A. T., Hoffstaedter, F., Gong, G., Laird, A. R., Fox, P. T., Evans, A. C., Amunts, K., & Eickhoff, S. B. (2017). A seed-based cross-modal comparison of brain connectivity measures. *Brain Structure and Function*, 222(3), 1131–1151.
- Rengachary, J., d'Avossa, G., Sapir, A., Shulman, G. L., & Corbetta, M. (2009). Is the posner reaction time test more accurate than clinical tests in detecting left neglect in acute and chronic stroke? *Archives of Physical Medicine and Rehabilitation*, 90(12), 2081–2088.
- Rengachary, J., He, B. J., Shulman, G. L., & Corbetta, M. (2011). A behavioral analysis of

4. References

- spatial neglect and its recovery after stroke. *Frontiers in Human Neuroscience*, 5, 29.
- Rescorla, R. A., & Wagner, A. R. (1972). A theory of Pavlovian conditioning: Variations in the effectiveness of reinforcement and nonreinforcement. *Classical Conditioning II: Current Research and Theory*, 2, 64–99.
- Reuter-Lorenz, P. A., & Cappell, K. A. (2008). Neurocognitive aging and the compensation hypothesis. *Current Directions in Psychological Science*, 17(3), 177–182.
- Robertson, I., & Halligan, P. W. (1999). *Spatial neglect: A clinical handbook for diagnosis and treatment*. Hove: Psychology Press.
- Robertson, I., Mattingley, J., Rorden, C., & Driver, J. (1998). Phasic alerting of neglect patients overcomes their spatial deficit in visual awareness. *Nature*, 395(6698), 169–172.
- Robertson, L. C., Knight, R. T., Rafal, R., & Shimamura, A. P. (1993). Cognitive Neuropsychology Is More Than Single-Case Studies. *Journal of Experimental Psychology: Learning, Memory, and Cognition*, 19(3), 710–717.
- Rode, G., Pagliari, C., Huchon, L., Rossetti, Y., & Pisella, L. (2017). Semiology of neglect: An update. *Annals of Physical and Rehabilitation Medicine*, 60(3), 177–185.
- Rojkova, K., Volle, E., Urbanski, M., Humbert, F., Dell'Acqua, F., & Thiebaut de Schotten, M. (2016). Atlasing the frontal lobe connections and their variability due to age and education: a spherical deconvolution tractography study. *Brain Structure and Function*, 221(3), 1751–1766.
- Rorden, C., Bonilha, L., Fridriksson, J., Bender, B., & Karnath, H.-O. (2012). Age-specific CT and MRI templates for spatial normalization. *NeuroImage*, 61(4), 957–965.
- Rorden, C., Karnath, H., & Bonilha, L. (2007). Improving Lesion-Symptom Mapping. *Journal of Cognitive Neuroscience*, 19(7), 1081–1088.
- Rorden, C., & Karnath, H. O. (2004). Using human brain lesions to infer function: A relic from a past era in the fMRI age? *Nature Reviews Neuroscience*, 5(10), 812–819.
- Rosenberg, M. D., Finn, E. S., Scheinost, D., Papademetris, X., Shen, X., Constable, R. T., & Chun, M. M. (2016). A neuromarker of sustained attention from whole-brain functional

4. References

- connectivity. *Nature Neuroscience*, 19(1), 165–171.
- Roser, M. E., Fiser, J., Aslin, R. N., & Gazzaniga, M. S. (2011). Right hemisphere dominance in visual statistical learning. *Journal of Cognitive Neuroscience*, 23(5), 1088–1099.
- Rushworth, M. F. S., & Behrens, T. E. (2008). Choice, uncertainty and value in prefrontal and cingulate cortex. *Nature Neuroscience*, 11(4), 389–397.
- Rushworth, M. F. S., Ellison, A., & Walsh, V. (2001). Complementary localization and lateralization of orienting and motor attention. *Nature Neuroscience*, 4(6), 656–661.
- Salazar, A. P. S., Vaz, P. G., Marchese, R. R., Stein, C., Pinto, C., & Pagnussat, A. S. (2018). Noninvasive Brain Stimulation Improves Hemispatial Neglect After Stroke: A Systematic Review and Meta-Analysis. *Archives of Physical Medicine and Rehabilitation*, 99(2), 355–366.
- Salvalaggio, A., De Filippo De Grazia, M., Zorzi, M., Thiebaut de Schotten, M., & Corbetta, M. (2020). Post-stroke deficit prediction from lesion and indirect structural and functional disconnection. *Brain*, 143(7), 2173–2188.
- Scherer, H. J. (1940). The forms of growth in gliomas and their practical significance. *Brain*, 63(1), 1–35.
- Shaqiri, A., & Anderson, B. (2012). Spatial probability cuing and right hemisphere damage. *Brain and Cognition*, 80(3), 352–360.
- Shaqiri, A., & Anderson, B. (2013). Priming and statistical learning in right brain damaged patients. *Neuropsychologia*, 51(13), 2526–2533.
- Shaqiri, A., Anderson, B., & Danckert, J. (2013). Statistical learning as a tool for rehabilitation in spatial neglect. *Frontiers in Human Neuroscience*, 7, 224.
- Shaqiri, A., Danckert, J., Burnett, L., & Anderson, B. (2018). Statistical Learning Impairments as a Consequence of Stroke. *Frontiers in Human Neuroscience*, 12, 339.
- Shulman, G. L., Astafiev, S. V., Franke, D., Pope, D. L. W., Snyder, A. Z., McAvoy, M. P., & Corbetta, M. (2009). Interaction of Stimulus-Driven Reorienting and Expectation in Ventral and Dorsal Frontoparietal and Basal Ganglia-Cortical Networks. *The Journal of*

4. References

- Neuroscience*, 29(14), 4392–4407.
- Siegel, J. S., Ramsey, L. E., Snyder, A. Z., Metcalfe, N. V., Chacko, R. V., Weinberger, K., Baldassarre, A., Hacker, C. D., Shulman, G. L., & Corbetta, M. (2016). Disruptions of network connectivity predict impairment in multiple behavioral domains after stroke. *Proceedings of the National Academy of Sciences*, 113(30), 4367–4376.
- Silvetti, M., Lasaponara, S., Lecce, F., Dragone, A., Macaluso, E., & Doricchi, F. (2016). The Response of the Left Ventral Attentional System to Invalid Targets and its Implication for the Spatial Neglect Syndrome: a Multivariate fMRI Investigation. *Cerebral Cortex*, 26(12), 4551–4562.
- Smitha, K. A., Akhil Raja, K., Arun, K. M., Rajesh, P. G., Thomas, B., Kapilamoorthy, T. R., & Kesavadas, C. (2017). Resting state fMRI: A review on methods in resting state connectivity analysis and resting state networks. *Neuroradiology Journal*, 30(4), 305–317.
- Sparing, R., Thimm, M., Hesse, M. D., Küst, J., Karbe, H., & Fink, G. R. (2009). Bidirectional alterations of interhemispheric parietal balance by non-invasive cortical stimulation. *Brain*, 132(11), 3011–3020.
- Sperber, C., & Karnath, H.-O. (2017). Impact of correction factors in human brain lesion-behavior inference. *Human Brain Mapping*, 38(3), 1692–1701.
- Sperber, C., & Karnath, H.-O. (2018). On the validity of lesion-behaviour mapping methods. *Neuropsychologia*, 115, 17–24.
- Sperber, C., Wiesen, D., & Karnath, H.-O. (2019). An empirical evaluation of multivariate lesion behaviour mapping using support vector regression. *Human Brain Mapping*, 40(5), 1381–1390.
- Staub, B., Doignon-Camus, N., Després, O., & Bonnefond, A. (2013). Sustained attention in the elderly: What do we know and what does it tell us about cognitive aging? *Ageing Research Reviews*, 12(2), 459–468.
- Stevens, J. (1996). *Applied multivariate statistics for the social sciences* (6th edition). Mahwah, NJ: Lawrence Erlbaum Associates.

4. References

- Stöttinger, E., Filipowicz, A., Marandi, E., Quehl, N., Danckert, J., & Anderson, B. (2014). Statistical and perceptual updating: Correlated impairments in right brain injury. *Experimental Brain Research*, *232*(6), 1971–1987.
- Stöttinger, E., Filipowicz, A., Valadao, D., Culham, J. C., Goodale, M. A., Anderson, B., & Danckert, J. (2015). A cortical network that marks the moment when conscious representations are updated. *Neuropsychologia*, *79*, 113–122.
- Stöttinger, E., Guay, C. L., Danckert, J., & Anderson, B. (2018). Updating impairments and the failure to explore new hypotheses following right brain damage. *Experimental Brain Research*, *236*(6), 1749–1765.
- Striemer, C., Ferber, S., & Danckert, J. (2013). Spatial working memory deficits represent a core challenge for rehabilitating neglect. *Frontiers in Human Neuroscience*, *7*, 334.
- Tales, A., Muir, J. L., Bayer, A., & Snowden, R. J. (2002). Spatial shifts in visual attention in normal ageing and dementia of the Alzheimer type. *Neuropsychologia*, *40*(12), 2000–2012.
- Thiebaut de Schotten, M., Dell'Acqua, F., Forkel, S. J., Simmons, A., Vergani, F., Murphy, D. G. M., & Catani, M. (2011). A lateralized brain network for visuospatial attention. *Nature Neuroscience*, *14*(10), 1245–1246.
- Thiebaut de Schotten, M., Dell'Acqua, F., Ratiu, P., Leslie, A., Howells, H., Cabanis, E., Iba-Zizen, M. T., Plaisant, O., Simmons, A., Dronker, N. F., Corkin, S., & Catani, M. (2015). From Phineas Gage and Monsieur Leborgne to H.M.: Revisiting Disconnection Syndromes. *Cerebral Cortex*, *25*(12), 4812–4827.
- Thiebaut de Schotten, M., Ffytche, D. H., Bizzi, A., Dell'Acqua, F., Allin, M., Walshe, M., Murray, R., Williams, S. C., Murphy, D. G. M., & Catani, M. (2011). Atlasing location, asymmetry and inter-subject variability of white matter tracts in the human brain with MR diffusion tractography. *NeuroImage*, *54*(1), 49–59.
- Thiebaut De Schotten, M., Tomaiuolo, F., Aiello, M., Merola, S., Silvetti, M., Lecce, F., Bartolomeo, P., & Doricchi, F. (2014). Damage to white matter pathways in subacute and chronic spatial neglect: A group study and 2 single-case studies with complete

4. References

- virtual “in vivo” tractography dissection. *Cerebral Cortex*, 24(3), 691–706.
- Toba, M. N., Zavaglia, M., Malherbe, C., Moreau, T., Rastelli, F., Kaglik, A., Valabrègue, R., Pradat-Diehl, P., Hilgetag, C. C., & Valero-Cabré, A. (2020). Game theoretical mapping of white matter contributions to visuospatial attention in stroke patients with hemineglect. *Human Brain Mapping*, 41(11), 2926–2950.
- Tzourio-Mazoyer, N., Landeau, B., Papathanassiou, D., Crivello, F., Etard, O., Delcroix, N., Mazoyer, B., & Joliot, M. (2002). Automated anatomical labeling of activations in SPM using a macroscopic anatomical parcellation of the MNI MRI single-subject brain. *NeuroImage*, 15(1), 273–289.
- Umarova, R. M. (2017). Adapting the concepts of brain and cognitive reserve to post-stroke cognitive deficits: Implications for understanding neglect. *Cortex*, 97, 327–338.
- Umarova, R. M., Nitschke, K., Kaller, C. P., Klöppel, S., Beume, L., Mader, I., Martin, M., Hennig, J., & Weiller, C. (2016). Predictors and signatures of recovery from neglect in acute stroke. *Annals of Neurology*, 79(4), 673–686.
- Umarova, R. M., Saur, D., Kaller, C. P., Vry, M. S., Glauche, V., Mader, I., Hennig, J., & Weiller, C. (2011). Acute visual neglect and extinction: Distinct functional state of the visuospatial attention system. *Brain*, 134(11), 3310–3325.
- Vaessen, M. J., Saj, A., Lovblad, K.-O., Gschwind, M., & Vuilleumier, P. (2016). Structural white-matter connections mediating distinct behavioral components of spatial neglect in right brain-damaged patients. *Cortex*, 77, 54–68.
- Vallar, G., & Perani, D. (1986). The anatomy of unilateral neglect after right-hemisphere stroke lesions. A clinical/CT-scan correlation study in man. *Neuropsychologia*, 24(5), 609–622.
- Van den Heuvel, M. P., & Hulshoff Pol, H. E. (2010). Exploring the brain network: A review on resting-state fMRI functional connectivity. *European Neuropsychopharmacology*, 20(8), 519–534.
- Varsou, O., Macleod, M. J., & Schwarzbauer, C. (2014). Functional connectivity magnetic resonance imaging in stroke: An evidence-based clinical review. *International Journal of*

4. References

- Stroke*, 9(2), 191–198.
- Vossel, S., Eschenbeck, P., Weiss, P. H., & Fink, G. R. (2010). The neural basis of perceptual bias and response bias in the Landmark task. *Neuropsychologia*, 48(13), 3949–3954.
- Vossel, S., Geng, J. J., & Fink, G. R. (2014). Dorsal and ventral attention systems: Distinct neural circuits but collaborative roles. *Neuroscientist*, 20(2), 150–159.
- Vossel, S., Mathys, C., Daunizeau, J., Bauer, M., Driver, J., Friston, K. J., & Stephan, K. E. (2014). Spatial attention, precision, and bayesian inference: A study of saccadic response speed. *Cerebral Cortex*, 24(6), 1436–1450.
- Vossel, S., Mathys, C., Stephan, K. E., & Friston, K. J. (2015). Cortical Coupling Reflects Bayesian Belief Updating in the Deployment of Spatial Attention. *The Journal of Neuroscience*, 35(33), 11532–11542.
- Vossel, S., Weidner, R., Driver, J., Friston, K. J., & Fink, G. R. (2012). Deconstructing the Architecture of Dorsal and Ventral Attention Systems with Dynamic Causal Modeling. *The Journal of Neuroscience*, 32(31), 10637–10648.
- Vossel, S., Weidner, R., Moos, K., & Fink, G. R. (2016). Individual attentional selection capacities are reflected in interhemispheric connectivity of the parietal cortex. *NeuroImage*, 129, 148–158.
- Vuilleumier, P., Hester, D., Assal, G., & Regli, F. (1996). Unilateral spatial neglect recovery after sequential strokes. *Neurology*, 46(1), 184–189.
- Vuilleumier, P. (2013). Mapping the functional neuroanatomy of spatial neglect and human parietal lobe functions: progress and challenges. *Annals of the New York Academy of Sciences*, 1296, 50–74.
- Wåhlin, A., Fordell, H., Ekman, U., Lenfeldt, N., & Malm, J. (2019). Rehabilitation in chronic spatial neglect strengthens resting-state connectivity. *Acta Neurologica Scandinavica*, 139(3), 254–259.
- Walthew, C., & Gilchrist, I. D. (2006). Target location probability effects in visual search: An effect of sequential dependencies. *Journal of Experimental Psychology: Human*

4. References

- Perception and Performance*, 32(5), 1294.
- Wang, R., & Benner, T. (2007). Diffusion toolkit: a software package for diffusion imaging data processing and tractography. *Proceedings of the International Society for Magnetic Resonance in Medicine*, 15, 3720.
- Weiss, P. H., Kalbe, E., & Kessler, J. (2013). *KAS: Kölner Apraxie-Screening*. Göttingen: Hogrefe.
- Weissman, D. H., & Prado, J. (2012). Heightened activity in a key region of the ventral attention network is linked to reduced activity in a key region of the dorsal attention network during unexpected shifts of covert visual spatial attention. *NeuroImage*, 61(4), 798–804.
- Wen, X., Yao, L., Liu, Y., & Ding, M. (2012). Causal Interactions in Attention Networks Predict Behavioral Performance. *The Journal of Neuroscience*, 32(4), 1284–1292.
- Whitfield-Gabrieli, S., & Nieto-Castanon, A. (2012). Conn: A Functional Connectivity Toolbox for Correlated and Anticorrelated Brain Networks. *Brain Connectivity*, 2(3), 125–141.
- Wilson, B., Cockburn, J., & Halligan, P. W. (1987). Development of a behavioral test of visuospatial neglect. *Archives of Physical Medicine and Rehabilitation*, 68(2), 98–102.
- Wirth, K., Held, A., Kalbe, E., Kessler, J., Saliger, J., Karbe, H., Fink, G. R., & Weiss, P. H. (2016). Das revidierte Kölner Apraxie-Screening (KAS-R) als diagnostisches Verfahren für Patienten mit rechtshemisphärischem Schlaganfall. *Fortschritte Der Neurologie-Psychiatrie*, 84(10), 633–639.
- Yeo, B. T. T., Krienen, F. M., Sepulcre, J., Sabuncu, M. R., Lashkari, D., Hollinshead, M., Roffman, J. L., Smoller, J. W., Zöllei, L., Polimeni, J. R., Fischl, B., Liu, H., & Buckner, R. L. (2011). The organization of the human cerebral cortex estimated by intrinsic functional connectivity. *Journal of Neurophysiology*, 106(3), 1125–1165.

5. Curriculum Vitae

Name: **Anne-Sophie Käsbauer**
 Mail: a.kaesbauer@fz-juelich.de
 Geburtsdatum: 15.04.1991 (Bochum)
 Nationalität: Deutsch

Ausbildung

10/2016 – heute	Promotionsstudium Department Psychologie Humanwissenschaftliche Fakultät der Universität zu Köln
10/2014 – 09/2016	M.Sc. in Cognitive-Affective Neuroscience (Psychologie), Technische Universität Dresden (Note 1,4)
10/2010 – 07/2014	B.Sc. in Psychology Ruhr-Universität Bochum (Note 1,6)
08/2001 – 06/2010	Allgemeine Hochschulreife Gymnasium am Ostring, Bochum (Note 1,2)

Forschungstätigkeiten

10/2016 – heute	Wissenschaftliche Mitarbeiterin (Doktorandin) Forschungszentrum Jülich, Institut für Neurowissenschaften und Medizin, Kognitive Neurowissenschaften (INM-3) Prof. Dr. Gereon R. Fink (Betreuung: Jun.-Prof. Dr. Simone Vossel)
01/2015 – 01/2016	Wissenschaftliche Hilfskraft Technische Universität Dresden, Fakultät Psychologie, Sonderforschungsbereich 940 Volition und kognitive Kontrolle Prof. Dr. Thomas Goschke (Betreuung: Dr. Franziska Korb und Dr. Uta Wolfensteller)
02/2013 – 07/2014	Wissenschaftliche Hilfskraft Ruhr-Universität Bochum, Fakultät Medizin, Abteilung für medizinische Psychologie und medizinische Soziologie, Prof. Dr. Monika Hasenbring (Betreuung: Jun.-Prof. Adina Rusu-Klappheck)
02/2012 – 05/2013	Forschungspraktikum Ruhr-Universität Bochum, Fakultät Psychologie, Abteilung Biopsychologie, AG Motivation Prof. Dr. Dr. Onur Güntürkün (Betreuung: Dr. Marlies Pinnow)

Konferenzen und Workshops

11/2019	N ² Meeting: From Research to Application, Umweltforum Berlin
10/2019	Annual Meeting of the Society for Neuroscience 2019 Chicago, IL, USA.
07/2018	NextGen@Helmholtz Konferenz Deutsches GeoForschungszentrum, Potsdam

5. Curriculum Vitae

07/2017	NextGen@Helmholtz Konferenz Geomar Helmholtz Zentrum für Ozeanforschung, Kiel
05/2017	Lesion Analysis Workshop Universitätsklinikum Tübingen
09/2015	Summerschool Human Action Control Babes-Bolyai University, Cluj-Napoca, Rumänien

Andere Tätigkeiten

12/2016 – 05/2020	Tourguide, Forschungszentrum Jülich
04/2016 – 05/2016	Klinisches Praktikum Tagesklinik für Somatoforme Störungen, Klinik und Poliklinik für Psychotherapie und Psychosomatik, UK Dresden
09/2013 – 08/2014	Studentische Hilfskraft Neurologisches Rehabilitationszentrum Rüttenscheid, Alfried Krupp Krankenhaus, Essen
02/2013 – 07/2014	Studentische Hilfskraft Alfried Krupp Schülerlabor, Ruhr-Universität Bochum

Erworbene Qualifikationen

Sprachen	Deutsch	Muttersprache
	Englisch	fließend in Schrift und Sprache
	Französisch	Grundkenntnisse
	Spanisch	Grundkenntnisse
	Schwedisch	Grundkenntnisse
	Latinum	
Software	Brainsight TMS Navigation, Brain Vision Analyser, Coral Draw, Matlab, MS Office (Excel, PowerPoint, Word), MRI Cron/NPM, NiiStat, Presentation (Neurobehavioral Systems), R Studio, SPM, SPSS	

Ehrenamt

- Sprecher und Mitglied des Docteams und der Helmholtz Juniors
- Mitglied des Advisory Boards des Career Centers, Forschungszentrum Jülich
- Mitglied der Arbeitsgruppe zur Anpassung der Richtlinien guter wissenschaftlicher Praxis, Forschungszentrum Jülich
- Mitglied des Programms Qualifizierung der Prozesslandschaft Wissenschaftskommunikation, Forschungszentrum Jülich
- Mitglied des Organisationsteams der INM-ICS Retreats, Forschungszentrum Jülich
- Sprecher und Mitglied des Fachschaftsrates der Fakultät Psychologie, Technische Universität Dresden
- Mitglied des Fachschaftsrates der Fakultät Psychologie, Ruhr-Universität Bochum